## The Journal of Gemmology

# Formation of large synthetic zincite (ZnO) crystals during production of zinc white

John W. Nowak[1†], R.S.W. Braithwaite[2], J. Nowak[3],
K. Ostojski[4], M. Krystek[5] and W. Buchowiecki[6]

1. 71 Glenhurst Avenue, Bexley, Kent, DA5 3QH
2. School of Chemistry, University of Manchester, Manchester, M13 9PL
   Email: willbraith@hotmail.com
3. Jelenia 4, 92-309 Lodz, Poland. Email: targi@interstone.net.pl
4. Olawa S.A. Foundry, Olawa, Poland
5. Geological Museum, University of Lodz, 90-142 Lodz, Kopcinskiego 31, Poland
   Email: pseudotachylit@wp.pl
6. Mieszczanska 17/40, 93-322 Lodz, Poland. Email: buchow@p.lodz.pl (corresponding author)

**Abstract:** *Remarkable zincite crystals have formed as a by-product of zinc white production in Olawa Foundry, Poland. Some are of gem quality and have been faceted. Small primary crystals formed by reaction of zinc vapour with carbon dioxide from fuel burning gases leaking through faults in a diaphragm of a retort furnace. Some of these have undergone carbon monoxide-promoted and zinc vapour-assisted sublimation to form large secondary crystals. Many of these crystals are brightly coloured and transparent, and have been found up to 2 kg in weight. Most of the crystals are fluorescent in ultraviolet light.*

**Keywords:** *chemical assisted sublimation, crystal growth, zinc oxide, zincite*

## Introduction

Zincite is a relatively rare natural oxide of zinc, with the ideal formula ZnO. The world's largest deposit of zincite is near Franklin and Ogdensburg, Sussex County, New Jersey, USA. The district is famous for its wide range of more than 250 minerals, including crystals of rare fluorescent species (Palache, 1935; Bancroft, 1984). Zincite occurs here mainly as a massive material or as small granules with other major zinc-bearing minerals such as willemite and franklinite, embedded in a white crystalline limestone.

† Sadly John W. Nowak died on 16 April 2007. An obituary notice is given on p. 355.

Zincite crystals are quite rare and generally tend to be small. The world's best crystals, transparent and several cm in length, are known only from Buckwheat mine, on Mine Hill close to Franklin. Only a few natural gem-quality zincite crystals, displaying a magnificent deep red colour have been cut. One example weighing 20.06 ct is on exhibit in the National Gem Collection at the Smithsonian Institution in Washington D.C. and others are in the American Museum of Natural History in New York City (Sinkankas, 1959).

Not surprisingly, the appearance in the early 1980s of very large transparent and brightly coloured zincite crystals at major mineralogical shows created considerable interest. This rare and exciting cutting material was attractive mainly to lapidary enthusiasts, and many have been faceted (Kammerling and Johnson, 1995) (*Figure 1*). Despite their aesthetic beauty, this zincite was far less appealing to conservative mineral collectors because its synthetic origin was unmistakeable. From the scientific point of view an intriguing issue was the question of the conditions in which such spectacular zincite crystals could grow.

The increasing demand for this synthetic zincite had been largely fulfilled for a time, but now the material is only available from dealers' old stocks. The mineralogical and gemmological communities had not been aware of the provenance of these zincite crystals (Crowningshield, 1985; Kammerling and Johnson, 1995) until information became available on the Internet. In this article we establish that the distinctive and exquisite zincite crystals which appeared in Europe and in the U.S.A. during the period 1980–2004 originated from the Olawa Foundry SA near Wroclaw in Poland. We also describe the major features of zinc white production technology that unexpectedly caused the formation of these large zincite crystals as an accidental by-product, and present unique photographs documenting this phenomenon.

Crystalline ZnO is a wide band-gap semiconductor for various high-tech applications. Especially promising is the use of ZnO crystals to produce blue lasers for digital video-disc systems and data storage, emitter devices in the blue and ultraviolet region, and piezoelectronic devices (Nause *et al.*, 1999).

Currently very few technologies can deliver centimetre-sized ZnO mono-crystals; one is based on hydrothermal growth (Kortunova and Lyutin, 1995; Suscavage *et al.*, 1999), another on chemical vapour transport (CVT) (Noritake *et al.*, 1991a,b; Fujitzu *et al.*, 1993; Mycielski *et al.*, 2004), and the most promising one, based on pressurized melting (Nause *et al.*, 1999), has the potential to produce low-cost ZnO wafers up to 100 mm in diameter. All the listed technologies require quite sophisticated processing equipment. In contrast, Olawa's simple furnace has delivered transparent ZnO crystals weighing up to 2 kg. Evidently, in this case the mechanism of crystal growth and vapour transport was highly effective. However, the plant was not designed to produce structurally uniform ZnO crystals, so unfortunately these crystals do not meet the requirements for electronic material.



Figure 1: *Faceted zincite crystal. Photograph by R.S.W. Braithwaite.*

1 mm

# Zinc white production at the Olawa Foundry SA, Poland

Zinc white is an important industrial product for numerous applications. Most is consumed in the rubber, dye, ceramic and pharmaceutical industries. Of the several production technologies described in the literature (Bailar, 1973; Kirk and Othmer, 1970), Olawa Foundry SA produces zinc white as a powder according to the so-called French method, by vaporizing pure zinc and burning it in air. The process is conducted in a single retort furnace of modified and patented construction (Jasinski *et al.*, 1987; Igielski *et al.*, 1988). A cross-section of the furnace is shown diagrammatically in *Figure 2*.

The furnace consists of two sections, the upper being the combustion chamber (3) and the lower the vaporizing chamber (2). Heating gas is burned in the combustion chamber, creating temperatures up to 1400-1500 C. The combustion chamber is separated from the vaporizing chamber by a ceramic diaphragm (1), conducting heat so that the metallic zinc (2a) placed in the lower section is heated by radiation, melted and vaporized. The zinc vapour is overheated to ~ 950 C and leaves the furnace through the burner opening (6) into the oxidation chamber (4), where
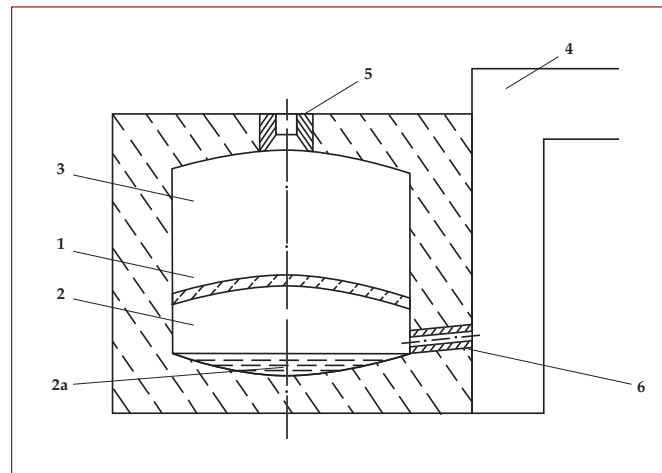
Figure 2: *Cross-section of a single retort furnace for zinc white production at Olawa (Jasinski et al., 1987): (1) ceramic diaphragm; (2) vaporizing chamber; (2a) metallic zinc melt; (3) combustion chamber; (4) zinc vapour oxidizing chamber; (5) gas burner; (6) zinc vapour burner.*

in contact with wet air it forms zinc white powder, which is then collected.

Initial exploitation of the plant exposed several minor technical difficulties, which have gradually been eliminated. The most serious problem was a slow increase in heating gas consumption per tonne production of zinc white. A periodic shutdown of the plant revealed that the top of the vaporizing chamber, against the lower part of the diaphragm, was virtually covered by hundreds of kilograms of small to giant colourful zincite crystals and many crystals had fallen to the bottom (*Figure 3*).
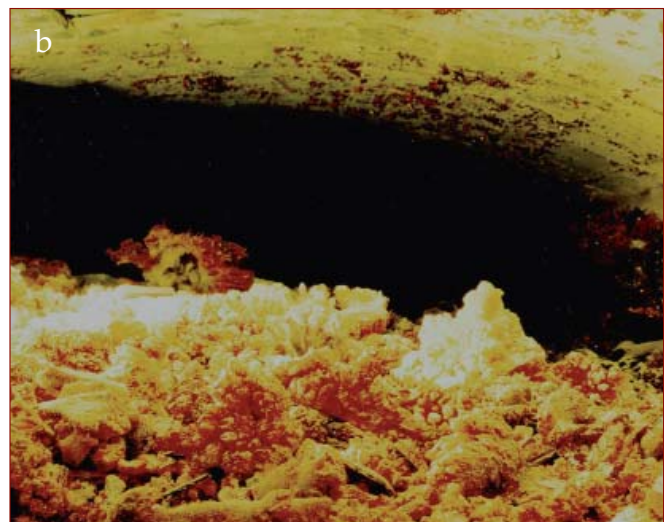
Figure 3: *Zincite crystals in vaporizing chamber: (a) on roof of chamber; (b) fallen crystals on floor of chamber. Photographs by R. Jaslan.*

As far as we know, other zinc white producers have not reported such a technological anomaly. From the very beginning the reason for the unexpected formation of zincite crystals was attributed to an unpredicted micro-porosity of the diaphragm. In order to improve the diaphragm there was a serious effort to select appropriate heat resistant ceramic materials, cements and seals, and apply an innovative construction technology.

After considerable experimentation, rewarding results have been achieved. At the maintenance shutdown of the furnace in 2002 no crystalline material was found, but some residual remains after zinc evaporation, such as for example an Fe-Al alloy, were found in addition to the usual ashes. Uninterrupted furnace runs have since been extended from four to six months to one full year and by February 2005 to over two years.

## Mechanism of the zincite crystal formation

The correct production process for zinc white in a single retort furnace should not create macro-crystals of zinc oxide. The necessary condition for the formation of crystals in the vaporizing chamber was the presence of micro-flaws in the defective ceramic diaphragm. As a result the fumes from the combustion chamber could slowly penetrate the vaporizing chamber. The fumes contain nitrogen, carbon dioxide and possibly some remaining oxygen in addition to other minor components. Contact of the zinc vapour with these fumes caused a rapid generation of apparently primary zincite crystals in an oxidizing atmosphere according to the following reactions:

(1) $Zn(g) + CO_2 \rightleftharpoons ZnO(s) + CO$

(2) $Zn(g) + \frac{1}{2}O_2 \; ZnO(s)$
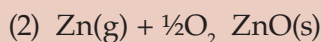
Distinctive zones of crystal formations on the diaphragm 'matrix' show variable local extension and peculiar spatial formations. The zones closest to the diaphragm display small needles of complex morphology (*Figure 3a*). The more distant zones show considerably larger secondary crystals displaying a habit typical of many synthetic zincite crystals (*Figures 3b* and *6*) as illustrated in the *Atlas der Krystallformen* (Goldschmidt, 1913) and many show dissolution or growth features. The following factors should be taken into account in considering the nature of the driving force involved in the sublimation:

• A high vertical temperature gradient reaching 350–400 C between the molten zinc at 907 C (bottom of the vaporizing chamber) and the diaphragm at 1250 C. This gradient was not constant and likely to vary over the diaphragm surface.

• ZnO crystals were formed on the lower diaphragm surface, and on the side walls of the vaporizing chamber.

• With a high, unstable vertical gradient of zinc vapour concentration, there could be horizontal transfer of zinc vapour.

Interestingly, the precise mechanism of ZnO(s) sublimation is not well known. Generally, the process is slow *in vacuo* at high temperatures (>1500 C). However, a number of additives, such as wet hydrogen, argon or chlorine can act as sublimation activators, which dramatically increase the sublimation rate at temperatures as low as ~1000 C (Triboulet *et al.*, 1991). This mechanism is called 'chemical assisted sublimation' or 'chemical vapour transport' and has been used in the laboratory synthesis of transparent ZnO mono-crystals (Noritake *et al.*, 1991a,b; Fujitzu *et al.*, 1993; Isshiki *et al.*, 2005b).

Reversible reaction (1) shows that gaseous zinc and solid zinc oxide can act in

association with a third key reactant, carbon dioxide (Bailar, 1973; Yu *et al.*, 2005). Consequently, equation (1) is important for an explanation of zincite crystal growth. From left to right, equation (1) describes ZnO crystal formation inside the vaporizing chamber. Initially, fast-rate stage needles of primary ZnO crystals were formed in an oxidizing micro-atmosphere containing concentrated $CO_2$ close to open cracks. The temperature of these crystals was nearly equal to the temperature of the diaphragm. In the reverse direction equation (1) actually describes the mechanism of carbon monoxide promoted sublimation of ZnO(s). This mechanism can be described in terms of a cycle (*Figure 4*).

CO released in the initial oxidation (equation 1) reacted with a crystal surface of ZnO(s) (A); the Zn(g/s) and $CO_2$ generated were flushed out from the crystal surface by a stream of Zn(g) (B). As a result, a diluted mixture of ZnO(g) and CO in flowing Zn(g) was formed instantly (C), this interacting with already formed ZnO(s) (D). One mole of CO can dissolve many molar equivalents of ZnO(s) because CO is regenerated during the oxidation reaction (C). The reductive mixture [ZnO(g) + CO + Zn(g)] formed the atmosphere of the upper part of the vaporizing chamber. This mixture was responsible for ZnO crystal growth, erosion, dissolution, habit changes, colouring and transport. Direct formation of ZnO(g) by sublimation of ZnO(s) under the sole influence of Zn(g) (reaction d) is doubtful, and unlikely at ambient pressure (Triboulet *et al.*, 1991).

Centres of sublimation and growth were randomly distributed over the diaphragm surface. They were subject to rearrangement in response to changes in heat transfer and concentration of [ZnO(g) + CO + Zn(g)] as well as a reaction to opening and closing of cracks.

Methane from the fuel gas would also be a very strong sublimation promoter if present in larger than trace amounts in the fumes entering the vaporizing chamber. The oxidation of methane by ZnO (equation 3) has recently been found very useful for producing metallic zinc and synthesis gas (CO + $2H_2$) (Jamshidi *et al.*, 2005).

(3)  $ZnO(s) + CH_4 = Zn(g) + CO + 2H_2$
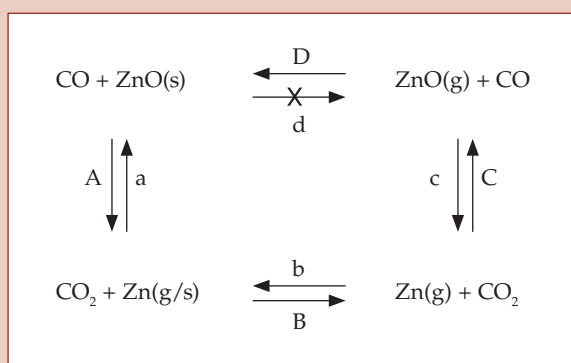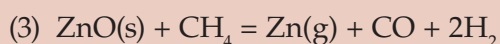


*Figure 4: Reaction cycle involved in the formation of the zincite crystals. ZnO(s) = surface of ZnO crystal; ZnO(g) = vapour of ZnO in Zn(g) solvent; Zn(g/s) = Zn atom adsorbed on ZnO(s); Zn(g) = Zn vapour. A = degradation of ZnO(s) surface under the influence of CO; B = desorption of Zn(g) from ZnO(s) surface by Zn(g) vapour; C = oxidation of Zn(g) by $CO_2$ to generate ZnO(g); D = growth of ZnO(s) crystal from ZnO(g) vapour; a, b, c, d = reverse reactions respectively of A, B, C, D.*

A recent patent briefly describes the synthesis of high-purity high quality ZnO crystals using CO and $CO_2$ as vapour transport agents, providing strong experimental support for our postulated sublimation mechanism (Isshiki *et al.*, 2005b).

Tons of zinc vapour run continuously through the plant every day. The transporting potential of this solvent at the top of the chamber was apparently adequate to keep increasing masses of zincite in constant transport.

# Coloration

Natural zincite crystals from Franklin display reds of variable intensity and hue (Sinkankas, 1959). The colour of these crystals is caused by the presence of $Mn^{2+}$ ions in tetrahedral sites and is additionally influenced by some $Fe^{3+}$ content (Bates *et al.*, 1966). ZnO crystals grown hydrothermally in the presence of $Mn^{2+}$ ions especially for jewellery purposes are red-orange (Kuz'mina *et al.*, 1991); those contaminated with iron are amber-coloured (Laudise *et al.*, 1960), and others are green as a result of incorporation of unknown impurities or lattice defects (Suscavage *et al.*, 1999).

Zincites from Olawa are free from colouring elements such as iron or manganese (Kammerling and Johnson, 1995) as even if traces of these elements were present in the raw zinc, which is of high purity, they would not co-evaporate with the zinc and would stay in the melting tank. Under laboratory conditions, when zinc oxide is heated in zinc vapour, additional neutral zinc atoms diffuse to octahedral interstices in the crystal lattice (Mohanty and Azaroff, 1961; Greenwood, 1968; Isshiki *et al.*, 2005a; Lott *et al.*, 2005). These n-type doped crystals are brightly coloured, just like the material from Olawa, and darker crystals are the most conductive. The hue and intensity of the colour largely depends on the concentration of the extra zinc atoms in the crystal lattice, but the physical mechanism of coloration remains to be elucidated (Kotera and Yonemura, 1992; Erhart *et al.*, 2005).

A striking feature of the zincites from Olawa is their high transparency and rather uniform colour distribution. We postulate that a sublimation process of ZnO(s) inside the furnace was CO promoted and Zn(g) assisted. As a consequence, the growing secondary crystals were easily doped by a Zn(g) incorporation mechanism. Variation in growth conditions resulted in some gradual colour changes, typically observed in the [0001] direction, e.g. yellow to pale yellow or colourless, green to colourless and red to yellow. Long lasting ageing at the high temperatures involved caused diffusive redistribution of doping centres. Presumably, the presence of lattice defects conjugated to electron donors such as neutral zinc atoms are responsible for colour development.

# Description of the zincite crystals from Olawa

Zincite crystals are hexagonal, of wurtzite structure, space group $P6_3mc$, with a = 3.250 Å, c = 5.207 Å; Z = 2. Refractive indices are high, with ω = 2.013, ε = 2.029; birefringence = 0.016; optically uniaxial, positive. Mohs hardness = 4.5 – 5; specific gravity = 5.67 (Bailar, 1973). Their gemmological properties have been described in detail by Kammerling and Johnson (1995) and readers are referred to their Table II for a concise summary.

The zincite crystals from Olawa display enormous diversity in size, habit and colour. They can be divided into two genetically different subgroups.

## 1. Primary crystals formed by oxidation of Zn(g) by $CO_2$ from furnace fumes (oxidizing environment)

These are small, from sub-millimetre to 5–8 mm, rarely larger. Thin needles with sharp edges and smooth faces are common, but frequently signs of dissolution over the full crystal length are present. Crystal tips are sharp or pinhead-like, with tiny pyramidal terminations (*Figure 5a*). Exceptional short needles terminated by {0001} plates of dendritic snowflake-like crystals have been found, as well as beautiful crystal aggregates (*Figure 5a* and *b*). These are formed by tiny needles growing in striking order perpendicularly on prismatic or pyramidal faces of larger needles, to form many patterns resembling flowers, brushes, combs or firs. The crystals are predominantly colourless, pale yellow or green, rarely intensely yellow to reddish yellow.

Analogous zincite crystals of complicated morphology but of nanometre size, obtained by a vapour transport process have been extensively studied by Yu *et al.* (2005).
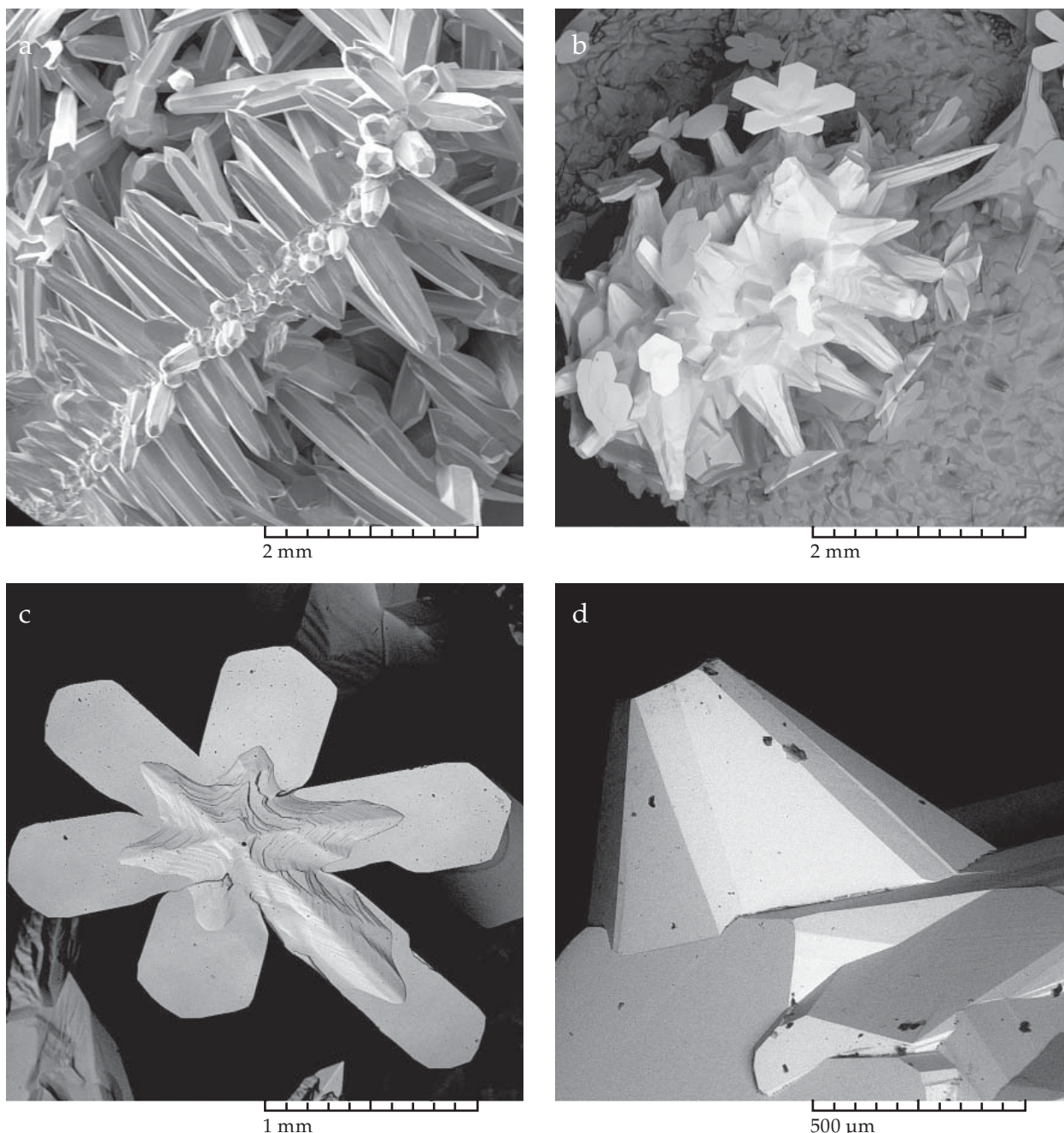
*Figure 5: SEM photographs of primary zincite crystals: (a–b) crystal clusters; (c–d) single crystals.*
*Photographs by K. Polanski. Vega © Tescan.*

## 2. Secondary crystals formed from ZnO(g) vapours by CO-promoted transformation of ZnO(s) in the presence of Zn(g) (reductive environment)

Secondary zincite crystals form complex groups, commonly on relict primary zincites, and are usually much larger, commonly reaching 10–12 cm in length and 1 cm in diameter. Gigantic transparent crystals 10–15 cm in length, 5–6 cm in diameter and weighing up to 2 kg have been found and a cluster is shown in *Figure 6*. The larger secondary zincites show a strong tendency to grow along the [0001] direction, and possess a typical hexagonal prismatic habit with diverse pyramidal terminations (*Figure 7*). Complex pyramidal crystals showing pronounced hemimorphism with the {0001} face are commonly observed. Most of the larger secondary zincite crystals display dissolution or growth features on somewhat rounded surfaces and edges.

Figure 6: *Giant zincite crystal cluster weighing 3.5 kg from the collection of A. Ignaciak: (a) front view; (b) back view; (c) view from underneath. Photographs by M. Krystek.*

Most secondary zincite crystals are transparent and are usually intensely coloured in shades of red, orange, yellow, green or brown. Their colour intensity varies from pale to deep and saturated. Colour distribution in the larger crystals is rather uniform, gradual or sectoral colour changes being uncommon. Yellow tones are clearly detectable in green and red crystals. Small, thick prismatic near-colourless crystals of almost blue-white hue were also observed; their lack of coloration is intriguing, and these crystals may be primary in genesis, being formed slowly in an oxidizing atmosphere in which doping was inhibited. The laboratory preparation of large colourless single crystals of ultra-pure zinc oxide by controlled oxidizing of zinc vapour at elevated temperature was described by Bailar (1973).

### Fluorescence

Most of the crystals display fluorescence under ultraviolet illumination (Kammerling and Johnson, 1995), typically of a yellowish green to white (*Figure 8*). The darker orange crystals are mostly inert under short-wave (254 nm) and variably fluorescent under long-wave (365 nm) or LED UV illumination; paler crystals of all colours, especially those growing on the orange crystals are usually strongly fluorescent. The small complex primary spiky crystals with snowflake-like overgrowths fluoresce pale yellow in short-wave UV, with bright green patches in their base areas, and are brighter under LED UV, the 'snowflakes' and branches being brightest. Natural very pale yellowish prismatic zincite crystals formed from volcanic vapours in Kamchatka show a strong, very similar fluorescence (e.g. specimen 01-68 in R.S.W. Braithwaite collection).

### Inclusions

A number of crystals were examined microscopically for the presence of inclusions. Many appeared to be free from obvious inclusions, but others contained wispy dark bands, fissures, glossy spherules or dull oval-shaped bodies (*Figure 9*). These complement the three examples illustrated by Kammerling and Johnson (1995).
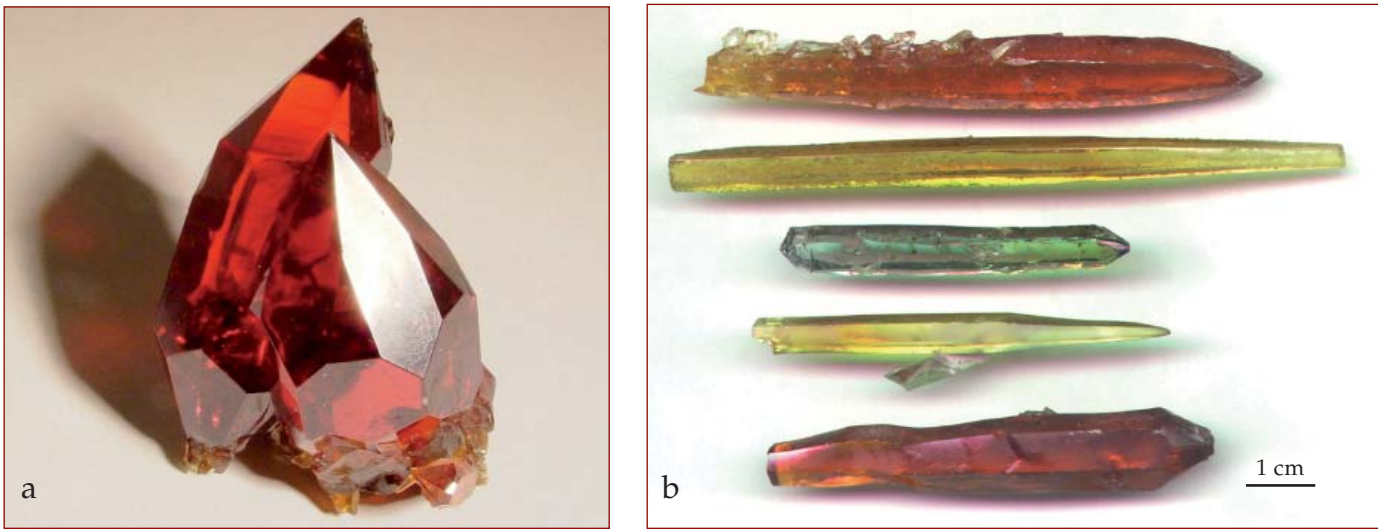
*Figure 7: Secondary zincite crystals: (a) two red 5 cm crystals from the collection of A. Miziolek, photograph by M. Krystek; (b) selection of long crystals from the collection of R.S.W. Braithwaite; photograph by R.S.W. Braithwaite.*

## Conclusions

Olawa's zinc-white production furnace has produced remarkable synthetic ZnO crystals, some in quantities and forms unlike any previously reported. We conclude that the formation of large ZnO crystals as a by-product has resulted from a defective porosity of a ceramic diaphragm in the furnace. In consequence, carbon dioxide from burning fuel gas penetrated cracks and oxidized zinc vapour to form small primary zincite crystals. These crystals underwent carbon monoxide-promoted, zinc vapour-assisted sublimation to form large secondary zincite crystals, some of gem quality.
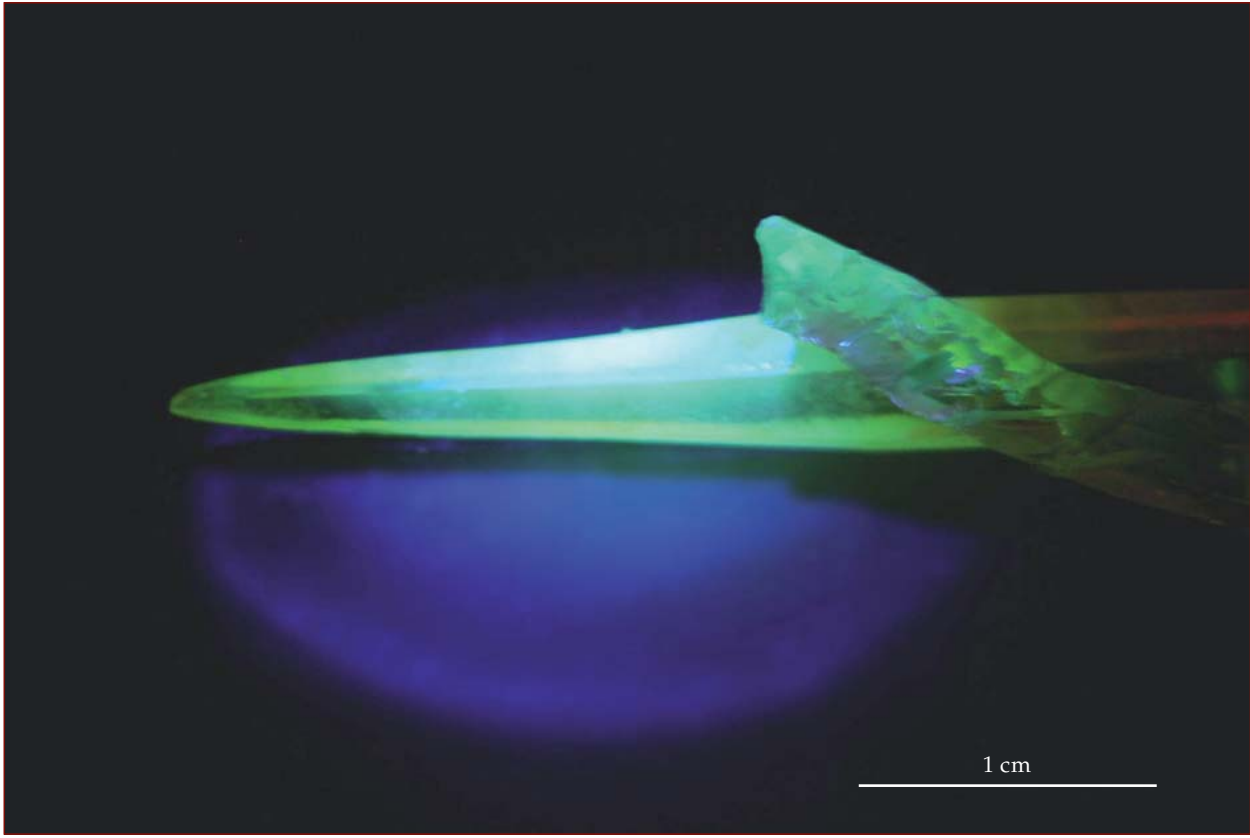


*Figure 8: Zincite crystal fluorescing under LED-UV illumination. Photograph by R.S.W. Braithwaite.*
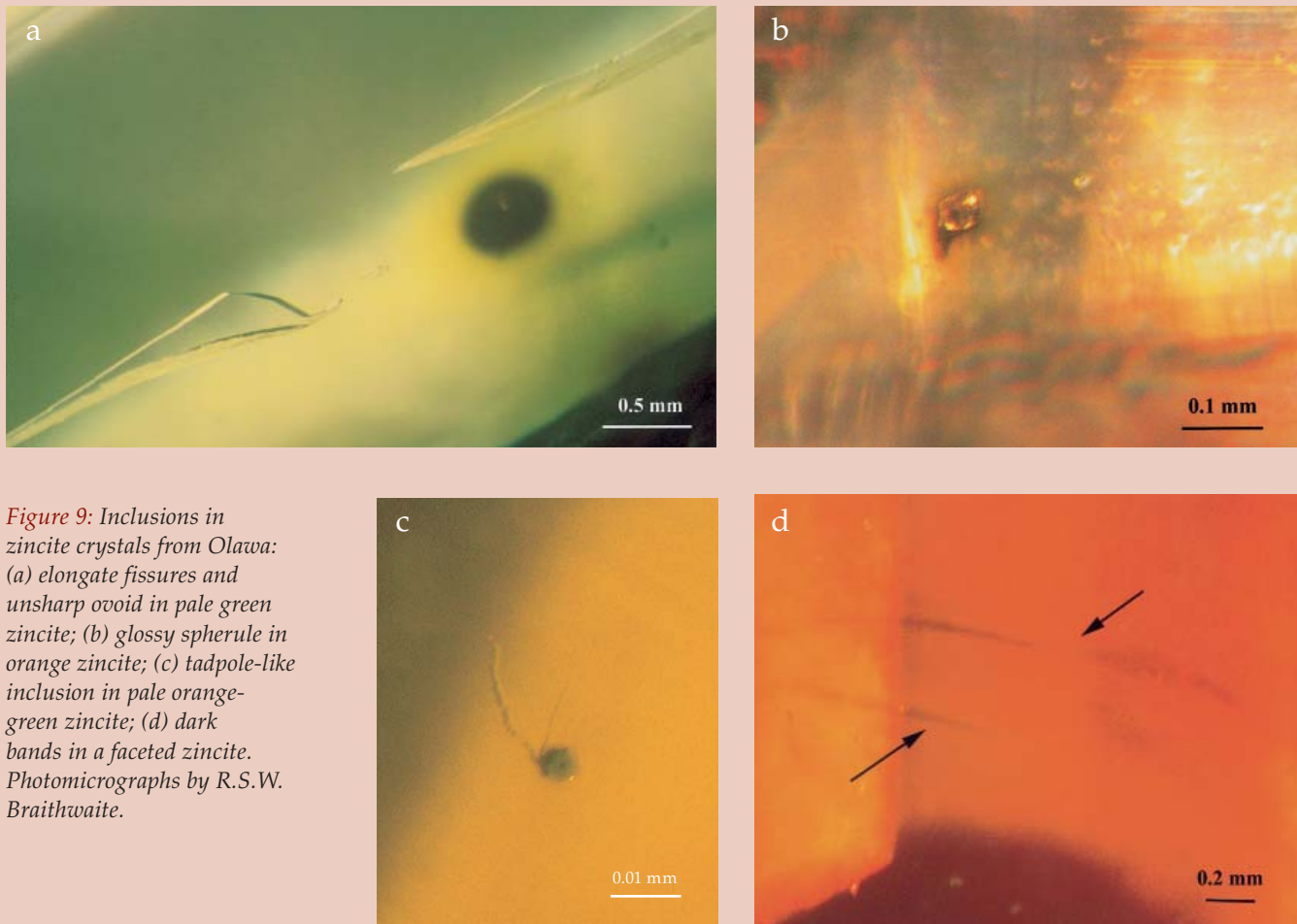
*Figure 9: Inclusions in zincite crystals from Olawa: (a) elongate fissures and unsharp ovoid in pale green zincite; (b) glossy spherule in orange zincite; (c) tadpole-like inclusion in pale orange-green zincite; (d) dark bands in a faceted zincite. Photomicrographs by R.S.W. Braithwaite.*

## Acknowledgements

## References

Bailar, J.C., 1973. *Comprehensive Inorganic Chemistry*, Vol. 3 (Ed. A.F. Trotman-Dickenson *et al.*). Pergamon Press Ltd., Oxford

Bancroft, P., 1984. *Franklin-Sterling Mines, Franklin, New Jersey*. In: *Gem and Crystal Treasures*, Western Enterprises and Mineralogical Record, Falbrook, California, U.S.A., 19-24

Bates, C., White, W.B., and Roy, R., 1966. The solubility of transition metal oxides in zinc oxide and the reflectance spectra of $Mn^{+2}$ and $Fe^{+3}$ in tetrahedral fields. *J. Inorg. Nucl. Chem.,* 28, 397-405

Crowningshield, R., 1985. Gem Trade Lab Notes: Synthetic zincites. *Gems & Gemology,* 21, 237-8

Erhart, P., Klein, A., and Albe, K., 2005. First-principles study of the structure and stability of oxygen defects in zinc oxide. *Physical Review B: Condensed Matter and Materials Physics*, 72(8), 085213/1-7

Fujitzu, S., Noritake, F., and Horiguchi, Y., 1993. Production of transparent zinc oxide. *Jpn. Kokai Tokkyo Koho* (Japanese patent) JP 0570286. *Chem. Abstr.,* 119, 238454b

Goldschmidt, V., 1913-1923. *Atlas der Krystallformen, Vol. 7.* Universitätsverlag Gmbh, Heidelberg

Greenwood, N.N., 1968. *Ionic crystals, lattice defects and nonstoichiometry*. Butterworths, London

Igielski, Z., Ostojski, K., Standio, J., and Przybyla, W., 1988. *Polish patent* P 140679 (19 Sept., 1983)

Isshiki, M., Wang, J., Mikami, M., and Sho, Y., 2005a. Heat treatment of zinc oxide crystals. *Jpn. Kokai Tokkyo Koho* (Japanese patent) 2005, 272283. *Chem. Abstr.*, 143, 357123y

Isshiki, M., Yoshitoyo, O., Mikami, M., and Tadashi, Y., 2005b. Growth of zinc oxide crystals. *Jpn. Kokai Tokkyo Koho* (Japanese patent) JP 2005, 272282. *Chem. Abstr.* 143, 357122x

Jamshidi, E., and Ale Ebrahim, H., 2005. Synthesis gas production by methane oxidation with zinc oxide. *Tahghigh dar Oloom va Mahandesi-i Naft*, 12(46), 46-51 (in Persian). *Chem. Abstr.*, 142, 8815r

Jasinski, R., Igielski, Z., Ostojski, K., Standio, J., and Wegrzynek, B., 1987. Method and apparatus for zinc oxide manufacture. *Polish patent* P 137089 (18 March, 1982)

Kammerling, R.C., and Johnson, M.L., 1995. An examination of "serendipitous" synthetic zincite. *Journal of Gemmology*, 24(8), 563-8

Kirk, R.E., and Othmer, D.F., 1970. *Encyclopedia of Chemical Technology*, *Vol. 22,* 2nd edn, Interscience Publishers, New York, 555-603

Kortunova, E.V., and Lyutin, V.I., 1995. Growth of zincite crystals. *Razvedka Okhrana Nedr.*, 3, 9-12 (in Russian). *Chem. Abstr.*, 123, 271133b

Kotera, Y., and Yonemura, M., 1992. The formation of color centres in zinc oxide. *Fontai oyobi Funmatsu Yakin*, 39(6), 515-518 (in Japanese). *Chem. Abstr.*, 117, 254286n

Kuz'mina, I.P., Nikitenko, V.A., Lazarevskaya, O.A., Komarova, E.E., Stoyukhin, S.G., and Tsur, O.V., 1991. Method of producing coloured zinc oxide single crystals. Russian patent SU 1673651. *Chem Abstr.*, 116, 117889b

Laudise, R.A., and Ballman, A.A., 1960. Hydrothermal synthesis of zinc oxide and zinc sulfide. *J. Phys. Chem.*, 64, 688-91

Lott, K., Shinkarenko, S., Kirsanova, T., Tuern, L., Grebennik, A., and Vishnjakov, A., 2005. Atomic absorption photometry of excess Zn in ZnO. *Physica Status Solidi C: Conferences and Critical Reviews*, 2(3), 1200-5

Mohanty, G.P., and Azaroff, L.V., 1961. Electron density distribution in ZnO crystals. *J. Chem. Phys.*, 35, 1268-70

Mycielski, A., Kowalczyk, L., Szadkowski, A., Chwalisz, B., Wysmolek, A., Stepniewski, R., Baranowski, J.M., Potemski, M., Witowski, A., Jakiela, R., Barcz, A., Witkowska, B., Kaliszek, W., Jedrzejczak, A., Suchocki, A., Lusakowska, E., and Kaminska, E., 2004. The chemical vapour transport growth of ZnO single crystals. *Journal of Alloys and Compounds*, 371(1-2), 150-2

Nause, J.E., Agarwae, G., and Hill, D.N., 1999. A new approach to growth of bulk ZnO crystals by melt solidification. *Ceram. Trans.*, 94 (Innovative processing and synthesis of ceramics, glasses and composites, 11), 483-91

Noritake, F., Yamamoto, N., Horiguchi, Y., Fujitsu, S.

Koumoto, K., and Yanagida, H., 1991a. Vapour-phase growth of transparent zinc-oxide ceramics with *c*-axis orientation. *J. Amer. Ceramic Soc.*, 74[1], 232-3

Noritake, F., Fujitsu, S., Kawamoto, K., Yanagida, H., and Yamamoto, N., 1991b. Production of transparent zinc oxide. *Jpn Kokai Tokkyo Koho,* Japanese patent JP 3279214. *Chem. Abstr.* 116, 154853f

Palache, C., 1935. *The minerals of Franklin and Sterling Hill, Sussex County, New Jersey*. U.S. Geological Survey Professional Paper 180. Washington, D.C. Reprinted 1960

Sinkankas, J., 1959. *Gemstones of North America.* D. Van Nostrand Company, Inc., New York

Suscavage, M., Harris, M., Bliss, D., Yip, P., Wang, S.-Q., Schwall,D., Bouthillette, L., Bailey, J., Callahan, M., Look, D.C., Reynolds, D.C., Jones, R.L., and Litton, C.W., 1999. High quality hydrothermal ZnO crystals. *MRS Internet J. Nitride Semicond. Res.*, 4S1, G3.40

Triboulet, R., N'Tep, J.M., Barbe, M., Mora-Sero, I., and Munez, V., 1991. Some fundamentals of the vapor and solution growth of ZnSe and ZnO. *J. Cryst. Growth*, 198/199, 968-74

Yu, W., Li, X., and Gao, X., 2005. Catalytic synthesis and structural characteristics of high-quality tetrapod-like ZnO nanocrystals by a modified vapor transport process. *Crystal Growth and Design*, 5[1], 151-5

# Colour zoning in heat-treated yellow to yellowish-orange Montana sapphires

Dr Karl Schmetzer[1] and Dr Dietmar Schwarz[2]

1. Taubenweg 16, D-85238 Petershausen, Germany
2. Gübelin Gem Lab, Lucerne, Switzerland

**Abstract:** *Heat-treated sapphires in the yellow to yellowish-orange colour range originating from Montana, U.S.A., were examined in order to determine if the growth patterns and colour zoning which are present after the heat treatment process are helpful for the distinction of this material from beryllium-diffusion-treated sapphires.*
*The investigations were performed in immersion on a diffused-light box at low magnification and with a horizontal immersion microscope at higher magnification.*

*The orange colour centres which are responsible for the intense yellow to yellowish-orange coloration of the samples are predominantly developed in intensely coloured basal growth sectors which are surrounded by rhombohedral and dipyramidal sectors with much lighter yellow coloration. This characteristic pattern of growth structures and colour zoning is useful for locality determinations as well as for a distinction from beryllium-diffusion-treated sapphires in the yellow to orange colour range.*

## Introduction

Untreated sapphires from the Rock Creek deposit in Montana, U.S.A., are light blue, bluish green, greenish blue, yellowish green, yellow or pink with low saturation. Due to this low colour saturation, only a small percentage of the untreated rough can be used for jewellery purposes. Consequently, the material is heat treated to develop more intense blue or yellow colours. A detailed description of heat treatment processes performed in reducing or oxidizing atmospheres was published by Emmett and Douthit (1993), who also discussed the causes of colour in heat-treated and untreated material.

Light yellow untreated or heat-treated Montana sapphires are coloured by minor amounts of iron. Upon heat treatment in an oxidizing atmosphere, an intense yellow coloration is developed in the central part of a certain percentage of the sapphire crystals, which is caused by magnesium-related colour centres. Consequently, a more intense yellow to yellowish-orange coloration is observed in such heat-treated sapphires. If the colour centres are developed by heat treatment in

the rarer chromium-bearing sapphires from Montana, a pinkish-orange to reddish-orange 'padparadscha' coloration is obtained. The colour zoning of both types of heat-treated Montana sapphires is readily visible in rough stones, but is more difficult to observe in faceted stones (see the examples given by Emmett and Douthit, 1993). A similar colour centre to that observed in Montana sapphires was described in heat-treated yellow, orange or reddish-orange sapphires from Sri Lanka by Schmetzer *et al.* (1983).

Since the appearance of large quantities of beryllium-diffusion-treated sapphires in the yellow to reddish-orange colour range at the end of 2001 (McClure *et al.*, 2002), the application of various microscopic criteria for a distinction of beryllium-diffusion-treated from simply heat-treated sapphires has been discussed by various authors, and a detailed summary is given by Emmett *et al.* (2003) and Schmetzer and Schwarz (2005). The high temperatures applied in 'normal' heat treatment and beryllium diffusion procedures mean that decomposed or even melted mineral inclusions can be caused by both processes with similar visible results. Thus, no single microscopic inclusion feature described so far can be used to determine whether a sapphire is diffusion-treated or simply heat-treated.

A direct beryllium determination as proof of beryllium diffusion treatment can be done by laser ablation-inductively coupled plasma-mass spectroscopy (LA-ICP-MS), secondary ion mass spectroscopy (SIMS) or laser-induced breakdown spectroscopy (LIBS). Although some of the major gemmological laboratories have established at least one of these techniques directly in their premises or have access to such analytical instruments, e.g. at university or other research laboratories, the situation in Bangkok (which may reflect the trade in general) was characterized by A. Peretti in June 2006 as follows:

"As we test beryllium-treated corundum by LIBS everyday in Bangkok, we have learned that smaller heated yellow sapphires goods are generally mixed with beryllium-treated yellow sapphires goods. The dealers (that I

have spoken to) have mostly given up on the 'beryllium-treated' versus 'non-beryllium-treated' small sapphire issue, because the costs of testing exceed the costs of the materials. Beryllium-treated corundums are most likely widespread, particularly in the smaller goods. Larger coloured sapphires, however, are more carefully handled (so far my opinion). Therefore, beryllium-treatment seems to establish itself in the smaller goods within the general term of 'heat-treatment'".

Consequently, a quick screening test for possible beryllium diffusion treatment, especially for larger lots of small sized samples, is still highly desirable and necessary.

Due to the development of colour centres by heat treatment only in specific growth sectors of sapphire crystals, the examination of growth patterns in combination with colour zoning was used for a distinction of untreated, heat-treated and beryllium-diffusion-treated sapphires from specific localities, especially for a recognition of simply heat-treated yellow or pinkish-orange to reddish-orange (padparadscha) sapphires from Sri Lanka (Schmetzer and Schwarz, 2005). Growth patterns in combination with colour zoning were also used for a characterization of heat-treated, chromium-bearing sapphires from Montana in the orange to pinkish-orange or reddish-orange colour range. Chromium-free, beryllium-diffusion-treated Montana sapphires with a homogeneous yellow, yellowish-orange or orange coloration were also studied, but no detailed investigation is available for chromium-free or almost chromium-free, heat-treated samples from Montana in the yellow to yellowish-orange colour range. Therefore, the present study was undertaken to determine whether the characteristic growth pattern and colour zoning found in chromium-bearing sapphires from Montana applies also for chromium-free samples; that is, to find out if a microscopic examination is also helpful for a recognition of this type of material and its distinction from homogeneously coloured beryllium-diffusion-treated samples in the same colour range.

Figure 1: *Faceted round Montana sapphires, diameters from 5.2 to 5.4 mm, weights from 0.60 to 0.80 ct.*



Figure 2: *Heavily waterworn sapphire crystals from Montana, sizes from about 3 to 5 mm, weights from 0.33 to 0.72 ct.*



Figure 3: *Slices of rough waterworn sapphire crystals from Montana, polished on both sides, diameters from about 5 to 6 mm, weights from 0.58 to 1.08 ct.*

*Most of these heat-treated samples shown in figures 1, 2 and 3 show a characteristic colour zoning with intensely coloured yellow, yellowish-orange or brownish-yellow zones surrounded by somewhat lighter yellow areas.*

# Materials and methods

Untreated lots of Montana sapphires from two major localities, i.e. from the Rock Creek and Missouri river deposits, were studied and reported on by Schmetzer and Schwarz (2005). The results of these examinations, especially the morphology and growth pattern of untreated material, will be cited shortly thereafter (for details of these occurrences, especially for information about history of the sapphire production and colour ranges of the sapphires, see Hughes (1997) and Kane (2003); the origin of the sapphire deposits was recently discussed by Berg and Dahy (2002)).

For the present study we examined three lots of heat-treated Montana samples:

a. 32 faceted round sapphires, diameters from 5.2 to 5.4 mm, weights in the range of 0.60 to 0.80 ct (*Figure 1*);

b. 40 rough heavily waterworn sapphire crystals, sizes from about 3 to 5 mm, weighing from 0.33 to 0.72 ct (*Figure 2*); and

c. 11 slices of rough waterworn sapphire crystals, polished on both sides, diameters from about 5 to 6 mm, weighing from 0.58 to 1.08 ct (*Figure 3*).

Lots (a) and (b) came from the stock of Fine Gems International, Helena, Montana; lot (c) was from the research and teaching collection of one of the authors (DS). All three lots have known treatment histories, and no beryllium diffusion was performed on any of the samples. Lots (a) and (b) consisted predominantly of Rock Creek sapphires, but some may come from the Missouri river deposit. Lot (c) was said to contain only Rock Creek samples.

A few of our samples have a very light yellow homogeneous body colour, but most show more intense yellow, orange or brownish-orange zones (*Figures 1* to *3*). These zones are easily visible in polished slices or in the rough material, but were more difficult to observe in some faceted stones.

The colour distribution in all samples was studied by immersing the stones in methylene iodide, simply placing them on a diffused-light box in a Petri dish. Although
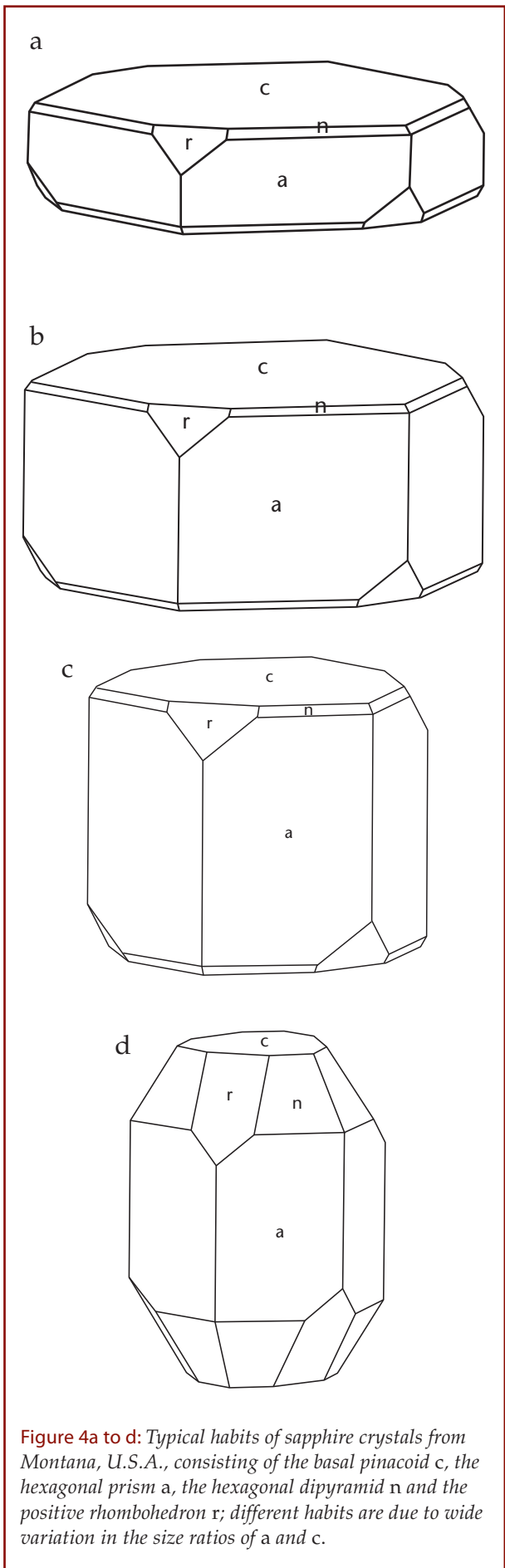
Figure 4a to d: *Typical habits of sapphire crystals from Montana, U.S.A., consisting of the basal pinacoid* c, *the hexagonal prism* a, *the hexagonal dipyramid* n *and the positive rhombohedron* r; *different habits are due to wide variation in the size ratios of* a *and* c.

the colour distribution within each stone can be seen with the unaided eye, examination with a loupe (10×) or with a microscope at low magnification (10× to 20×) provides better results. Exact determination of growth structures and colour zoning related to growth patterns was performed with a horizontal immersion microscope using a special sample holder with two rotation axes and specially designed eye-pieces.

Trace and minor element contents of 40 samples were obtained using EDXRF spectroscopy. The analyses were performed with a Tracor Northern Spectrace 5000 system, using a program specially developed for trace element geochemistry of corundum. Non-polarized absorption spectra of 20 samples were recorded using a Perkin-Elmer Lambda 19 spectrophotometer.

# Results

## *Morphology and growth patterns of untreated Montana sapphires*

The habits of Montana sapphires from both the Rock Creek and Missouri river deposits, are predominantly formed by the hexagonal prism *a* {$11\bar{2}0$} and the basal pinacoid *c* {0001}, with subordinate rhombohedral *r* {$10\bar{1}1$} and dipyramidal *n* {$22\bar{4}3$} faces. Due to large variations in the relative size of the hexagonal prism *a* compared to the basal pinacoid *c*, there is a large habit variation between tabular, thick tabular, equidimensional and prismatic (*Figure 4*).

In the immersion microscope, growth patterns consisting of the four crystal forms mentioned above are visible. In a view perpendicular to the *c*-axis, there is either a pattern consisting of the basal pinacoid *c* in combination with the hexagonal dipyramid *n* and the prism *a* (*Figure 5a*) or a pattern consisting of the basal pinacoid *c* in combination with the rhombohedron *r* (*Figure 5b*). The two characteristic views are related to each other by a rotation of 30° about the *c*-axis (for further details refer to Schmetzer and Schwarz (2005)).

Figure 5a,b: *Growth pattern and colour zoning in an untreated greenish-blue sapphire from Montana, U.S.A. a) View perpendicular to the c-axis, the basal pinacoid* c, *two hexagonal prism faces* a *and two hexagonal dipyramids* n *are visible. b) View perpendicular to the* c-axis, *the basal pinacoid* c *and the positive rhombohedron* r *are visible; Figures a) and b) are related by a rotation of 30° about the* c-axis.
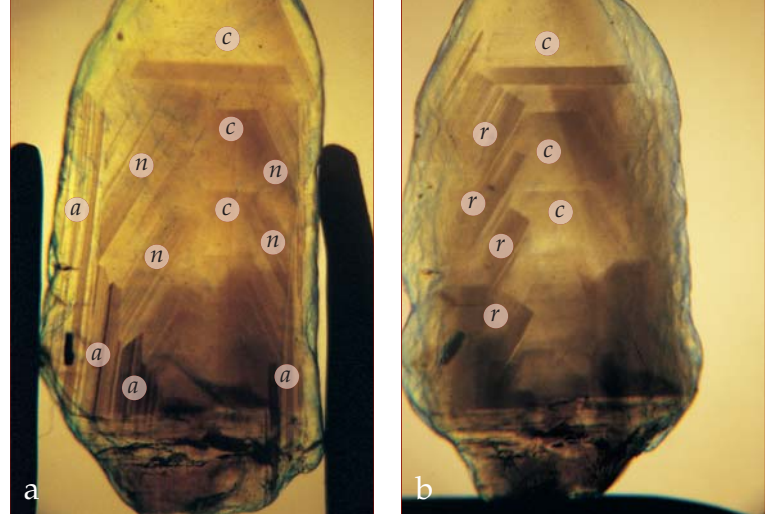


## Chemical and spectroscopic properties and causes of colour

X-ray fluorescence analysis showed a large variation of iron contents between 0.19 and 0.94 wt.% $Fe_2O_3$. Although the chromium contents of 22 sapphires were below the detection limit of the analytical method (0.005 wt.% $Cr_2O_3$), 18 contained minor amounts of chromium (between 0.005 and 0.013 wt.% $Cr_2O_3$). The chromium versus iron distribution of the 40 analysed

research samples is plotted in *Figure 6* and compared with chromium and iron contents in padparadscha-type heat-treated Montana sapphires studied previously (Schmetzer and Schwarz, 2005).

The spectroscopic properties of our sapphires (*Figure 7*) are consistent with the chemical data. All spectra showed the dominant iron-related absorption bands at 450, 388 and 376 nm. In a few samples with a homogeneous light yellow coloration, no additional absorption bands were observed.
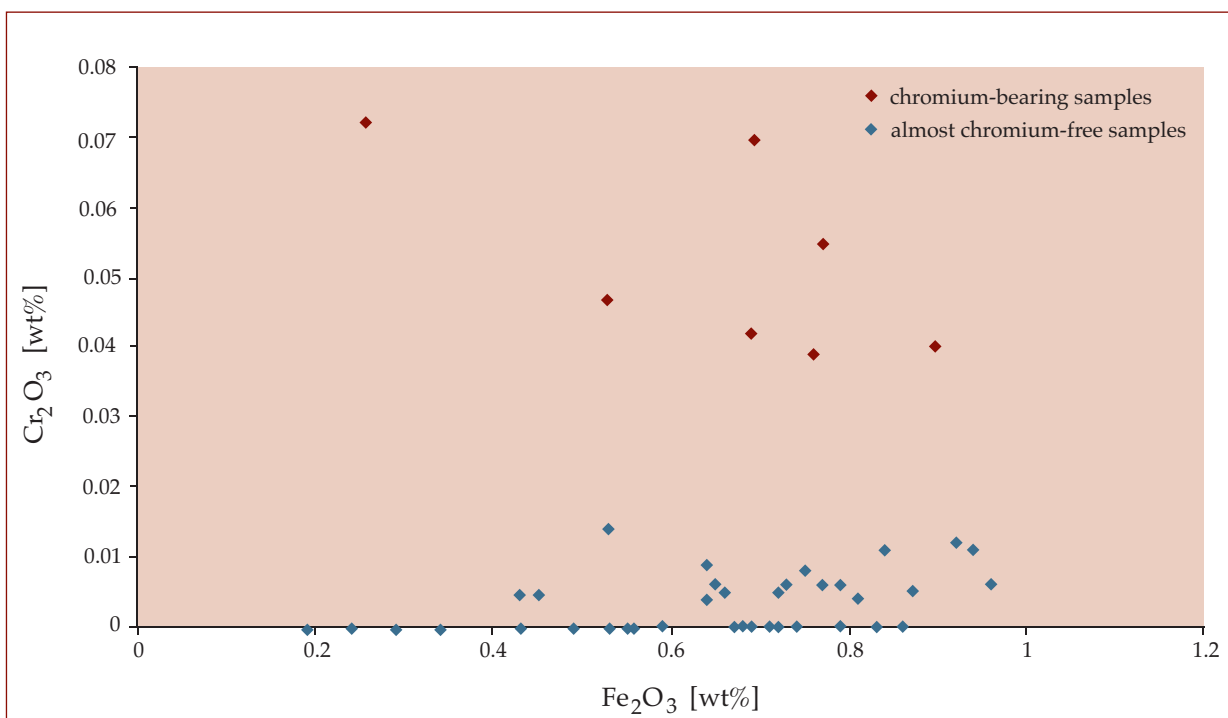


Figure 6: *Graphic representation of iron and chromium contents as determined for 40 heat-treated yellow to yellowish-orange sapphires from Montana, U.S.A., by energy-dispersive X-ray fluorescence spectroscopy (EDXRF); iron contents vary widely between 0.19 and 0.94 wt.% $Fe_2O_3$, chromium contents of the sapphires are very low (18 samples) or below the detection limit of the instrument (22 samples, <0.005 wt.% $Cr_2O_3$; because of identical iron values, the points of three samples overlap). The iron and chromium contents of seven chromium-bearing orange to reddish-orange heat-treated Montana sapphires (Schmetzer and Schwarz, 2005) are given for comparison.*
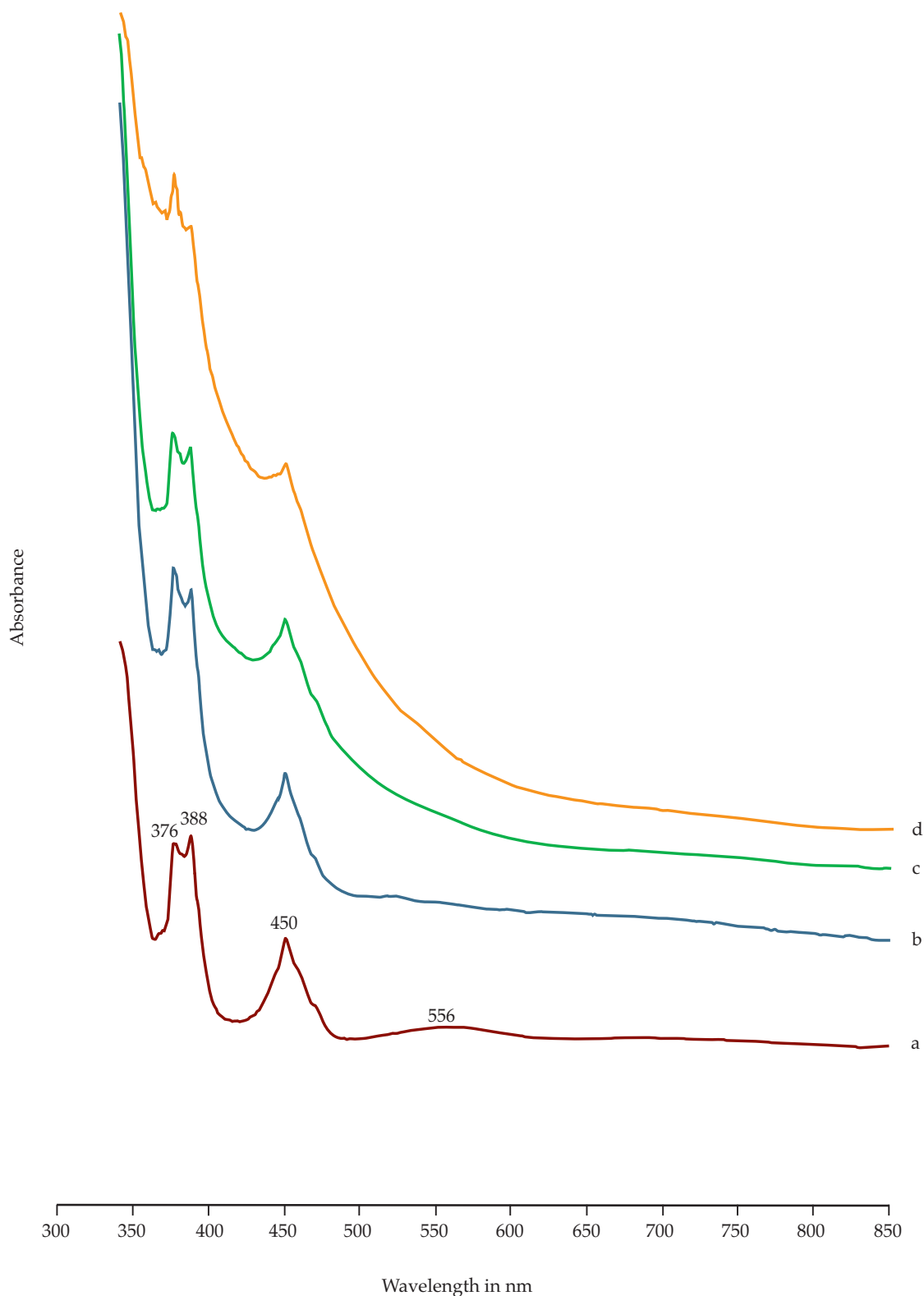
Figure 7: *Absorption spectra of heat-treated sapphires from Montana, U.S.A. in the yellow, yellowish-orange or brownish-yellow colour range; all samples show the characteristic absorption spectrum of iron-bearing sapphires with dominant absorption maxima at 450, 388 and 376 nm. In sample (a) with homogeneous yellow body colour, a small absorption band of chromium at about 556 nm is also visible (chromium contents of this sample 0.005 wt.% $Cr_2O_3$), but no orange colour centres were developed by heat treatment. Spectra (b) to (d) indicate that increasing numbers of orange colour centres were developed by the heat treatment process, which are macroscopically seen as intensely coloured yellow, yellowish-orange or yellowish brown growth sectors within the surrounding lighter yellow areas. Thus, in (b) to (d), the iron-related absorption spectrum is superimposed on that of the orange colour centres; spectra (b) to (d) are vertically displaced for clarity.*

Figure 8 (a) to (f): *In heat-treated Montana sapphires, orange colour centres are developed predominantly in central areas which are related to basal growth sectors; in a view approximately parallel to the c-axis of each sample, central darker areas are visible, mostly with a distinct fine structure. In the surrounding lighter yellow areas, small zones with residual blue colour zoning are present in some stones, an original colour not completely removed by the heat treatment process. Immersion, sizes of samples about 4 to 5 mm.*

All samples that showed – in addition to the light yellow homogeneous body colour – at least one more or less intense orange to brownish-orange growth sector, also showed a continuously increasing absorption from the visible to the ultraviolet region, which is superimposed on the iron absorption bands. This absorption is related to thermally stable orange colour centres which are developed by heat treatment. Due to the high intensity of the iron-related absorption band at 450 nm, an additional absorption of this orange colour centre which was expected at about 470 nm was not seen. No chromium absorption bands were observed in most of our spectra compared to the spectra pictured by Schmetzer and Schwarz (2005) for Montana sapphires with higher chromium contents (in the range of 0.040 to 0.073 wt.% $Cr_2O_3$). Only a few of our yellow sapphires showed a weak chromium absorption band at 556 nm; such samples have chromium contents near 0.01 wt.% $Cr_2O_3$.

Consequently, the colour of light yellow sapphires which do not have any intensely coloured yellow to orange growth sectors is solely due to their iron content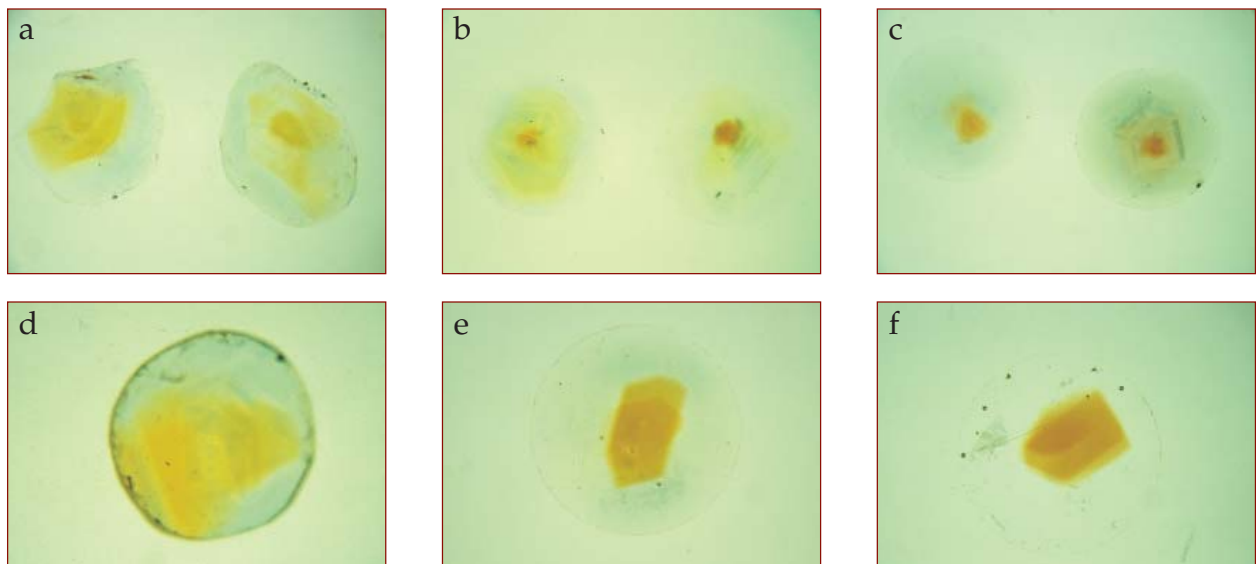s. If orange colour centres were developed by heat treatment, the absorption related to these colour centres would be superimposed on the iron-related absorption spectrum and affect the resulting colour. These data and interpretations are consistent with the results given in the paper of Emmett and Douthit (1993) and with the recent papers of Emmett *et al.* (2003) and Schmetzer and Schwarz (2004, 2005).

### Growth pattern and colour zoning

Even in random orientation, most of the rough or faceted sapphires in this study, in immersion show the presence of intense yellow, orange, or brownish-orange zones when immersed in liquid. In many samples, we observed a dark central core surrounded by lighter yellow parts of the sapphire crystals (*Figures 8* and *9*). In addition to distinct fine structures, which are present in most of the intense yellow to orange or brownish-orange cores, the darker areas may also be composed of several distinguishable parts. In the central zone or in these central darker growth sectors, the orange colour centres are developed by the heat treatment process, whereas in the surrounding areas, only a light yellow iron-related coloration is visible. In the rims of some heat-treated sapphires, the original blue or greyish-blue
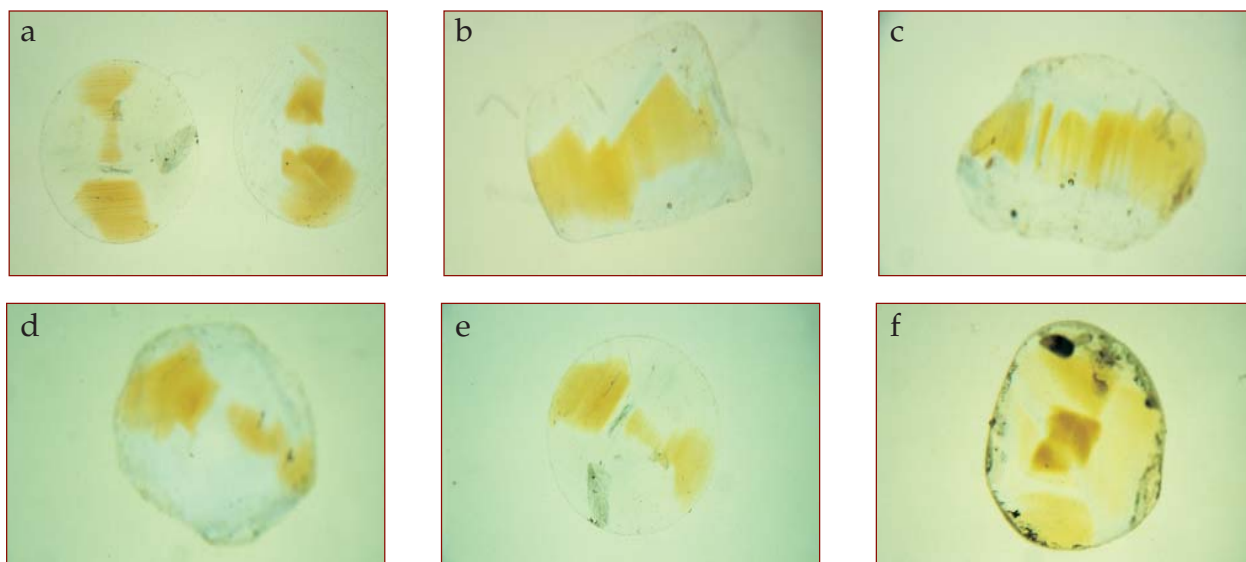
Figure 9 (a) to (f): *In heat-treated Montana sapphires, orange colour centres are developed predominantly in central areas which are related to basal growth sectors; in a view approximately perpendicular to the* c*-axis of each sample, elongated darker areas are visible in the centres of the stones, mostly with a distinct fine structure due to varying diameters of the darker basal growth sectors along the* c*-axis. Immersion, sizes of samples about 4 to 6 mm.*

coloration was not completely removed by the heat treatment process and a residual blue remains.

With different orientations of the rough and faceted sapphires, the outlines of the core or the darker central zones change. If the samples are examined in a direction approximately parallel to the *c*-axis of the sapphire crystal, a dark, more or less compact central core may be observed in most stones (*Figure 8*). In an orientation approximately perpendicular to the *c*-axis, a more or less elongated darker central part (*Figure 9*) is visible. The diameters of these darker centres are very variable along the *c*-axis and in some stones, the darker core is discontinuous consisting of several parts separated by lighter yellow growth zones.

With a more exact orientation of the sapphires in the immersion microscope, the measurements indicate that the growth structures and colour zoning are closely comparable to the growth pattern of untreated samples (see *Figures 5 a,b*). In heat-treated sapphires, the darker cores, in which the orange colour centres were developed by the heat treatment process, consist of basal growth sectors with diameters that change along the *c*-axis. These darker basal growth zones show sharp boundaries to

rhombohedral *r* and dipyramidal *n* growth sectors (*Figure 10*). Growth striations (i.e. growth planes) are also visible within the outer (lighter yellow) *r*, *n* and *a* growth sectors, but these growth striations are not combined with an intense colour zoning. This pattern of growth and colour zoning, i.e. the intensely coloured basal growth sectors confined either by lighter yellow dipyramidal *n* growth sectors (*Figure 11*) or by lighter yellow rhombohedral *r* growth sectors (*Figure 12*), is typical for the locality, and also indicates that heat treatment only, in the absence of beryllium, was performed.

## Discussion

The results of the present study represent another example for the applicability of growth patterns and colour zoning as a focal point of a microscopy-based screening system to distinguish heat-treated and beryllium-diffusion-treated sapphires in the yellow to reddish-orange colour range. We can summarize, that heat-treated yellow, yellowish-orange or orange (chromium-free to almost chromium-free) Montana sapphires show characteristic growth patterns consisting of basal, rhombohedral, dipyramidal and prismatic growth zones.
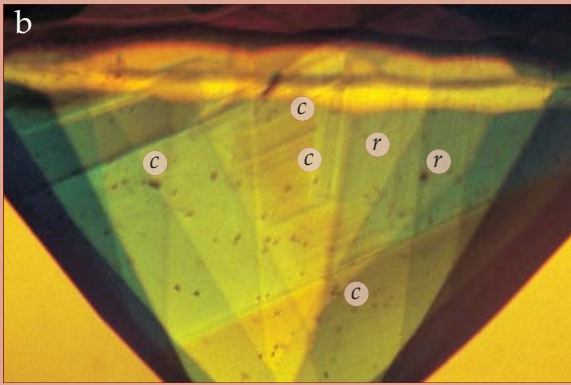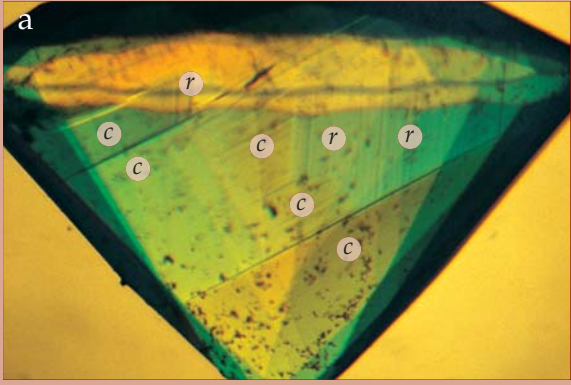
Figure 10 (a) to (c): *In heat-treated Montana sapphires, intensely coloured basal c growth sectors are surrounded by lighter yellow rhombohedral r and lighter yellow dipyramidal n growth sectors; (a) gives an overview of the sample (40×), (b) is the sample in an identical orientation (60×), and (c) is the same sapphire rotated about the c-axis through an angle of 30° (60×); all photos in immersion.*
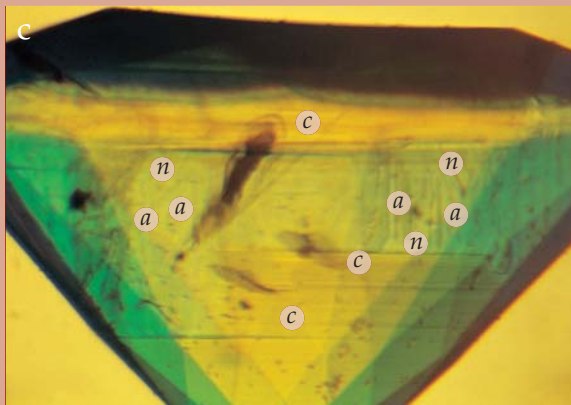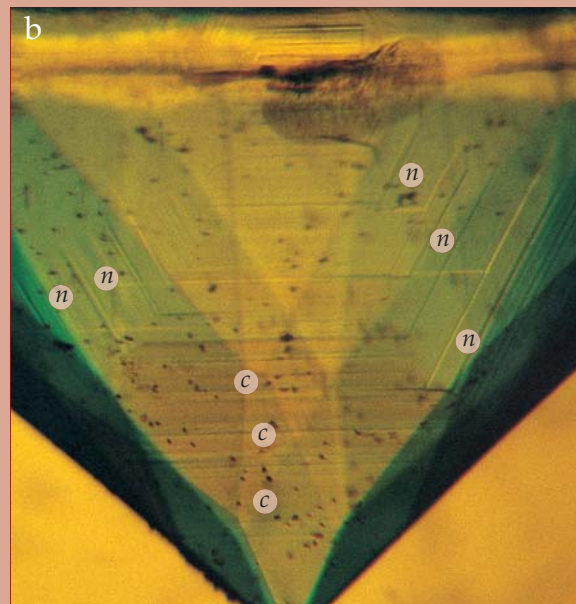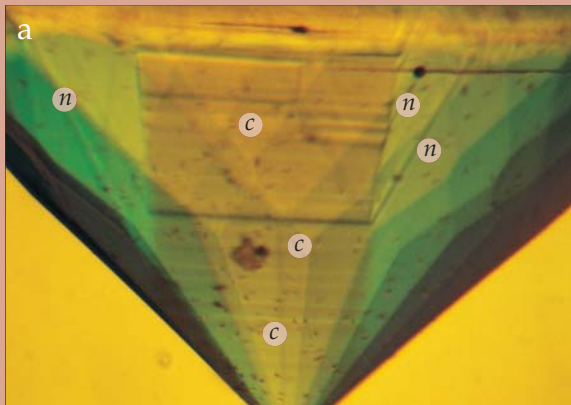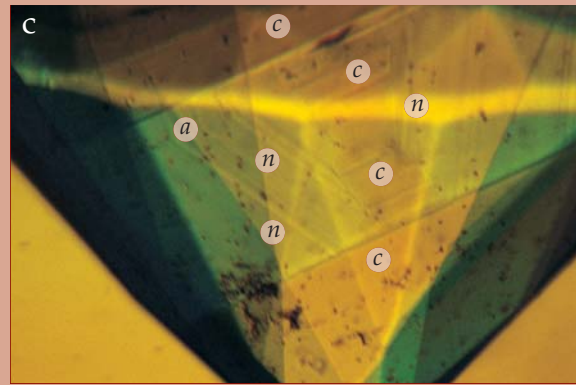
Figure 11 (a) to (c): *Heat-treated Montana sapphires with darker basal c growth sectors confined by lighter yellow dipyramidal n growth sectors; occasionally light yellow prismatic a growth zones are also visible; (a) 50×, (b) 50×, (c) 60×, all photos in immersion.*
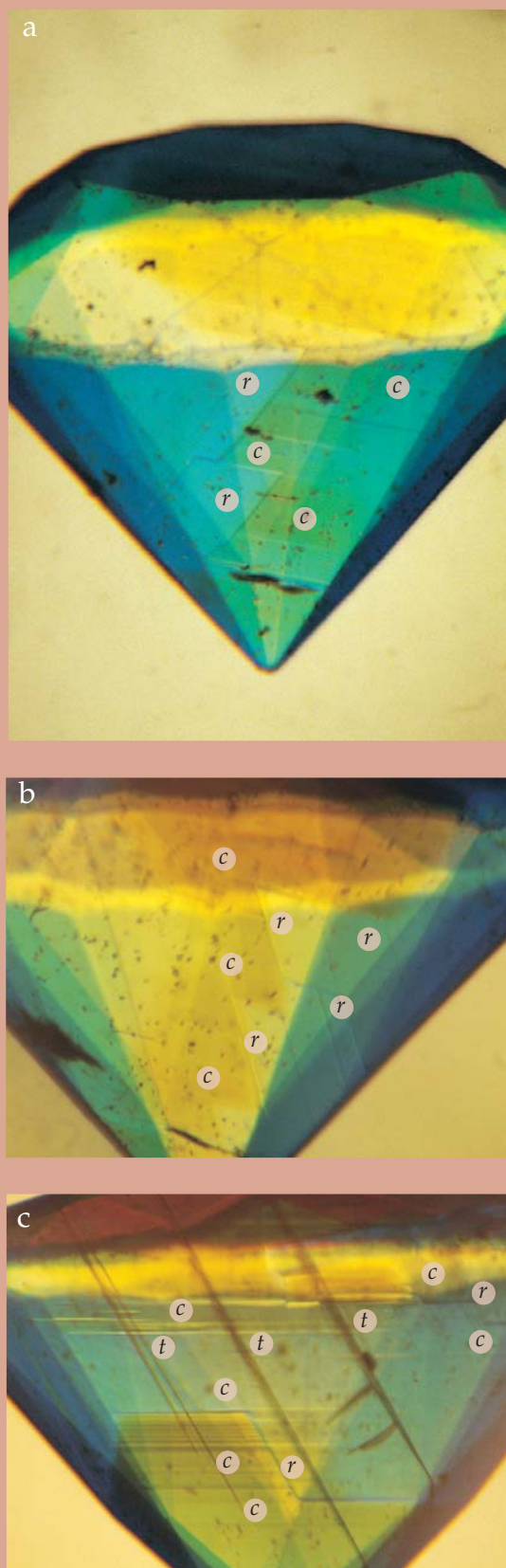
Figure 12 (a) to (c): *Heat-treated Montana sapphires with darker basal* c *growth sectors confined by lighter yellow rhombohedral* r *growth sectors; occasionally twin planes* t *parallel to the rhombohedral faces are also visible; (a) 30×, (b) 60×, (c) 50×, all photos in immersion.*

These internal growth patterns are consistent with the morphology of the untreated rough sapphire crystals. It is evident that the characteristic features described may be observed also in relatively small samples (between 0.3 and 1.1 ct) and, thus, the applicability of the method for the distinction of lots of smaller yellow to yellowish-orange sapphires is clearly demonstrated.

Darker growth zones, in which the orange colour centres are developed by heat treatment, are related to basal growth sectors with sharp boundaries to lighter yellow rhombohedral or dipyramidal growth zones. This is a characteristic pattern of growth zoning combined with an extreme colour zoning, which is typical for the locality. A similar pattern was found in heat-treated chromium-bearing Montana sapphires with a padparadscha-like reddish-orange or pinkish-orange colour. In these sapphires, orange colour centres are also developed in basal growth sectors only, but these samples contain elevated amounts of chromium (Schmetzer and Schwarz, 2005).

In beryllium-diffusion-treated Montana sapphires, in contrast, a homogeneous yellow to yellowish-orange coloration is developed throughout the entire stone (Schmetzer and Schwarz, 2005). Consequently, the observation of the characteristic growth patterns and colour zoning described in this paper are extremely useful for locality determinations and are conclusive for the separation of heat-treated and diffusion-treated sapphires.

## Acknowledgements

Colour zoning in heat-treated yellow to yellowish-orange Montana sapphires

# References

Berg, R.B., and Dahy, J.P., 2002. Montana sapphires and speculation on their origin. In: Scott, P.W., and Bristow, C.M. (eds) *Industrial Minerals and Extractive Industry Geology*. The Geological Society of London, 199-204

Emmett, J.L., and Douthit, T.R.,1993. Heat treating the sapphires of Rock Creek, Montana. *Gems & Gemology*, 29 (4), 250-72

Emmett, J.L., Scarratt, K., McClure, S.F., Moses, T., Douthit, T.R., Hughes, R., Novak, S., Shigley, J.E., Wang, W., Bordelon, O., and Kane, R.E., 2003. Beryllium diffusion of ruby and sapphire. *Gems & Gemology*, 39 (2), 84-135

Hughes, R.W., 1997. *Ruby and Sapphire.* RWH Publishing, Boulder, CO, U.S.A.

Kane, R.E., 2003. The sapphires of Montana. *Gem Market News*, 22, Issue 1, Part 1, 1, 4-10

McClure, S., Moses, T., Wang, W., Hall, M., and Koivula, J.I., 2002. A new corundum treatment from Thailand. *Gems & Gemology*, 38 (1), 86-90

Peretti, A., 2006. To whom it may concern. gem-a@mailtalk.ac.uk; June 24, 2006.

Schmetzer, K., Bosshart, G., and Hänni, H.A., 1983. Naturally-coloured and treated yellow and orange-brown sapphires. *Journal of Gemmology*, 18 (7), 607-22

Schmetzer, K., and Schwarz, D., 2004. The causes of colour in untreated, heat treated and diffusion treated orange and pinkish-orange sapphires – a review. *Journal of Gemmology*, 29 (3), 149-82

Schmetzer, K., and Schwarz, D., 2005. A microscopy-based screening system to identify natural and treated sapphires in the yellow to reddish-orange colour range. *Journal of Gemmology*, 29 (7/8), 407-49

# Cape Breton ruby, a new Canadian gemstone discovery, Cape Breton Island, Nova Scotia

David J. Mossman[1], James D. Duivenvoorden[2] and Fenton M. Isenor[3]

1. Department of Geography, Mount Allison University, 144 Main Street, Sackville, New Brunswick E4L 1A7, Canada

2. 627 Saint Terese Sud, Robertville, New Brunswick E4K 2W3, Canada

3. Department of Mathematics, Physics and Geology, Cape Breton University, P.O. Box 5300, Sydney, Nova Scotia B1P 6L2, Canada

**Abstract:** *Ruby was discovered near Frenchvale, Cape Breton, Nova Scotia, in mid-August 2004, in a geological context closely resembling that in the Hunza Valley, Kashmir. Although only relatively low grade stones from this newest Canadian gemstone locality have been recovered so far, the terrain holds promise of quality ruby. The potential for future discoveries in Atlantic Canada are excellent*

## Introduction

The Frenchvale area in the Boisdale Hills, southeastern Cape Breton Island, contributed carbonate flux to the steel mills of Sydney, Nova Scotia, over several decades. Here, as elsewhere in the extensive Precambrian terrain of Cape Breton, exploration has long been carried out sporadically for metalliferous deposits of lead, zinc and copper, and more recently for precious metals. Then in mid-August 2004, during the course of a mineral exploration programme, ruby corundum was serendipitously discovered in the environs of a disused quarry at Frenchvale, Cape Breton county.

The village of Frenchvale is located about 18 km west southwest of Sydney (*Figure 1*).

The Frenchvale quarry is a boomerang-shaped excavation 0.63 km long east-west, and 0.33 km north-south, located about 0.7 km northwest of the village (*Figure 2*). Readily accessed by a network of secondary roads in the area, the quarry is situated in the midst of the Boisdale Hills, a beautiful, gently rolling terrain intersected by streams and dotted with lakes.

## History

During the 1960s Mosher Limestone Ltd., through its affiliate Scotia Limestone Ltd., supplied 'purifying stone', namely limestone and dolomite, the main natural fluxes in

steel making, to the Sydney Steel works. Iron ore feedstock, not available locally, arrived in Sydney by ship from mines in Newfoundland and Labrador.

## Geology

Sir William Dawson made first mention of geological associations in the area in his classic *Acadian Geology* (1855, p. 322) and Weeks (1954) provides an overview of the results of early geological studies.

The results of subsequent work (Barr and Setter, 1986; Hill, 1987, 1989; Barr and Raeside, 1989; Raeside, 1989; Raeside and Barr, 1990) on the Precambrian geology of Cape Breton has led to the reallocation to other units, of some rocks previously assigned to the George River Group (Raeside, 1989), considered the oldest rocks in the region. For example, the migmatite within a gneiss complex at Lime Hill on North Mountain, southwestern



Figure 1: *Sketch map shows the extent of Precambrian metasedimentary rocks on Cape Breton Island; main occurrences of George River Group rocks (BH - Boisdale Hills, NM - North Mountain, CH - Creignish Hills, WM - Whycocomagh Mountain) are restricted to the Bras d' Or tectonostratigraphic terrane (modified from Raeside, 1989).*

Cape Breton, contains "... minor spinel- and corundum-bearing neosomes..." (Raeside, 1989). This earliest discovery of corundum on the island is in a unit within the Bras d'Or terrane viewed by Raeside and Barr (1990) as distinct from the George River Group *(Figure 1).* For the purpose of this report, however, the term is retained in order to highlight areas of particular interest in the exploration for Cape Breton rubies. The focus here is on a small window of the George River Group, centred in the Boisdale Hills, a locality which Milligan (1970) considered as the type. This report is based on over four months geological mapping and sampling, and a follow-up drilling programme as part of an on-going mineral exploration programme within a 4000 Ha claim block in the Boisdale Hills held by Mount Cameron Minerals Inc. (MCMI). Mineral collecting is prohibited in this claim block without the permission of MCMI.

Although no type section has been formally proposed for the George River Group, the term has been loosely applied to many interbedded carbonate and clastic and minor volcanic rocks of variable metamorphic grade on Cape Breton Island. As noted above, the informal type locality is the Boisdale Hills, where a Late Precambrian sequence of schists, gneisses and siliceous dolomitic marbles has been regionally metamorphosed to upper amphibolite facies. These rocks are intruded by predominantly late stage shallow level hybrid igneous dykes and sills ranging from granite through hornblende diorite to diabase. Ratio of metasediments to intrusives is estimated at 3 : 1.

Results of radiometric age determinations reported by White *et al.* (1994) identify the intrusive igneous rocks from the northern Boisdale Hills as late Cambrian to early Ordovician. In the environs of Frenchvale quarry, upper amphibolite grade metamorphism is represented by the presence of two-mica schist, garnetiferous (grossular-andradite, so-called 'grandite')-sillimanite-andalusite gneiss, and in metacarbonates in the quarry itself, by the presence of corundum and a suite of calc-silicate minerals. Both fault-bounded and intrusive contacts with
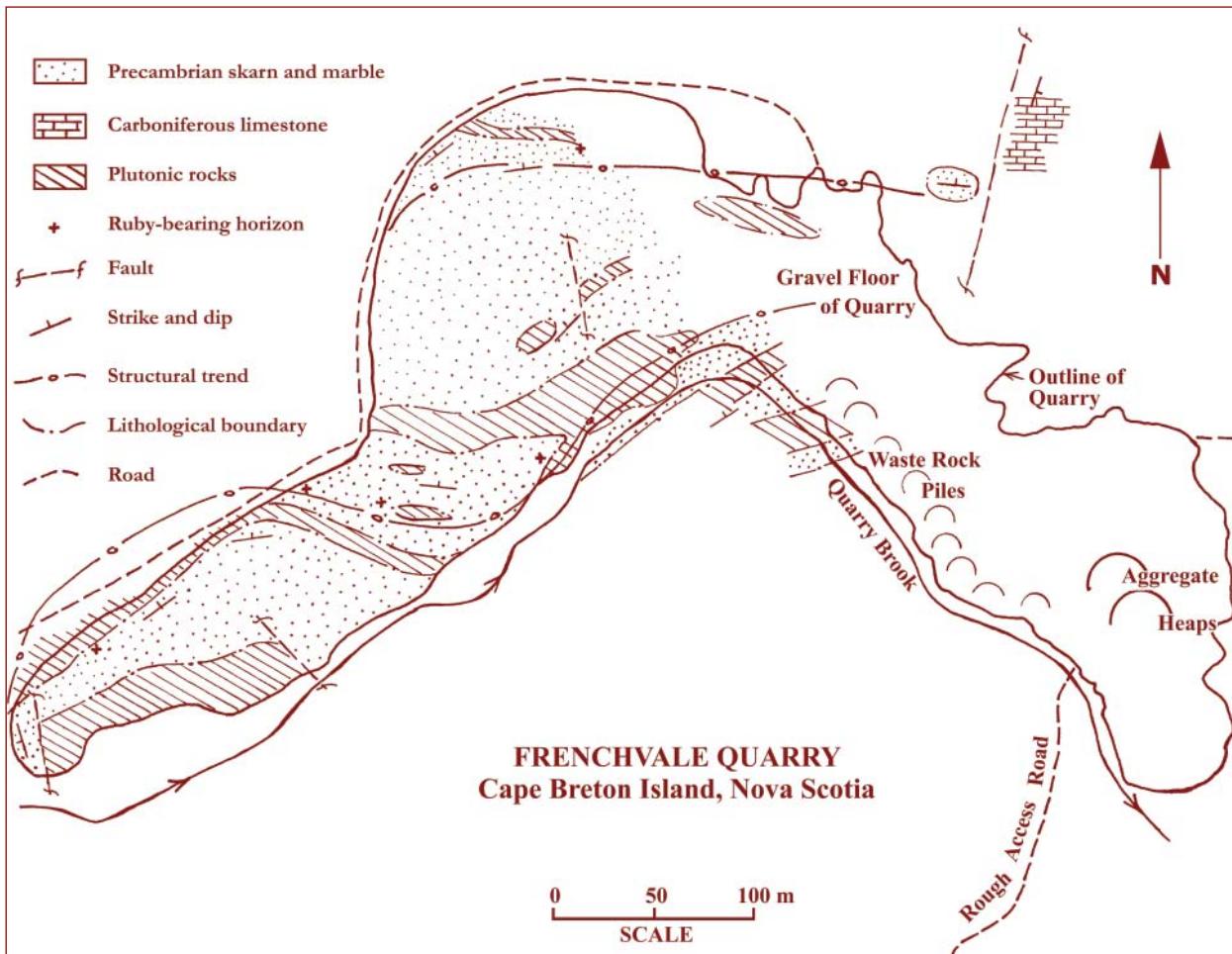
Figure 2: *Geological sketch map of Frenchvale quarry, situated 0.7 km northwest of the village of Frenchvale, and approximately 18.7 km west southwest of Sydney, Cape Breton Island, Nova Scotia.*



Figure 3: *Discovery specimen (untrimmed) of prismatic (1.2 cm diameter) ruby in skarn from the northeast wall of Frenchvale quarry. Photograph by D. Mossman.*

country rock metasediments are encountered in the area. The largest fault occurs near the east end of the quarry and separates Carboniferous limestones from the more ancient skarns of the quarry *(Figure 2)*.

Lower grade (in part retrograde) metamorphism is evident in chloritization, development of talc, widespread silicification and serpentinization, and the presence of exsolved aluminium hydroxides in corundum (Schmetzer, 1987). Overall the metasediments have been made over into skarn, or more specifically 'skarnoid rocks', a term describing relatively fine-grained, iron-poor, calc-silicate rocks which reflect the compositional control of the original sediment (Einaudi *et al.*, 1981). Skarns and skarnoid

Table I: *Minerals from the George River Group, Frenchvale and environs, Cape Breton Island (this study; Chatterjee, 1977; Hill, 1989)*

| | |
|---|---|
| Andalusite | Orthoclase |
| Antigorite | Pargasite |
| Apatite | Phlogopite |
| Biotite | Plagioclase (peristerite and anorthite)` |
| Calcite | Prehnite |
| Chalcopyrite | Pyrite |
| Chlorite | Pyrrhotite |
| Cordierite | Quartz |
| Corundum | Scapolite |
| Diopside | Serpentine |
| Dolomite | Sillimanite |
| Epidote | Sphalerite |
| Forsterite | Sphene |
| Garnet ('grandite') | Spinel |
| Goethite | Talc |
| Graphite | Titanite (sphene) |
| Hematite | Tremolite-actinolite |
| Magnetite | Vesuvianite |
| Marcasite | Wollastonite |
| Monticellite | Zoisite |
| Muscovite (including var. fuchsite) | |

rocks develop in response to either localized contact metamorphism adjacent to an igneous intrusion, or regional metamorphism whereby mineral changes in the rocks occur over an extensive area. The latter hypothesis is believed to apply to the ruby occurrences at Frenchvale (*Figure 3*). Unlike classic skarns, however, the Frenchvale metacarbonates are not dominated by garnet and pyroxene.

## Mineralogy

Many minerals, including some relatively exotic species, have been identified (Chatterjee, 1977; Hill, 1989) in the George River Group metasediments (*Table I*). Dolomite and to a much lesser extent, calcite, are of course major components of the purest marbles; fine-grained, disseminated flake graphite is virtually ubiquitous. Calc-silicate minerals, for the most part coarse-grained, are widely developed especially in what were originally impure limestones/marbles but which have undergone a measure of silicification. In these, a relict banding and sporadic stylolitization suggest the original stratification, and wollastonite, scapolite and vesuvianite are common.

Metamorphic mineral assemblages are characteristic of upper amphibolite grade facies (Chatterjee, 1977). Forsterite (usually heavily serpentinized), diopside, and tremolite are widespread in the metacarbonates. Spinel has likewise been reported (Chatterjee, in Milligan, 1970) though not seen by the writers. In gneiss, sillimanite and andalusite can accompany phlogopite and/or biotite, muscovite and plagioclase, attesting to a former high temperature, low pressure

regime. Various minerals, including sulphides, quartz, calcite, talc, serpentine, scheelite and tourmaline (schorl) are common in the vicinity of shear zones which provided the channels for a relatively late stage non-focused flow of mineralizing fluids.

Retrograde metamorphic minerals are locally conspicuous, a good illustration being green chromian-muscovite (fuchsite), which commonly envelopes corundum crystals. As a result of weathering, goethite, magnesite, and kaolin are locally abundant. Among sulphides, pyrrhotite, pyrite and marcasite are of widespread occurrence, with chalcopyrite least evident.

## Cape Breton ruby

Here, we follow Hughes' (1997, p. 401) carefully considered recommendation that "... all corundums of a red colour, regardless of its depth or intensity should be termed rubies, just as was done prior to the 20th century." Cape Breton ruby was first recognized in mid-August 2004 as pea-sized crystals more or less enveloped by fuchsite along the northeastern rim of the Frenchvale quarry. Outcrops of ruby-bearing rock were subsequently identified at several other locations in the quarry and environs.

Corundum at Frenchvale ranges from white to dark grey, but rose, purple, red-violet and various shades of lavender are the most



Figure 4: *A Cape Breton ruby (~ 1 ct) cut by Hans Durstling and set in a gold ring by Donald Baird. Photograph by D. Mossman.*

prevalent (*Figures 4* and *5*). More than one colour can occur at any given locality; several very small blue crystalline portions within red corundum have been recovered. The term 'oriental amethyst' has been suggested for the purple variety. However, the true nature of corundum being now well understood (Hughes, 1997), use of such a misleading term serves little purpose.

Comparing the colours of faceted Cape Breton ruby under various light sources reveals weak change of colour effects, with tungsten light producing the strongest rose red. Refractive indices of rose red crystals at the discovery site give $n_e$ = 1.766, $n_o$ = 1.776, values characteristic of the middle of the field for the mineral.

Typically, the crystals have a 'fat' rather than flat habit. However, tabular to blocky hexagonal prisms are common as are various pinacoid combinations with well-developed rhombohedron faces. Flattened bladed crystals are less common. On fold limbs, ruby crystals tend to be oriented parallel to the foliation of the enclosing rock, having been deformed at the same time as the enclosing rock.

Cape Breton ruby shows rhombohedral parting and prominent basal parting, the former giving nearly cubic angles. Only one imperfectly developed set of needle-like rutile inclusions has been observed, although prismatic rutile crystals (to 0.5 mm dia), and less often pyrite, occur around the rims of ruby crystals at some localities. Exsolved diaspore and/or boehmite are present (John Emmett, pers. comm., 2004) and doubtless contribute to the opacity/translucency of the stones. Heat treatment carried out under oxidizing conditions for 12 hours at 980 C and more, result in a colour change to bright pink, but at the cost of complete opacity.

Deformation was a late stage geological event. Indications are that some Cape Breton rubies initially formed as a progressive stage of amphibolite facies metamorphism. Then, a second generation crystallized as a consequence of retrograde metamorphism. A third mode of occurrence of corundum at Frenchvale is its presence in several small

granitic pegmatites, and this suggests that the mineral may also have been locally produced under conditions of partial anatexis at the peak of metamorphism by the breakdown of muscovite to corundum, K-feldspar and water.

During an extensive shallow drilling programme undertaken by MCMI in late 2004, true stratigraphic thicknesses of 15 m or more of ruby-bearing skarn were intersected immediately north and west of the Frenchvale quarry. Results of drilling confirm that ruby crystallized at specific horizons in the metamorphic sequence at Frenchvale – in some instances remote from intrusive rocks. Further, oblique, non-faulted contacts between ruby-containing horizons and granodiorite supply additional evidence in support of the concept that regional metamorphism and not contact metamorphism played the major role in ruby genesis. This finding has important implications for further exploration in the region, because together with the presence of corundum in the gneiss complex at North Mountain (Lime Hill), it means that rubies may be found in the George River Group whether igneous intrusions are present or not.

## Comparison with ruby from the Hunza Valley

The corundum-muscovite association common at several ruby localities in Frenchvale, along with other principal characteristics of the deposit, highlights the remarkable resemblance to the Hunza, Kashmir, occurrences (Okrusch *et al.,* 1976, Hughes, 1997; Hammer, 2004). Evidently, at the old Hunza mines much of the material recovered was cracked and had more value as specimens than as rough, although some was suitable for producing cabochons or carvings. This contrasts with the much higher quality material presently being recovered from modern workings a few kilometres distant (Syed M. Shah, pers. comm., 2005). Cape Breton ruby shares the following geological and gemmological characteristics with ruby from Hunza:

1. Primary deposits consist of a siliceous corundum-bearing marble enclosed in gneisses and mica schist;
2. Colour, red to deep purple, violet to purple, some blue; most crystals are opaque to translucent;
3. Stones show a strong chromium spectrum;
4. Crystal habits are generally prisms, rhombohedra or bi-pyramids with development of pinacoid faces;
5. Strong fluorescence in red to orange-red; long wavelength UV response stronger than short wavelength;
6. Cavities and negative crystals are common inclusions;
7. Some crystals are coated with a thin waxy 'veneer' of translucent white mica and talc;
8. Corundum forms intercalations within garnetiferous mica schists and biotite-plagioclase gneisses, which are cut by pegmatites and aplite dykes;
9. A green scaly mineral closely associated with ruby is muscovite which contains traces of Cr (and V) (O'Donoghue, 1988, p. 164).

## Conclusions

Cape Breton ruby is an exciting new gemstone find in Atlantic Canada. Aside from a few detrital grains of ruby found in British Columbia, and rumours of gem quality sapphire in the Northwest Territories and the Yukon, Ontario, is usually said to have Canada's most important corundum deposits, especially sapphire from several counties, albeit in small quantities as gems (Hughes, 1997). There is also an exciting new find of ruby from Baffin Island (Brad Wilson, pers. comm., 2006), certainly one of the more challenging gemmological exploration frontiers.

In Precambrian times, western Scotland and eastern Canada were probably very close, and Cartwright *et al*. (1985) have documented an area in Lewisian gneiss near Stoer, northern Scotland, of (pink) corundum associated with staurolite in a chromian muscovite matrix, although the Scottish gneiss is Archean and considerably older than the Late Precambrian

Figure 5: *Pendant of Cape Breton ruby set in silver; fashioned by Hans Durstling. Photograph by F. Isenor.*

metamorphic sequences in Cape Breton.

Although faceted Cape Breton rubies are not at present of the finest quality, they are attractive and may eventually support a vigorous local market in jewellery. Collectors, too, will find mineral specimens of interest. Prospects for future field discoveries in Atlantic Canada are excellent, especially if, as Raeside and Barr (1989) postulate, units equivalent to the Bras d'Or terrane exist in southern New Brunswick and in Newfoundland. Certainly on Cape Breton Island, lithologies traditionally considered to belong to the George River Group deserve close attention, especially the stream and glacial gravel deposits. It will be worthwhile also to bear in mind the analogy with Hunza, Kashmir, an area in which newer prospects within kilometres of old workings are currently producing high quality rubies and sapphires.

## Acknowledgements

# References

Barr, S.M., and Setter, J.R.D., 1986. Petrology of granitoid rocks of the Boisdale Peninsula, central Cape Breton Island, Nova Scotia. *N. S. Dept. Mines and Energy Pap., 84-1, 75 pp*

Barr, S. M., and Raeside, R.P., 1989. Tectonostratigraphic divisions of Cape Breton Island, Nova Scotia: implications of terranes in the northern Appalachian Orogen. *Geology,* 17, 822-5

Cartwright, J., Fitches, W.R., O'Hara, M.J., Barnicoat, A.C., and O'Hara, S., 1985. Archean supracrustal rocks from the Lewisian near Stoer, Sutherland. *Scottish Journal of Geology*, 21(2), 187-96

Chatterjee, A.K., 1977. Tungsten mineralization in the carbonate rocks of the George River Group, Cape Breton Island, *Nova Scotia. N. S. Dept. Mines Pap., 77-7,* 26 pp

Dawson, J.W., 1855. *Acadian Geology: an Account of the Geological Strucure and Mineral Resources of Nova Scotia, and portions of the Neighbouring Province of British Columbia.* Oliver and Boyd, Edinburgh, 694 pp

Einaudi, M.T., Meinert, L.D., and Newberry, R.J., 1981. Skarn deposits. *Econ. Geol.*, 75th Anniversary Volume, 317-91

Hammer, V.M.F., 2004. Red, blue and green gemstones from Hunza (pp 54-5). In: G. Agozzino, D. Blauwet, M. Jarnot, S. Muhammad, G. Neumeier, G. Staebler and T. Wilson (eds), Pakistan: Minerals, Mountains and Majesty. *Lapis International, English edition No. 6,* 96 pp

Hill, J.R., 1987. Geology and geochemistry of Precambrian carbonate rocks, Cape Breton Island, Nova Scotia. *Geol. Surv. Can.,* Open File 1597. 43 pp

Hill, J.R.,1989. Follow-up geology and geochemistry of metacarbonate formations and their contained mineral occurrences, Cape Breton Island, Nova *Scotia. Geol. Surv. Can.,* Open File 2077, 50 pp

Hughes, R.W., 1997. *Ruby and Sapphire.* RWH Publishing, Boulder, Colo. 511 pp

Milligan, G.C., 1970. The geology of the George River Series, Cape Breton. *N. S. Dept. Mines,* Memoir 7, 111 pp

O'Donoghue, M., 1988. *Gemstones.* Chapman and Hall. London, 372 pp

Okrusch, M., Bunch, T.E., and Bank, H., 1976. Paragenesis and petrogenesis of a corundum-bearing marble at Hunza (Kashmir). *Mineralium Deposita,* 11, 278-97

Raeside, R.P., 1989. Geology of the metamorphic rocks of the Boisdale Hills, Cape Breton Island. *N. S. Dept. Mines and Energy, Mines and Minerals Branch, Rept. Activities, 1989, Part A: N. S. Dept. Mines and Energy,* Report 89-3, 145-8

Raeside , R.P., and Barr, S.M., 1990. Geology and tectonic development of the Bras d'Or suspect terrane, Cape Breton Island, Nova Scotia. *Can. J. Earth Scis.,* 27, 1371-81

Schmetzer, K., 1987. Lamellare einschaltungen von Diaspor in Korund. *Aufschluss,* 38, 335-7

Weeks, L.J., 1954. Southeast Cape Breton Island, Nova Scotia. *Geol. Surv. Can.,* Memoir 277, 112 pp

White, C.E., Barr, S.M., Bevier, M.L., and Kamo, S., 1994. A revised interpretation of Cambrian and Ordovician rocks in the Bourinot belt of Central Cape Breton Island, Nova Scotia. *Atlantic Geology,* 30, 123-42

# Better refractometer results with the Bright Line technique

## Dr D. B. Hoover FGA, FGAA (Hon.)[1] and C. Williams FGA[2]

1. 1274 E. Crystal Wood Lane, Springfield MO 65803, U.S.A.
   Email dbhoover@aol.com
2. P. O. Box 104504, Jefferson City MO 65110-4504, U.S.A.
   Email cara@beargems.com

**Abstract:** *Grazing incidence illumination of gemstones on the gemmologist's refractometer is now little used, but offers some significant advantages. The authors review the history of such use, give detailed explanations of how it is accomplished, and provide suggestions for its application to practical problems. There are three principal applications of grazing incidence illumination that can aid the gemmologist in practical discrimination between gems. One is in easier and better determination of the refractive index, or indices for birefringent stones. The second is in estimation of relative dispersion, and the third is in being able to observe polarized absorption spectra of gems.*

**Keywords:** *bright line technique; grazing incidence; polarized spectra; refractive index; refractometer*

## Introduction

*"It is a wise precaution in a doubtful case to study the effect when the stone is illuminated from above and not below."*

G. F. Herbert Smith (1940, 31) in discussing use of the refractometer.

Many gemmologists may not be aware of the 'bright line' technique (Anderson, 1959) for obtaining refractive index (RI) readings with the common, critical angle refractometer or if aware, do not make use of it. This is not surprising due to the limited discussion of the technique in modern gemmological texts and the design of many modern instruments, which can make it awkward to properly position the light source. The authors have taken a new look at the 'bright line' method, which is an old variation of stone illumination, and have found that it has distinct advantages that are not currently utilized. This paper examines the technique and explains how to get more from your standard gemmological refractometer.

### History

Most readers will be familiar with the workings of the standard gemmologist's critical angle refractometer, where light enters a dense glass prism from behind and below, and is reflected at the glass/gem interface, so that a shadow edge defines the critical angle of reflection on a scale within the instrument. In using the 'bright

Figure 1: *A critical angle refractometer with the light shield removed and illuminated for grazing incidence using a torch.*



Figure 2: *Modern style refractometer with small LED light directed at grazing incidence.*



Figure 3: *Pulfrich refractometer, catalog scan taken from Arthur H. Thomas Co. Laboratory Apparatus and Reagents. Philadelphia (1921).*

line' technique, the normal light port of the instrument is not used, and light enters the gem directly, so that some of the light is at grazing incidence to the glass/gem interface (*Figures 1* and *2*). With this technique, the light and dark parts of the refractometer scale are reversed, and importantly, a very bright spectrum is seen at the boundary, hence the term 'bright line'. The authors believe that the dramatic difference in the appearance of the readings between the two illumination methods, shown in *Figure 8*, has not been adequately noted in the literature. Traditional illumination with white light produces a diffuse shadow edge with hints of blue on the low side and red on the high side, but monochromatic light or a polarizing filter can make the reading more distinct. Grazing incidence produces one or two very bright, clear spectra that show the absorption spectrum of the gem. In pleochroic stones, the differing spectra can be observed side by side. This means of comparison is a valuable educational and identification tool. Anderson (1959, 1980) indicates that C. J. Payne used this method when it was difficult to obtain readings by traditional means. The light hood of the instrument was removed and Anderson (1959, 33) says that the light was "… so adjusted as to provide light at grazing incidence on the stone …". No other lighting details are given. He goes on to note that it may be necessary to rotate the stone to see the effect clearly, again without further explanation.

G. F. Herbert Smith, the father of the gemmologist's refractometer, was certainly aware of the utility of grazing incidence illumination, as shown by the quotation given at the introduction above. His 1913 text *Gemstones* does not include instruction on grazing incidence illumination, but by his 9th edition (1940) he includes it. Smith even shows a photograph of a Zeiss pocket refractometer designed for jewellers, that provides for illumination to either the glass hemisphere or the stone. A schematic drawing of this instrument is shown by Diniz Gonsalves (1949), clearly showing that an adjustable mirror is moved to provide

Figure 4: *Sketch of the light path in the sample and prism of a Pulfrich refractometer when solids are measured.*

either type of illumination and indicating that the grazing illumination is directed along the plane of the prism/gem interface. Diniz Gonsalves notes that it is one of the instruments most often used by the experts.

Critical angle refractometers used in other industries may use either type of illumination. The Pulfrich refractometer (*Figure 3*), designed for grazing incident light, provides much needed information on the use and limitations of such refractometers. A sketch of the principal optics of this instrument when measuring a solid is shown in *Figure 4*. In order to obtain good results, the material being tested must have an optically flat surface (for example, a polished facet surface) with an adjacent surface intersecting at a clean, 90-degree angle (Cooper, 1946). These two factors are critical in obtaining accurate results with the instrument. Light entering the solid at grazing incidence will exit into the dense glass at the critical angle. Light entering the solid at angles less than grazing will be refracted into the dense glass at angles less than the critical angle, lightening the lower part of the refractive index scale. In other respects it is the same as a gemmologist's refractometer. This explains the reversal of the dark and light parts of the scale.

The technique is mentioned in the 3rd edition of Webster's *Gems* (1975), but was dropped by the 5th edition (1994). Webster (1975) emphasizes that the technique is sometimes useful for those difficult cases when an RI cannot be obtained by normal means, adding that best results are for trap-cut [rectangular step-cut] gems, without explanation. He makes another comment regarding colour fringes seen when using white light for RI determinations in the traditional manner that will be important for our story later. Webster (1975, 627) says: "The sharpness or otherwise of the coloured fringe of the shadow edge in white light will give some idea of the dispersive power of the stone … and this may give useful confirmatory information." This technique gives a strong indication of relative dispersion, not easily available by other
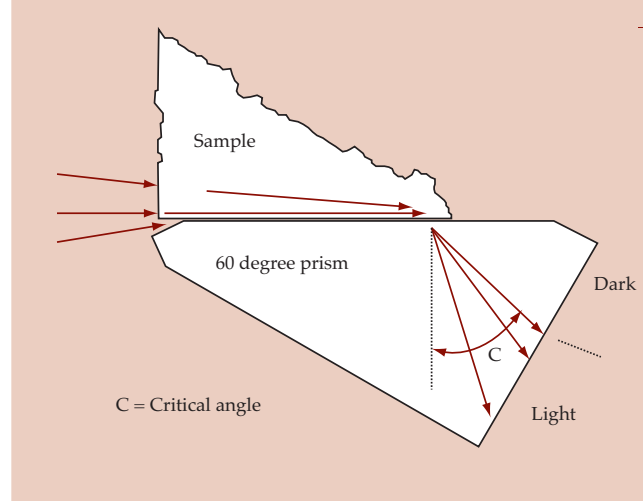
testing methods. Hoover and Linton (2000, 2001), and Linton (2005) are the only authors we know of who have recently made much use of the 'bright line' technique, as noted in their papers on dispersion measurement. There are few other references to the technique in the current literature, other than Liddicoat (1989), who makes passing mention of it. Liddicoat states that the light source should be directed from above and behind the stone, not mentioning grazing incidence. We shall address this aspect later. Liddicoat (1989) notes the reversal of the bright and dim parts of the scale, and further states that the spectrum when using the bright line scheme is predominantly red, as opposed to the blue-green seen in normal operation.

The authors suspect that the principal reasons for the lack of interest in the 'bright line' technique are the lack of instruction in its use and the redesign of most modern instruments, limiting the size of light source that can be used to obtain grazing incidence. Many gemmologists may have tried it but have become discouraged in their attempts to get proper lighting. Understanding the illumination requirements permits one to adjust the measuring technique so that, with practice, useful measurements can be quickly and easily obtained.

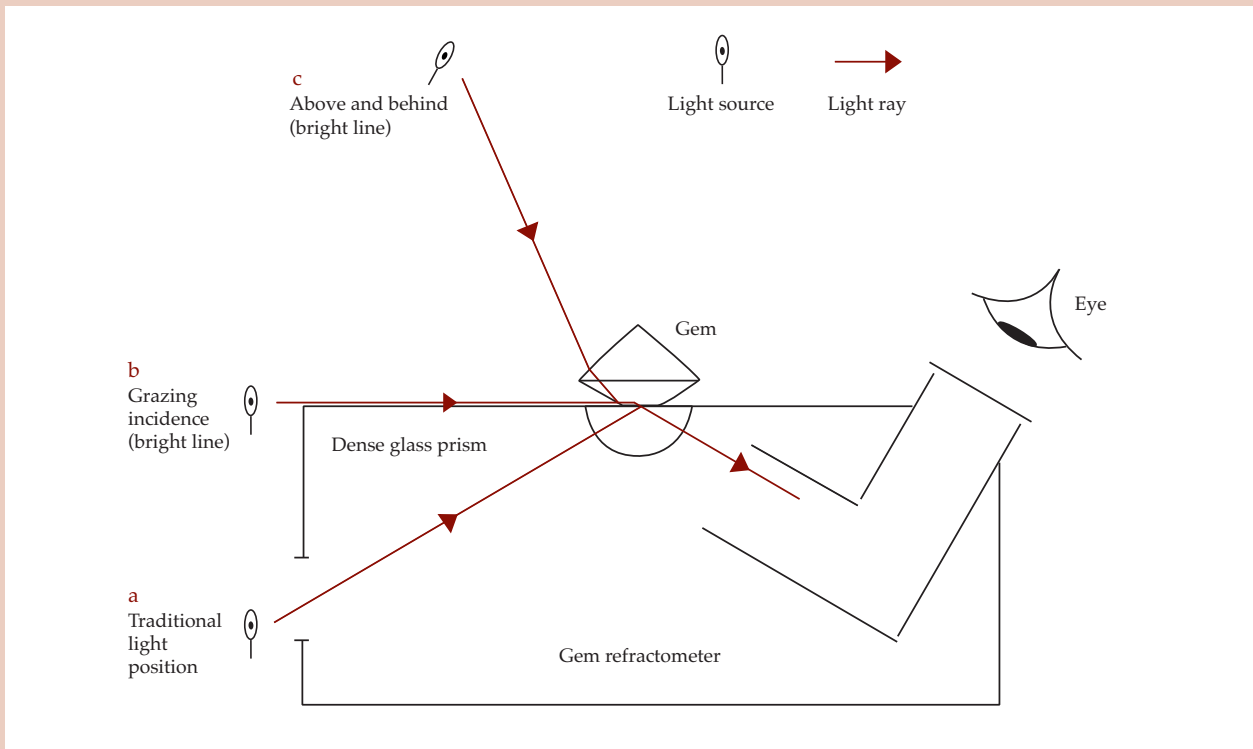Figure 5: *Diagram of a refractometer showing the positions a, b and c of a light source for traditional illumination, and for grazing incidence.*
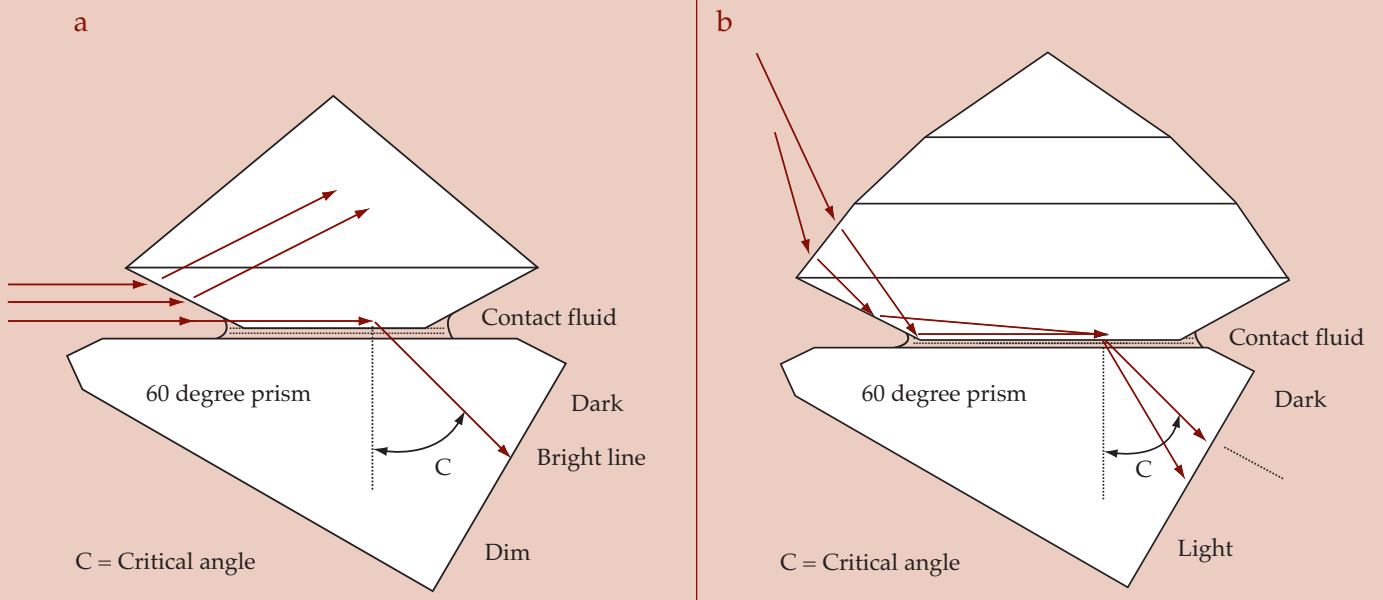
Figure 6: *Sketch of the light paths in the prism of a gemmologist's refractometer when grazing incidence is used. In position (a) light is directed in the plane of the prism surface. In position (b), light is directed into a pavilion facet from above and behind.*

# Obtaining grazing illumination

The review above shows that for the 'bright line' technique to be practised; a simple, reversible alteration to the standard gemmologists' refractometer is required to allow for grazing incidence mode (*Figure 1*). The light shield must be removed. The Eickhorst refractometers have easily removable light shields, making them ideal for practicing the technique. Alternatively, a small light source can be used, as in *Figure 2*. We prefer to remove the cover. *Figure 5* shows a conventional refractometer with the dense glass prism, and a 90-degree telescope with scale for viewing the critical angle. Three possible positions (a, b and c) for the light source are also indicated. In this diagram the plane of the paper is the optical plane of the instrument. Position a is the traditional mode of illumination from below. Position b may be easier to obtain with the light shield removed (*Figures 1* and *2*). Position c will vary depending on the RI and facet angles of the stone under test.

*Figure 6* shows details of two ways in which grazing light may be introduced into a gem placed table-down on a refractometer with the light shield removed. *Figure 6a* shows a light beam travelling at grazing incidence along the instrument path, and parallel to the gem/prism interface. The thickness of the contact fluid layer is exaggerated in this figure for clarity, and we only consider the facets adjacent to the table. This mimics the light path in the Pulfrich instrument, except that when using a faceted gem, having the adjacent facet at 90 degrees to the table is generally not possible, nor is it necessary. The adjacent facet must still be oriented at 90 degrees to the plane of the refractometer, as shown in the diagram (*Figure 7*). Within a small range, the light can also be oriented at 90 degrees to any facet adjacent to the table, as long as the light path still roughly follows the light path of the refractometer. This explains Anderson's statement that a stone may have to be rotated in order to obtain a reading, and Webster's

comment on trap-cut stones being best. Certainly, rectangular step cut stones are best for learning the technique. Light directly entering crown facets will refract light away from grazing incidence (*Figure 6a*). Light entering the contact fluid film between the gemstone and the instrument table will be refracted at the critical angle of the fluid, or upward into the stone, and lost (not shown). It is only if there is a sufficient bead of contact liquid on the adjacent crown facet (*Figure 6a*) that light at grazing incidence will be able to enter the stone. Therefore, it is key that one should use sufficient RI fluid so that a small bead of fluid forms at the facet edge. A consequence of using the small 'window' of liquid rather than a facet at 90 degrees is that the lower part of the refractometer scale will not be so brightly lit as with a 90 degree face due to the lower quality of light at appropriate angles entering the gem. The scale in this case remains quite dark, with only the one (or two if birefringent) bright spectrum clearly seen; a shadow edge(s) will be seen if monochromatic light is used.
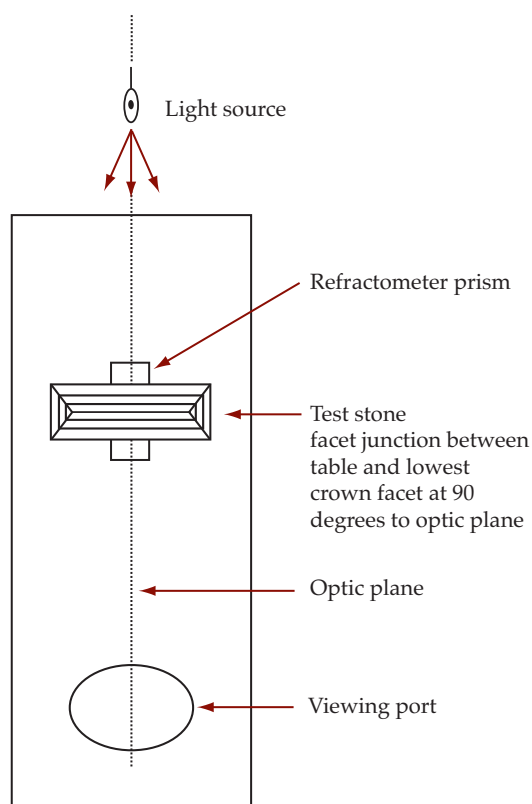


Figure 7: *Diagram of a refractometer showing the placement of a gem with respect to the optic plane of the refractometer.*

*Figure 6b* shows another method of getting light into a faceted gem at grazing incidence. By holding the light source above and slightly behind the stone, the light entering the pavilion is internally reflected off of a crown facet at its intersection with the table. The optimum position of the light source will vary depending on the RI and facet angles of the stone. With normal faceting angles, as in most stones, the reflection within the gem at the crown facet will be at or above the critical angle providing good light intensity at grazing incidence. Placing the stone so that the facet junction between the table and crown facet is perpendicular to the optical plane of the refractometer remains crucial. Tracing this light path back within the stone and out, one sees that generally the light source should be above the stone, and away from the viewer. This explains Liddicoat's suggestion (op. cit.) that the source be "from above and behind".

It is most important to note that there are a number of possible light paths which may produce line or spectral images on the scale at other than the critical angle. These false readings can cause some confusion to the novice, but are simple to detect. Smith (1940) gives us the clue; one should check the gem with illumination from both above and below (traditional refractometer testing). If illumination is correct, then shadow edges and spectra will be at the same positions. Continue to adjust the light position until the readings match and are consistent. What none of the quoted writers has said is that when using white light and traditional illumination, both the boundary and the spectrum seen at the boundary are very weak, while with grazing illumination the spectrum is bright and well defined (*Figure 8*).

This aspect will turn out to be a major asset, especially in cases where it is difficult to get clear readings by the traditional method. In these cases, the 'bright line' technique is ideal for confirming both R.I. and birefringence. This supports what C. J. Payne found many years ago. Two bright spectra would be seen for a birefringent gem. Pleochroic stones may show two slightly different spectra due to the variation in absorbance along different polarization directions. If one uses monochromatic illumination, then for grazing incidence the 'shadow edge' is not really a shadow edge, but one sees the edge defined by a very bright sharp spectral line that marks the RI for that wavelength, against a generally dark background. In essence one has a prism spectroscope with a birefringent prism. It is these bright, sharp lines that make it much easier to read the scale of the instrument at any particular colour.

## Making a measurement

At first the user may have difficulty obtaining clear readings by grazing illumination, but practice will quickly bring proficiency. Unfortunately, it is not entirely without problems. Poorly cut stones and included stones will give significant problems, scattering or distorting the light beam in its passage through the stone. Such defects prevent greater application of the technique. Mounted stones have obvious limitations in orientation, but many will still yield good results with bright line if an RI reading is possible. It is suggested that the beginner
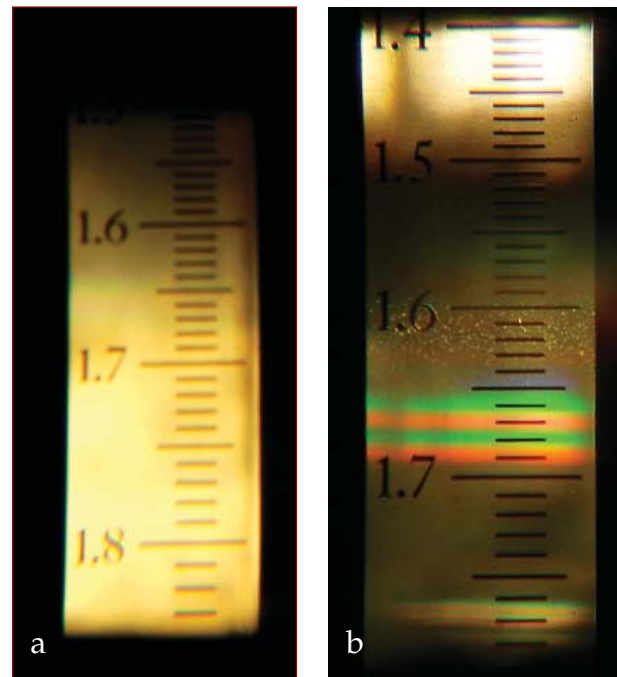


Figure 8: *Refractometer readings for a peridot when illuminated by white light with (a) traditional illumination, and with (b) grazing illumination.*

start with a well-cut, clean, rectangular step-cut quartz and use white light. For some refractometers, it will be helpful to remove the top cover. Use a light source that is easily moved so comparisons can be made quickly between the a, b and c illumination positions shown in *Figure 5*. A small key-chain white LED source is ideal.

Remember to use sufficient contact liquid, and to orient the stone so that one of the facet junctions with the table will be perpendicular to the refractometer axis. This is illustrated in *Figure 7*, which shows a step-cut stone on a refractometer. *Figure 9* illustrates the direction that the optic plane of the refractometer should take with respect to three different cuts. With a stone on the refractometer, find the shadow edge using traditional illumination methods. Look carefully and you will find a very faint spectrum at the shadow edge. With your head held in this viewing position, take your light source and raise it slowly to shine on the stone in the b position shown in *Figure 5*. As the light is raised, a very bright spectrum should suddenly appear in the same position as the shadow edge under traditional illumination. Note that there may be additional spectra at other positions on the scale. These are to be ignored. Practise until you can easily find the bright spectrum. Next, raise the source to be above the stone in the c position of *Figure 5*, and move it up and down to find the bright spectrum from light reflecting within the stone. If you have difficulty, practise with other clean, well-cut stones.

Various light sources can be used with this technique, and a small LED light is one example, as shown in *Figure 2*. If using white LED, it is important to note that it is not a true, full-spectrum light; and while it will produce accurate RI readings, the spectrum may not be accurate enough for positive identifications. Today's well-stocked lab should have several white and monochromatic LED lights. Yellow LEDs are ideal for traditional RI readings when a monochromatic filter is not available. It should be obvious how much brighter and sharper the readings are with grazing incidence. If the room is very dimly lit, the refractometer scale may be difficult to read;
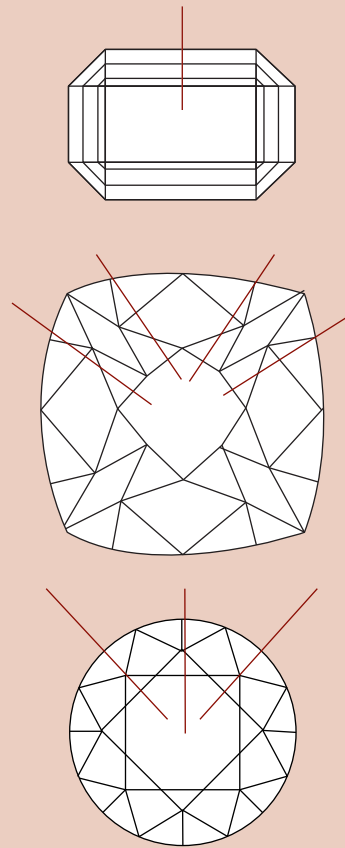


Figure 9: *Diagrams of emerald-, cushion- and brilliant-cut gems, showing the orientation of the gem facets to the light path /optical plane of the refractometer (as in* Figure 7) *for grazing illumination.*

it will help to introduce some diffuse light into the rear light port in order to light the scale. Once seen, the bright line effect is quite impressive. But remember, poorly cut and/or included stones can give poor results.

### *Summary of steps to obtain a bright line reading*

1. Obtain RI reading through traditional lighting method (*Figure 5*, position a).
2. Remove light cover from refractometer (*Figure 1*). (Optional)
3. Apply sufficient RI fluid to create a small bead along table/facet edge interface (*Figure 6*).
4. Align a facet (chosen facet must be adjacent to the table) at ninety degrees to light path/optic plane (*Figures 7* and *9*).
5. Direct light along grazing incidence (*Figure 5*, position b).
6. Observe bright line spectrum (*Figure 8*).
7. Direct light from above and behind (*Figure 5*, position c).
8. Confirm reading by comparison with position a (*Figure 5*, position a and b).

# Utilization of grazing incidence

There are three key areas where grazing incidence will be of benefit to gemmologists in facilitating gem identification. The first is in better and easier reading of refractive index or indices, for birefringent stones. The second is in estimation of dispersion, and lastly as a simple prism spectroscope.

### Refractive index or indices measurements

Gemmologists will occasionally come across a specimen that gives vague or unclear readings on the refractometer by traditional methods. The 'bright line' technique is ideal for obtaining RI measurements on such stones, as grazing incidence gives much better definition of the shadow edge(s). Even for clear and simple RI measurements, the authors recommend that Smith's (1940) advice be heeded, and that both illumination techniques be used whenever possible. It is quick and simple, and provides much greater confidence.

Orienting a stone for maximum birefringence readings may be difficult due to the requirement that the facet through which the light enters the stone must be at 90-degrees to the light path, limiting the number of positions for gem. Accurate birefringence readings should be taken using traditional illumination, and then confirmed with bright line technique if the facets allow. Displacing the light source slightly to one side or the other when using bright line (*Figure 5* positions b and c) can still provide good readings within a given range, depending on the facet arrangement.

# Dispersion estimation

If a white light source is used for grazing incidence a clear, bright spectrum should be visible, including its absorption features. Because these spectral colours may cover a wide span on the refractometer scale, it might be tempting to assume this would provide a good measure of dispersion, by simply taking the difference in readings at either end. This is not the case. The spread of the spectrum across the scale is an apparent dispersion, not a true dispersion; and its width is inversely proportional to the dispersion of the gem. If the refractometer reading indicates a large apparent dispersion, then that gemstone will have a low actual dispersion. For example quartz will show a wide, spread spectrum across the refractometer scale, whereas a spinel will show a narrower spectrum. Imitation gems of glass typically have high dispersions and show relatively low apparent dispersion on the refractometer. These glass imitations have become more sophisticated and more prevalent in the market, with their optical and physical properties often overlapping with known natural materials. While intense colours may mask the observed dispersion, the apparent dispersion in the bright line method can be a strong indicator of their true nature.

The amount of apparent dispersion a gem may show depends on the type of refractometer, prism or hemisphere, and the nature of the dense glass used (see Hoover and Linton, 2000, 2001 for details). In order to qualitatively estimate dispersion, one needs to become familiar with an instrument by checking known materials and standards representing a range of dispersion. Once familiar, then relative dispersions may be estimated, based on the width in RI units of the colour spectrum relative to known gems.

It should be emphasized that the above discussion concerns relative dispersion. True dispersion is difficult to measure, but Hoover and Linton (2000, 2001) have given details of the problem using a critical angle refractometer; they show that it is only practical for those instruments with a hemispherical or hemicylindrical dense glass element.

In general, dispersion follows closely the refractive index of a material, so is not expected to be a simple means of discrimination except for glasses and liquids, which tend to have higher dispersions than crystalline solids. Care also needs to be taken if estimates are made from the spectrum produced from white light: absorptions in the gem at the red or blue end of the spectrum may make the apparent dispersion appear less than it really is (e.g. selenium glass).

# Absorption spectra definition

When trying the 'bright line' technique with a ruby and white light, it will become immediately apparent that the coloured fringe shows the absorption spectrum of the ruby, and appears similar to that seen using the 'Visual Optics' method (Hodgkinson, 1995). Other strongly absorbing gems also show typical spectra, e.g. almandine; emerald; gold, cobalt, and selenium glass imitations; and cobalt coloured synthetic spinels. Thus, for some stones, the spectroscope may be avoided simply by resorting to grazing incidence illumination. We believe this significantly adds to the importance of the refractometer as a determinative instrument for gemmologists.

Another advantage is that for anisotropic gems, both polarized spectra are visible at the same time, a feature not previously available to most gemmologists. This can yield additional information, which may help to identify a gem such as alexandrite or tourmaline. The polarized spectra of anisotropic gems commonly overlap, especially in those with relatively low birefringence and/or dispersion, so that use of a polarizing filter may be needed to clearly separate them. The difference in absorption spectra of strongly pleochroic stones can be observed and easily compared. Of course, it helps if the stone is oriented for maximum birefringence, although this may not be possible if facet geometry is unfavourable. As with traditional RI measurement, if the *c*-axis is perpendicular to the facet under test, only one spectrum will be seen. With ruby the difference in the red end of the spectrum is easily seen by the shift from red to orange-red. With green and blue tourmaline the distinct differences in absorption along the ordinary and extraordinary rays across the entire spectrum can be seen. The spectrum of the ordinary ray in most tourmalines will be much weaker than that of the extraordinary ray. Distinct differences in the polarized spectra of properly oriented dark emeralds may also be seen by this method. In alexandrite, distinct differences in the spectra

of each ray are visible and easily compared, side-by-side. The low-index ray passes much of the yellow, while the high index ray has an absorption in the yellow easily seen by its absence. Liddicoat (1989) shows examples of such polarized spectra.

Although the spectra produced by grazing incidence illumination are quite clear, minor or very narrow absorption lines may not be easily visible, especially at the blue end. The width or spread of the spectrum will also be an inverse function of the gem's dispersion. For the serious gemmologist, a simple addition can be used to spread the spectrum a little. If a small 45-90 degree prism is made of low dispersion glass (or better fluorite which has very low dispersion) then the apparent dispersion will cover a range of about 0.05 units on the refractometer. The prism is placed on the refractometer, similar to that for a Pulfrich refractometer as illustrated in *Figure 4*. It can then act as a 'poor man's' spectroscope, but without the capacity to produce polarized spectra. Light simply has to be introduced to the vertical end of the prism after passing through a gem whose spectrum is to be observed.

## Summary

The authors believe that use of the long-neglected 'bright line' technique to measure refractive indices can be a significant aid to gemmologists. This tool can significantly increase the confidence in measurements of refractive indices, especially for difficult cases. Further, it may assist in identifying glass or paste by providing estimates of relative dispersion, or provide polarized absorption spectra without resorting to other instrumentation. The authors suggest that students of gemmology should also be exposed to the technique, as an aid in learning how to measure refractive indices, and for better understanding of refractometers. Renewed use of the 'bright line' method will hopefully inspire more equipment manufacturers to build refractometers that enable easier implementation of this valuable technique.

# Acknowledgements

# References

Anderson, B.W., 1959. *Gem Testing.* 2nd edn. Emerson Books, New York. 324 pp

Anderson, B.W., 1980. *Gem Testing.* 9th edn. Butterworths, London. 434 pp

Cooper, H.J., 1946. *Scientific Instruments.* Chemical Publishing, Brooklyn. 305 pp

Diniz Gonsalves, A., 1949. *As Pedras Preciosas* (in Portuguese). Grafica Olimpica, Rio de Janeiro. 457 pp

Hodgkinson, A., 1995. *Visual Optics.* Gem World International, Northbrook, Ill. 50 pp

Hoover, D.B., and Linton, T., 2000, Dispersion measurements with a gemmologist's refractometer, part 1. *Australian Gemmologist,* 20(12), 506-16

Hoover, D.B., and Linton, T., 2001. Dispersion measurements with a gemmologist's refractometer, part 2. *Australian Gemmologist,* 21(4) 150-60

Liddicoat, R.T., 1989. *Handbook of Gem Identification.* 12th edn. Gemological Institute of America, Santa Monica, CA., 364 pp

Linton, T., 2005. Practical application for measuring gemstone dispersion on the refractometer. *Australian Gemmologist,* 22(8) 330-44

Smith, G.F.H., 1940. *Gemstones.* 9th edn. Methuen, London. 443 pp

Webster, R., 1975. *Gems.* 3rd edn. Newnes-Butterworths, London. 931 pp

Webster, R., 1994. *Gems.* 5th edn. Butterworth-Heinemann, Oxford. 1026 pp

# The effect of heat treatment on colour, quality and inclusions of aquamarine from China

Yang Ruzeng, Xu Hongyi and Li Minjie

*School of Ocean and Earth Science, State Key Laboratory of Marine Geology, Tongji University, Shanghai 200092, China*

**Abstract:** *Aquamarine from Altai, Siukiang, China, is heat treated from yellowish green to blue to make it more attractive for the gem market. Treatment is carried out at 480-500°C and results in both colour change and changes to the inclusions. The nature of these changes is illustrated and the appearance of tiny black inclusions is attributed to carbon which resulted from reduction of original fluids in the inclusions.*

**Keywords:** *aquamarine, China, heat treatment, inclusions*

## Introduction

Gem quality aquamarine comes from many countries but the main sources are Brazil, Russia, China and Pakistan. Of these, Brazil produces the finest stones. In China, aquamarine can be found in the provinces of Sinkiang, Mongolia, Hunan, Yunnan and Hainan, and the quantity and quality range from Altai, Sinkiang is especially large. However, much of the rough is not of gem quality – it has a pale colour and may be extensively fractured (Wang, 1999). With increasing demands for aquamarine in the gem market, the supply of natural high-quality stones has declined and consequently prices have risen.

One way to address this problem is to improve the colour of originally pale-coloured rough and since this can be achieved to some extent by heat treatment, this technique has become very important for the Chinese gem industry (He *et al.*, 1995). This has consequences for both the home and export markets.

This account reports the results of heat treatment applied to aquamarine from Altai, Sinkiang, and especially its effects on the inclusions.

## Materials, equipment and methods

The samples of aquamarine from Altai, Sinkiang, include randomly shaped lumps and step-cut faceted stones (*Figure 1*) in the



Figure 1: *Aquamarine crystals and cut stones from Altai, Sinkiang, typical of those studied for this report.*
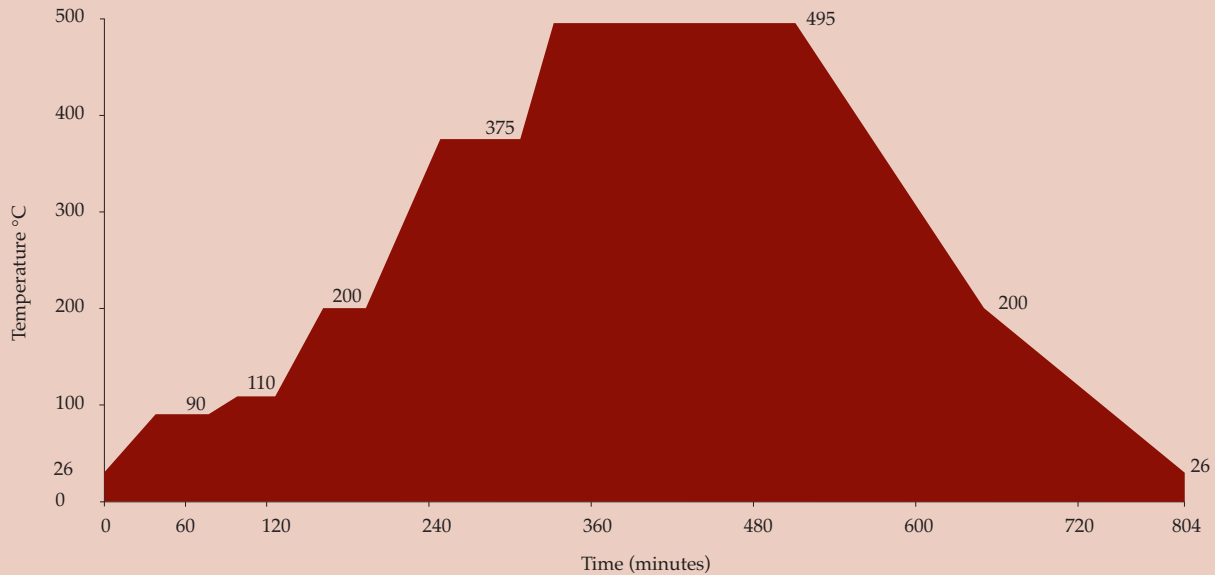
*Chinese aquamarines are heated to 495°C at 3°C/min. in the stages shown. They are held at 90°C for 60 min., at 110° and 200° for 30 min. each, at 375° for 60 min. and at 495° for 180 mins.*
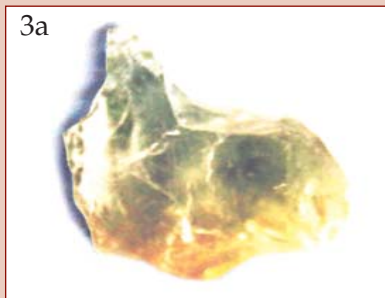

3a


3b

Figure 3: *Untreated aquamarine (a) and heat-treated crystal showing the colour change from yellow-green to blue.*

weight range of 10-15 ct (natural rough) and size range 4 x 6 to 6 x 9 mm (faceted). The natural colour is blue-green.

To heat the stones, a Resistance Furnace (SG2-3-12, made in China) using up to 3kW and delivering temperatures up to 1200 C, was used. Compositions of the stones and their inclusions were determined by coating them with gold and using a Philips scanning electron microscope (SEM model type EL30ESENTMP) fitted with an EDAX energy dispersive spectrometer.

The procedure for heating the aquamarine was as follows:

- aquamarines were mixed with hollow alumina granules and placed in an alumina pot;
- the pot with its load was placed in the furnace and slowly heated in a reducing atmosphere to 480-500 C;
- the load was held at this temperature for three hours and then the temperature was slowly reduced to room temperature.

Great care is needed in increasing and decreasing the temperature slowly to minimize any cracking from vapour pressures in the inclusions. Heating rate up to 495 C and down to 200 C is 3 C/min. and is slower from 200 C to room temperature. The whole cycle is shown in *Figure 2*.

## Results

An example of the colour change in aquamarine caused by the procedure described above is shown in *Figure 3*. The colour in *Figure 3b* is considered much more attractive in the gem market. In order to understand further the changes caused by heat treatment, inclusions were studied in detail under the gemmological microscope. Most Altai aquamarines contain cavities which are tube-shaped (many together look like rain), negative crystals or are of irregular shape, and

Figure 4: *Inclusions in natural untreated aquamarine: (a) crystal with clear curved face; (b) tube inclusions, 'rain'; (c) curved plane with abundant liquid-filled inclusions, 'fingerprints'; (d) crystal inclusion with clear straight boundaries.*
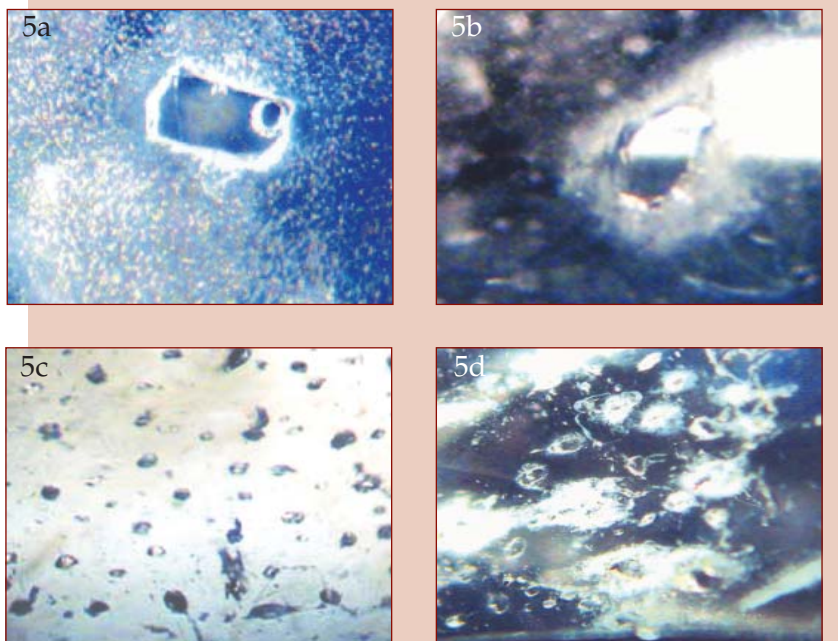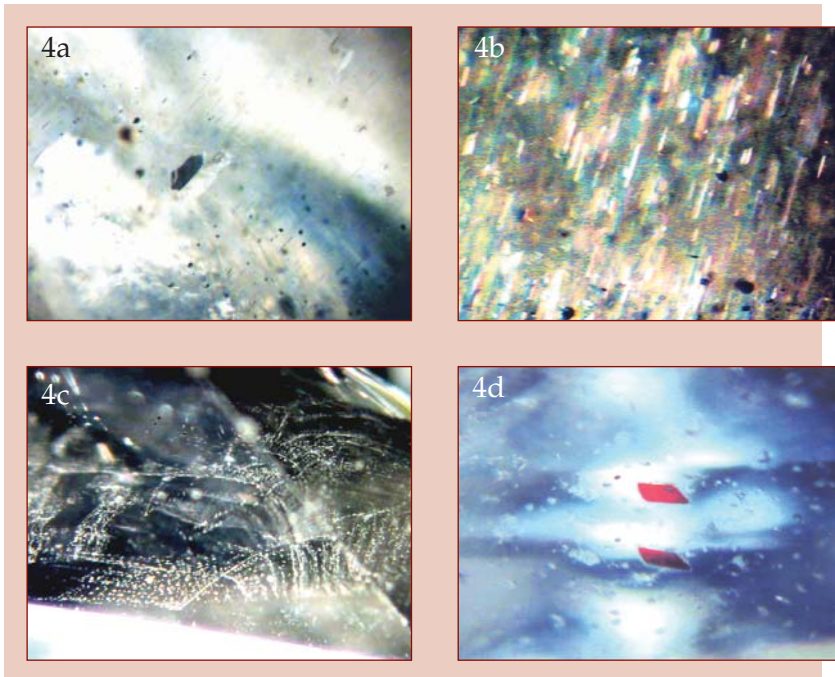


Figure 5: *The changes visible in inclusions after heat treatment: (a) negative crystal with two-phases, liquid and gas, clearly defined; (b) after heat treatment the cavity has changed shape, is empty and the surrounding host crystal is 'frothy' with local shattering; (c) two-phase inclusions in a 'fingerprint'; (d) disc-shaped fractures around the inclusions in (c) after heat treatment*

these may contain liquid, gas or both; some stones contain also tiny cavities in an overall fingerprint pattern (*Figure 4*). Solid inclusions (*Figure 4d*) have typically clean and distinct margins in natural untreated aquamarines.

Heat treatment changes most inclusions quite significantly. Examples are shown in *Figure 5* where a negative crystal cavity containing liquid and a round bubble of gas (a) transforms on treatment to an irregular cavity surrounded by a 'frothy' zone where escape of the volatiles has affected the host crystal (b). Changes of a similar nature affect the tiny cavities in a 'fingerprint' (*Figures 5c* and *d*) where disc-shaped fractures are formed around the original liquid-filled cavities and these resemble poached eggs.

More irregular zones of alteration may form around other inclusions (*Figure 6*).

If the heat treatment is not strictly controlled or if the aquamarine contains too many liquid-filled inclusions, an excessive number of fractures may be formed. Commonly these are disc-shaped, parallel to
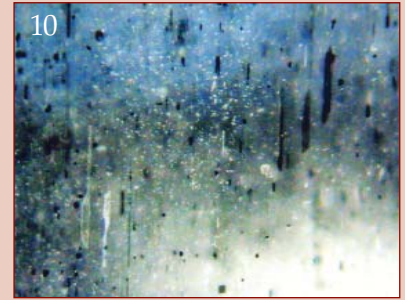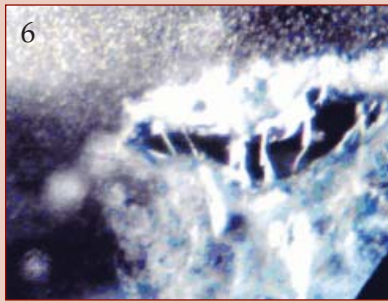
.**Figure 6:** *Cloudiness or frothiness around a cavity formed by heat treatment of an aquamarine.*

**Figure 7:** *Disc-shaped fractures penetrated by tube inclusions in close-up (a) and in a cut aquamarine (b).*

**Figure 8:** *Some disc-shaped fractures display iridescence.*

**Figure 9:** *Typical cracks formed in aquamarine when it is heated too quickly.*

**Figure 10:** *Tube inclusions showing black carbon deposits after heat treatment.*

the basal pinacoid {0001} and perpendicular to the *c*-axis (*Figure 7*) and some show iridescence on their surfaces (*Figure 8*). Where the discs are penetrated by tube inclusions, they resemble lotus leaves on a stalk. Rapid heating may lead to abundant tiny fractures creating very much reduced transparency in the stones (*Figures 9* and *10*).

After heat treatment in a reducing atmosphere, most colourless inclusions showed spider-like structures (*Figure 11*) or black spots on inclusion surfaces which resembled smog. The most likely explanation for this phenomenon is that the liquid in the inclusions was $CO_2$ and not water, and that the treatment reduced it to carbon which was deposited on the inclusion walls. Microprobe analysis of the black substance indicates the main component as carbon and supports this interpretation (*Figure 12*).
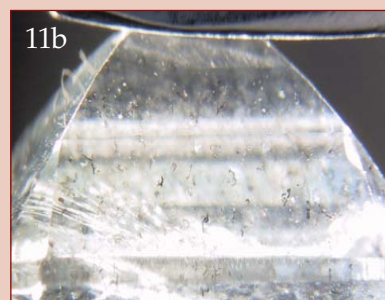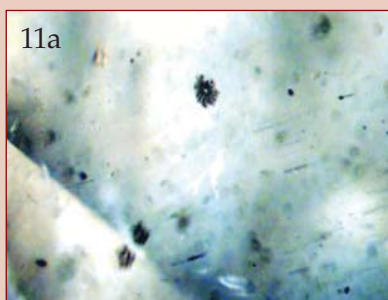
**Figure 11:** *Spider-like inclusions are probably black carbon deposits in disc fractures after heat treatment (a). A combination of fractures and black carbon makes a treated aquamarine look as if it contains 'smog'.*

Figure 12: *Spectra showing the major elements in aquamarine (except for Be) in (a), and the relatively high carbon peak from a black spot on a fracture caused by heat treatment (b).*
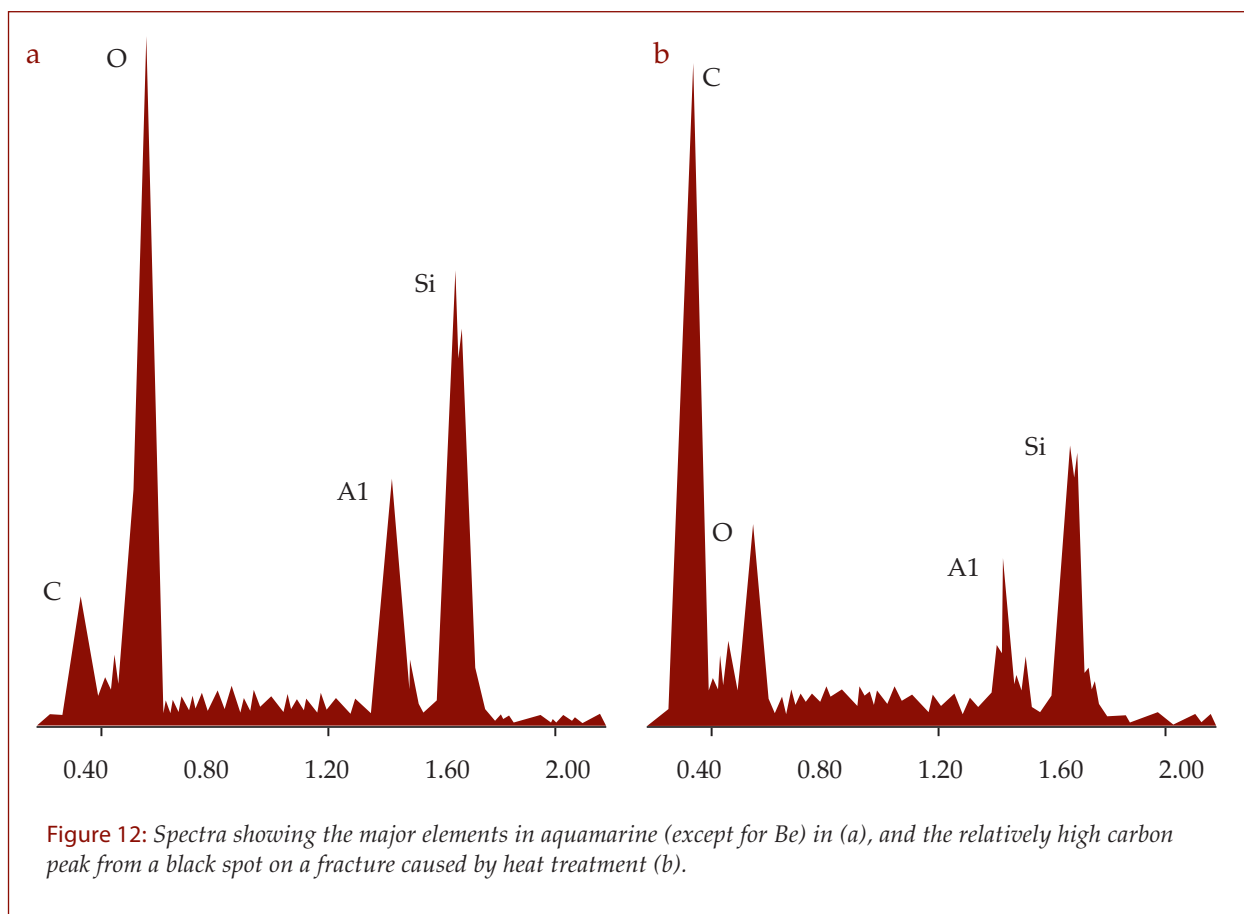
# Conclusions

a  Heat treatment of Altai aquamarine produced the best results when rough or cut stones were slowly heated to 480-500 C, held at that temperature for 3 hours and slowly cooled.

b  Heat treatment altered the characteristics of inclusions such that natural and treated stones can readily be distinguished.

c  Inclusions with spidery structures or dark spots have resulted from the reduction of their contents of carbon-bearing fluids during heat treatment.

# References

He, J.M., Shi, J., Guo, F.W., and Lai, J.Z., 1995. *Gemstone color-altering crafts and identification*. Xinjiang people publishing house, Xinjiang

Nassau, K., 1998. *Gemstone enhancement*. Butler and Tanner Ltd, Frome and London

Wang, S., 1999. *China gemstone resources*. Scientific and technical documents publishing house, Beijing

# A remarkably large clinohumite

Gagan Choudhary and Chaman Golecha

*Gem Testing Laboratory, Rajasthan Chamber Bhavan, Mirza Ismail Road,*
*Jaipur 302 003, India*
*Email gtljpr_jpl@sancharnet.in*

**Abstract:** *Recently a remarkably large clinohumite weighing 9.45 ct was identified at the Gem Testing Laboratory, Jaipur, India. This bright brownish-orange specimen of clinohumite was said to be from the Pamir Mountains, Tajikistan. Clinohumite, a rare magnesium silicate, is a monoclinic member of the humite group of minerals and is usually found in weights below three carats. This study reviews the gemmological properties, internal features and IR spectrum of the specimen. The colour, its remarkable size and the observed magnification features proved it a collectors' gem.*

## Introduction

Most commonly found only as small grains, large clinohumite crystals are rare and sought by collectors; some are fashioned into bright yellow-orange gemstones. Though the mineral has been known for a long time, gemmy crystals have been available in the international market only for the past two decades or so. Gem-quality clinohumite is known to occur in two important localities — the Pamir Mountains (at Kukh-i-lal, Sumdzin and Changin), in Tajikistan in association with spinel and in the Taymyr region (Basin of Kotui River) in Siberia (O'Donoghue, 2006, p.400; Henn *et al.*, 2001; Laurs and Quinn, 2004). Another find of clinohumite has been reported in association with spinel in Mahenge, Tanzania (Hyrsl, 2001). Recently, a large brownish-orange clinohumite was submitted for identification at the Gem Testing Laboratory, Jaipur.

## Specimen description

The specimen (*Figure 1*) is an oval mixed cut measuring 15.13 × 10.41 × 7.78 mm and weighing 9.45 ct. It is transparent and has a bright brownish-orange colour resembling some hessonite and spessartine garnets. The stone is slightly included with eye-visible inclusions (again *Figure 1*) and was reported to be from Tajikistan.



Figure 1: *Brownish-orange clinohumite of 9.45 ct. Photo by G. Choudhary.*

# Gemmological properties

Using traditional gemmological equipment, the stone's properties were determined and are summarized in *Table I*. Refractive index (RI) and birefringence are consistent with the values mentioned in literature (O'Donoghue, 2006; Henn *et al.*, 2001; Laurs and Quinn, 2004; Arem, 1987, p.113-14). The specimen exhibited a strong pleochroism with yellow, orange and brownish yellow being the three hues, and under the short wave ultraviolet light (SWUV) it displayed strong orange-yellow fluorescence with a surface-related greenish-yellow chalkiness (*Figure 2*). The surface-related chalkiness under SWUV reminded us of the fluorescence commonly associated with brown glass coloured by uranium.

# Internal features

Inclusions and other features were observed in the stone under immersion using both vertical and horizontal type microscopes.

Table I: *Gemmological properties of a clinohumite weighing 9.45 ct*

| Colour | Brownish orange |
|---|---|
| Diaphaneity | Transparent |
| RI | 1.646 - 1.670 |
| Birefringence | 0.024 |
| Optic character/ sign | Anisotropic, biaxial positive |
| Pleochroism | Strong trichroism: yellow, orange and brownish yellow |
| SG | 3.21 |
| Visible spectrum | Complete absorption of wavelengths shorter than 430 nm |
| SWUV | Strong orange-yellow with surface greenish- yellow chalkiness |
| LWUV | Inert |
| Chelsea colour filter | No change to body colour |

## *Growth-related features*

The specimen exhibits dominant zones in one direction throughout most of the stone, but there is an angular pattern at the narrow end. The overall complex pattern of the growth zoning is probably an indication of the shape of the original crystal. Colour zoning is coincident with the growth zoning only in patches (*Figure 3*).

## *Swirl-like features*

Swirl-like structures are present almost throughout the stone and these may indicate the outlines of intergrown individual crystals (*Figure 4*). Swirl features are commonly present in glasses and may occur in some natural gemstones, such as Mogok ruby. To our knowledge, such inclusions have not been reported in clinohumite.

## *Reflective planes*

The specimen exhibited flat, parallel and highly reflective planes (*Figure 5*) at an inclination to the dominant growth zones. These may represent incipient cleavage although clinohumite cleavage is reported as poor.

## *Fluid inclusions*

Feathers: The stone contains fluid inclusions in various structures, the most obvious of which are the 'feathers' or 'fingerprints' (*Figure 6*). These have the appearance of fine hair and show high reflection strongly resembling the inclusions common in tourmaline which have been described as 'trichites'. At higher magnification two phase inclusions within the trichites may be visible.

Oriented multiphase inclusions: Many multiphase (mainly two-phase but some also with black crystals) inclusions were observed in certain parts of the stone. They are contained in long, tubes with a slightly corroded appearance which are oriented in a single direction. The nature of the inclusions can be complex (*Figure 7*) and some reminded us of those seen in kunzite.
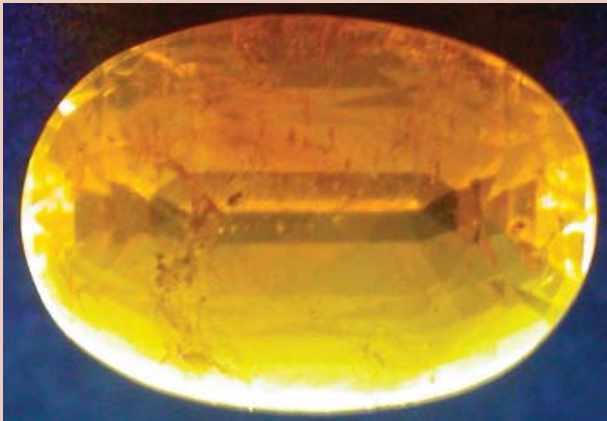
Figure 2: *Strong yellow-orange fluorescence of the clinohumite under SWUV radiation; also note the surface-related greenish-yellow chalkiness. Photo by G. Choudhary.*
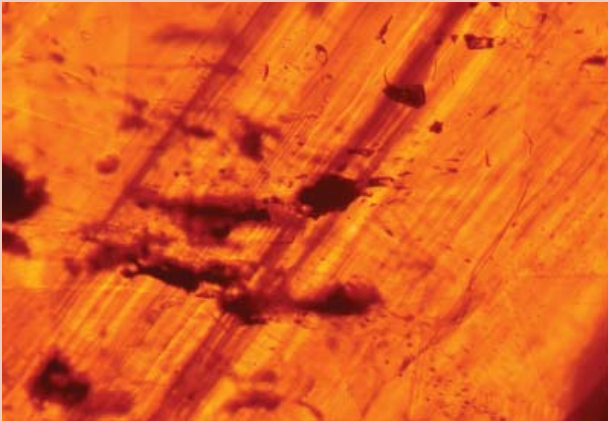


Figure 3: *Strong colour zoning is visible along the dominant growth zones; in some parts of the stone it gave a patchy effect. Diffused; magnified 30×. Photo by C. Golecha.*
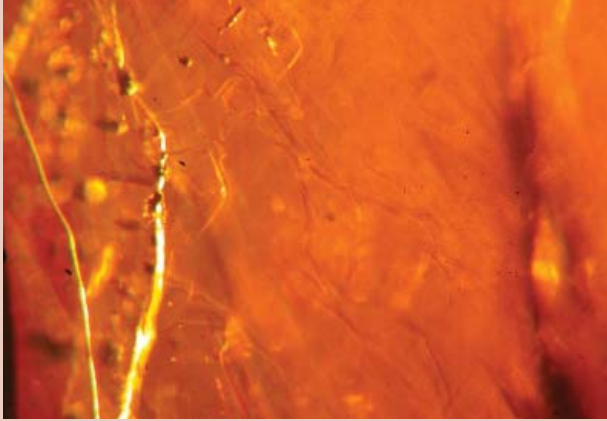


Figure 4: *Swirl like patterns resembling those in some glasses; magnified 35×. Photo by G. Choudhary.*



Figure 5: *Highly reflective, flat, one directional planes of weakness were observed. Note the fine tube like inclusions vertically oriented on the right side. Crossed polars; magnified 25×. Photo by M.B. Vyas.*
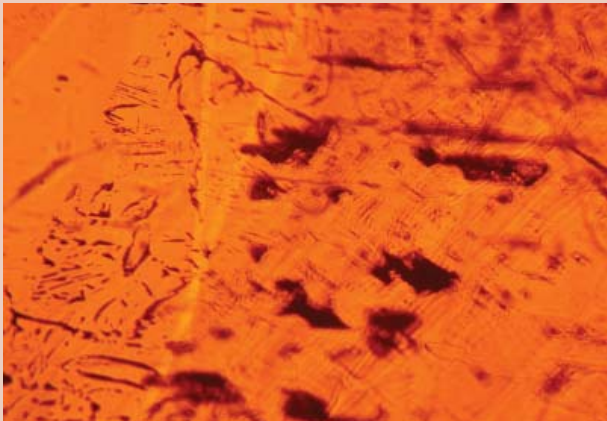


Figure 6: *The clinohumite is host to many types of fluid inclusions, most striking of which are inclusions resembling the 'trichites' seen in tourmaline. Magnified 35×. Photo by C. Golecha.*
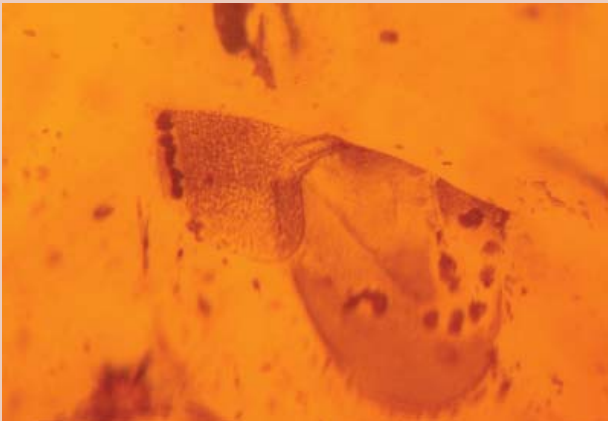


Figure 7: *Fluid inclusions are also present in the form of 'fingerprints' with a hazy or folded appearance. Diffused light; immersion; magnified 35×. Photo by C. Golecha.*

**Figure 8:** *Infrared spectrum of the clinohumite.*
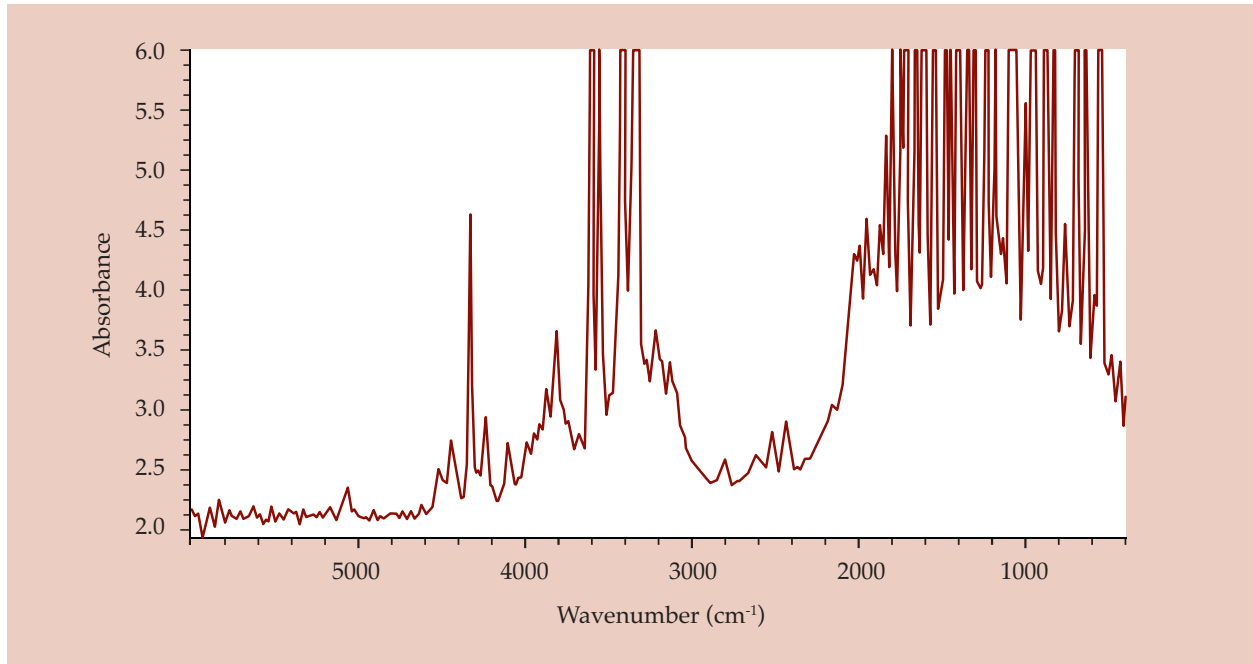


## Infrared spectrum

An infrared spectrum was obtained using a Fourier Transform Infrared Spectroscopy (FTIR) Avatar Nicolet 360 ESP model. The range recorded was 400 to 6000 cm$^{-1}$ (*Figure 8*) and the spectrum showed complete absorption between 400 and 2000 cm$^{-1}$ with numerous peaks between 2400 and 4500 cm$^{-1}$. The authors were unable to obtain a standard infrared spectrum of clinohumite for comparison so this spectrum is presented as a basis for further work.

## Discussion

The 9.45 ct specimen described is a rare example of a large gem-quality clinohumite. More and more stones are making their way to the gem trade in Jaipur from neighbouring countries such as Pakistan and Afghanistan, a fact reflected in the increase in the stones received for identification at the Gem Testing Laboratory in Jaipur. This specimen was submitted to us by a gem merchant with the information that it had been recovered from the spinel mines in the Pamir Mountains and had been transported through Afghanistan. However, the dealer had no idea that it was clinohumite, a gem that was new to him.

## Acknowledgement

## References

Arem, J.E., 1987. *Color Encyclopedia of Gemstones,* second edition. Van Nostrand Reinhold, New York, 248 pp

Henn, U., Hyrsl, J., and Milisenda, C.C., 2001. Gem-quality clinohumite from Tajikistan and the Taymyr region, Northern Siberia. *Journal of Gemmology,* 27(6), 335-9

Hyrsl, J., 2001. Gem News International. Spinel with clinohumite from Mahenge, Tanzania. *Gems & Gemology,* 37(2), 144-5

Laurs, B.M., and Quinn, E.P., 2004. Gem News International. Clinohumite from the Pamir Mountains, Tajikistan. *Gems & Gemology,* 40(4), 337-8

O'Donoghue, M., 2006. *Gems: Their Sources, Descriptions and Identification*, sixth edition. Butterworth-Heinemann, Burlington, USA, 873 pp

# Gem-quality garnets: correlations between gemmological properties, chemical composition and infrared spectroscopy

Ilaria Adamo[1], Alessandro Pavese[1,2], Loredana Prosperi[3], Valeria Diella[2] and David Ajò[4,5]

1. Dipartimento di Scienze della Terra, Sezione Mineralogia, Università degli Studi di Milano, Via Botticelli 23, 20133 Milano, Italy
2. Istituto per la Dinamica dei Processi Ambientali (I.D.P.A.), Consiglio Nazionale delle Ricerche (C.N.R), Sezione di Milano, Via Botticelli 23, 20133 Milano, Italy
3. Istituto Gemmologico Italiano (I.G.I.), Viale Gramsci 228, 20099 Sesto San Giovanni, Milano, Italy
4. Istituto di Chimica Inorganica e delle Superfici (I.C.I.S.), Consiglio Nazionale delle Ricerche (C.N.R.), Corso Stati Uniti 4, 35127 Padova, Italy
5. Gruppo di Coordinamento per la Ricerca sui Materiali Gemmologici, Progetto Finalizzato Materiali Speciali per Tecnologie Avanzate II, Consiglio Nazionale delle Ricerche (C.N.R.), Italy

**Abstract:** *A suite of 19 natural gem-quality garnets has been investigated to determine the correlations between those measurable quantities which are effective in their identification. The results reveal that IR spectroscopy, along with gemmological and chemical analyses, can provide sufficient data to enable positive characterization of garnet gemstones. In particular, the IR active bands over the 1150-800 and 650-450 cm$^{-1}$ ranges allow a discrimination between pyralspite and ugrandite series. Furthermore, pyrope, spessartine and andradite garnets exhibit such mid-infrared patterns that are potentially useful in their identification.*

**Keywords:** *chemical composition, garnet, gem testing, infrared spectroscopy*

## Introduction

The garnet group, or family, hosts a variety of minerals which have often aroused significant interest as gemmological materials for their chromatic and morphological properties (see, for instance, the overview by Stockton and Manson, 1985).

# Analytical methods

We have examined 19 faceted gem-quality natural samples (from 0.20 to 6.84 ct) of different garnet species (*Figure 1*); 17 are transparent and two are opaque (the latter are hydrogrossular garnets). The localities of our specimens are listed in *Table Ia* and *b*.

All the samples have been investigated using standard gemmological methods to determine colour, refractive indices (by means of a Kruss refractometer, using methylene iodide as a contact liquid), specific gravity and absorption lines over the visible energy range, using a hand spectroscope.

The chemical compositions of the samples have been determined in a non-destructive way using an Applied Research Laboratories electron microprobe equipped with five wavelength dispersive spectrometers (WDS) and a Tracor Northern energy dispersive spectrometer (EDS), using an accelerating voltage of 15 kV, a sample current on brass of 15 nA, and counting time of 20 sec on peaks and 5 sec on backgrounds. Natural kaersutite (for Si, Fe, Ti, Al, Mg and Na), chromite (for Cr), rhodonite (for Mn) and pure V have been employed as standards. For determining iron in almandine garnets (samples 2 and 3), natural fayalite was chosen as a standard instead of kaersutite. Ca contents in *pyralspite* and *ugrandite* were determined using standard kaersutite and standard diopside, respectively. $VK\alpha$ and $TiK\beta$-radiations give rise to a well-known interference which has been corrected by an appropriate re-scaling. By normalizing analyses to 12 oxygens and 8 cations, ferric iron contents have been calculated using the method of Droop (1987). The matrix effects have been accounted for through a conventional PAP routine of the SAMx series of programs.

Mid-infrared (4000-400 cm$^{-1}$) spectroscopic investigations have been carried out on all the samples, using a Nicolet NEXUS FTIR spectrophotometer, and results recorded in both reflection and transmission mode. Infrared spectra in reflectance mode, of interest for jewellery applications because it is non-destructive, were recorded using a diffuse reflectance accessory (DRIFT); four spectra at a resolution of 4 cm$^{-1}$ were recorded from each randomly oriented specimen. Further IR-measurements in transmittance mode at a resolution of 4 cm$^{-1}$ have been carried out using KBr compressed pellets with a sample to KBr weight ratio of 1:100, to provide support to the interpretation of the IR-data collected in reflectance mode.



*Figure 1: The 19 faceted garnet samples (from 0.20 to 6.84 ct) investigated in the present study (left: ten pyralspite garnets; right: nine ugrandite garnets) Pictures by Loredana Sangiovanni (IGI).*

As silicates with a general formula $X_3Y_2Si_3O_{12}$ (where X corresponds to $Mg^{2+}$, $Fe^{2+}$, $Mn^{2+}$ or $Ca^{2+}$, and Y to $Al^{3+}$, $Fe^{3+}$, $Ti^{4+}$, $Cr^{3+}$, or $V^{3+}$), almost all natural garnets are solid solutions between two or more end-members of the group. Most garnets belong to two series known as *pyralspite* (pyrope-almandine-spessartine; Y = $Al^{3+}$ and X = $Mg^{2+}$, $Fe^{2+}$, and $Mn^{2+}$, respectively) and *ugrandite* (uvarovite-grossular-andradite; X = $Ca^{2+}$ and Y = $Cr^{3+}$, $Al^{3+}$, and $Fe^{3+}$, respectively). A comprehensive survey of the chemistry and the structure of the garnet group is provided by Deer *et al.* (1997).

Notwithstanding the relevant role that garnets play as gemstones, relatively few studies have been published which relate the gemmological, chemical and spectroscopic features of garnets to enable one to precisely attribute a given specimen to the appropriate series, species and/or variety [the term variety in this context has been defined by Stockton and Manson (1985)].

In the present paper, we combine the results obtained from a suite of gem-quality garnets from some different localities by techniques ranging from traditional gemmological tests to 'modern' spectroscopic approaches (IR-spectroscopy) and advanced chemical determination methods (electron probe micro-analysis), with the aim to:

(i) discover any correlations between gemmological properties, chemical composition and IR vibrational frequencies;

(ii) increase the general knowledge of gemmologically relevant features of garnet gemstones;

(iii) provide a detailed set of spectroscopic and chemical data to help link macroscopic observations to microscopic properties, enabling precise identification.

In such a context, our work joins that of Stockton and Manson (1985) and adds data from the infrared spectra obtained from a range of garnets. Hereafter we adopt the gemmological nomenclature according to Stockton and Manson (1985), complemented by that of Johnson *et al.* (1995), so that one classifies garnet gemstones into nine species (pyrope, almandine, pyrope-almandine,

spessartine, almandine-spessartine, pyrope-spessartine, grossular, andradite and grossular-andradite) and eight varieties (chrome pyrope, rhodolite, malaya, colour-change, tsavorite, hessonite, demantoid and topazolite).

# Gemmological properties

The gemmological properties of the garnets, the colour, refractive index, specific gravity and spectral absorption lines, are summarized in *Table Ia* and *b* (see pages 314-317). Such properties are the foundation of precise identification of the species and/or variety of a given garnet gemstone.

# Chemical composition

The quantitative chemical analyses of the 19 faceted garnets are summarized in Table *Ia* and *b*. The molar composition in terms of end members enables a positive attribution of a specimen to a given garnet series/species/variety to be made. The results are consistent with those obtained from gemmological testing, though they do provide a significantly more detailed characterization.

The compositions of garnets lying in the *pyralspite* range (see *Table Ia* and *Figure 2*), namely pyrope (variety chrome pyrope), almandine, pyrope-almandine (variety rhodolite), spessartine and almandine-spessartine are consistent with those in the literature (Deer *et al.*, 1997; Eeckhout *et al.*, 2002). The pyrope-spessartine variety known by some in the gem trade as 'malaya garnet' contains 52.75 mol.% pyrope, 33.65 mol.% spessartine, 6.10 mol.% grossular and 7.50 mol.% almandine (sample 9), which is consistent with results reported by Schmetzer *et al.* (2001), and shows just small contents of $Cr^{3+}$ and $V^{3+}$. The chromatic behaviour of the colour-change pyrope-spessartine (sample 10) from green in day/fluorescent light to purple in incandescent light, is attributable to a relatively high combined $V_2O_3 + Cr_2O_3$ content of 1.58 wt. %; this is a diagnostic feature of such gemstones with respect to the other pyrope-spessartine garnets (Manson and Stockton,
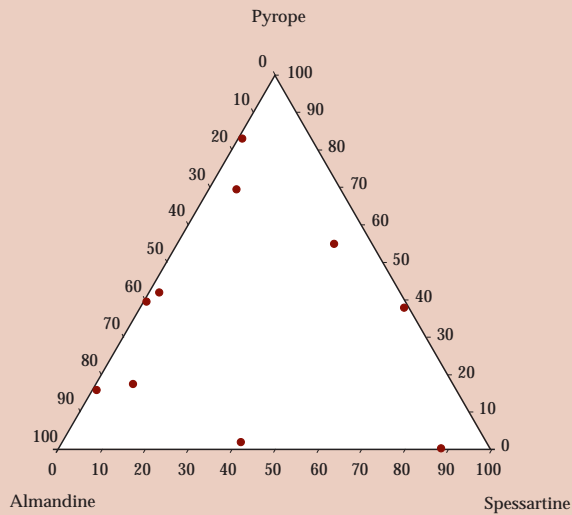
Figure 2: *Pyrope-almandine-spessartine triangular plot of the ten samples belonging to the pyralspite series. For details see Table Ia.*

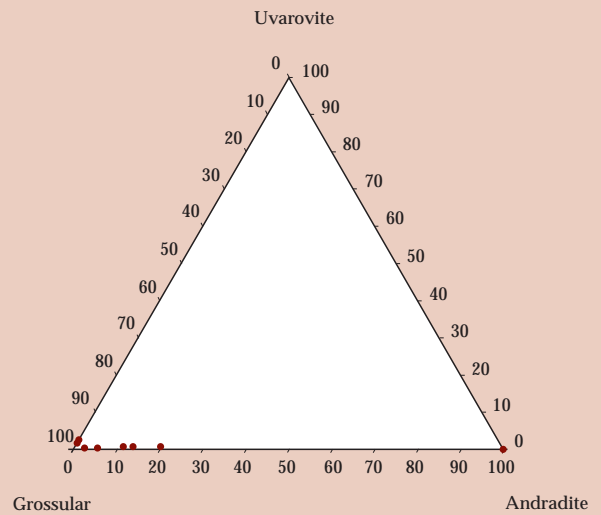Figure 3: *Uvarovite-grossular-andradite triangular plot of the nine samples belonging to the ugrandite series. For details see Table Ib.*
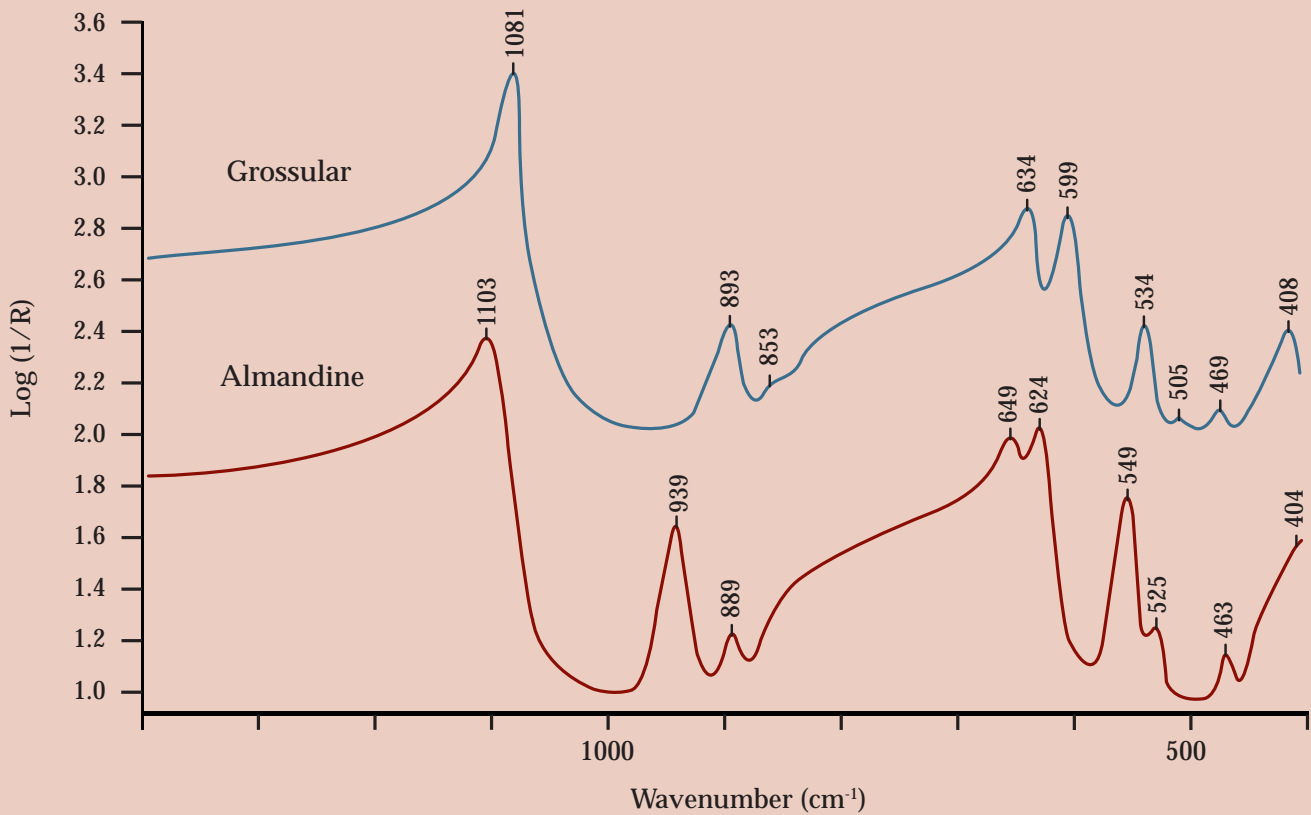


Figure 4: *Mid-infrared spectra (1400-400 cm⁻¹) in reflectance mode for two garnets (almandine and grossular) representative of the pyralspite and ugrandite series.*

1984; Schmetzer and Bernhardt, 1999; Krzemnicki *et al.*, 2001).

Five samples in the *ugrandite* series (see *Table Ib* and *Figure 3*) have compositions typical of grossular (Deer *et al.*, 1997). The tsavorite varieties are distinguishable from pure grossular on the basis of their significant $V_2O_3$ and lesser $Cr_2O_3$ contents, causing a green hue (Kane *et al.*, 1990; Mercier *et al.*, 1997). The grossular variety known as hessonite contains sufficient $Fe^{3+}$ to cause the orange-yellow colour (Kanis and Redmann, 1994; Phillips and Talantsev, 1996). Our andradite sample 16 is greenish yellow, due to its ferric iron content, and has less than 0.02 wt % of $Cr^{3+}$ (Deer *et al.*, 1997; Phillips and Talantsev, 1996). The grossular-andradite, from Mali, has a composition similar to that reported by Johnson *et al.* (1995) and its colour is entirely due to its content of $Fe^{3+}$.

# Infrared spectroscopy

Infrared spectroscopy is sensitive to the composition of a gemstone, as vibrational frequencies are dependent on the nature of the cations involved (Tarte and Deliens, 1973).

The observed infrared bands and frequencies in the 1400-400 cm$^{-1}$ range for all the garnets examined here are listed in *Table II* and *Table III* (see pages 318 and 319), obtained using the diffuse reflectance and transmittance modes respectively. Infrared reflectance patterns in the mid-infrared energy range of two specimens representative of the *pyralspite* and *ugrandite* series [almandine (sample 3) and grossular (sample 11), respectively] are shown in *Figure 4*, by way of example.

With reference to the data collected in reflectance mode (*Table II*), all the spectra are characterized over the 1150-800 cm$^{-1}$ range by three strong absorption bands assigned to the ν3-asymmetric stretching mode of the $SiO_4$ tetrahedron in the garnet structure (Hofmeister and Chopelas, 1991; Hofmeister *et al.*, 1996). The *pyralspite* frequencies range from 1094 to 1125 (mean 1111); from 924 to 945 (mean 938); from 876 to 892 (mean 886) cm$^{-1}$ which are distinct from the *ugrandite*

frequencies which range from 1044 to 1082 (mean 1075); from 867 to 897 (mean 891); and from 825 to 853 (mean 849) cm$^{-1}$, as shown in *Figure 5*. Such frequencies are related to the unit cell edge *a* of the garnet structure (Launer, 1952; Moore and White, 1971; Tarte and Deliens, 1973; Hofmeister *et al.*, 1996; Chaplin *et al.*, 1998) and allow one to immediately say whether a garnet lies in the *pyralspite* or *ugrandite* series (mean *a* 11.535 and 11.968 Å, respectively; see Deer *et al.*, 1997). By comparison with other *pyralspite* and *ugrandite* garnets investigated, our spessartine and andradite samples show lower frequencies of the three bands in question (see for details *Table II* and *Figure 5*).

Similar conclusions are achieved by inspecting patterns in transmission mode over the same energy range, apart from some differences revealed in terms of active bands (four instead of three) and of their related positions (compare *Table II* with *Table III*; for a survey on infrared transmittance bands see also: Moore and White, 1971; Tarte and Deliens, 1973; Hofmeister *et al.*, 1996; Chaplin *et al.*, 1998).

Over the 650-450 cm$^{-1}$ range, absorbance peaks recorded in reflectance mode are ascribable to the ν2-symmetric and ν4-asymmetric bending modes of the $SiO_4$ tetrahedra (see *Table II*, *Table III* and *Figure 6*). In *ugrandites* such frequencies (in cm$^{-1}$) range from 595 to 639 (mean 630), from 549 to 606 (mean 594), from 492 to 535 (mean 529), and from 467 to 506 (mean 499), and are at lower values than in *pyralspite*s which range from 644 to 650 (mean 648), from 612 to 639 (mean 627), from 543 to 559 (mean 552), and from 522 to 528 (mean 525), thus providing a useful marker for discrimination between the two series (Moore and White, 1971; Tarte and Deliens, 1973; Hofmeister and Chopelas, 1991; Hofmeister *et al.*, 1996; Chaplin *et al.*, 1998). At these frequencies, as for the higher frequencies (cf. *Figures 5* and *6*), our spessartine shows lower values than other *pyralspite* garnets and our andradite likewise shows lower values than other *ugrandite* garnets. Pyrope gives IR-patterns with a single band at 639 cm$^{-1}$ (*Table II*,
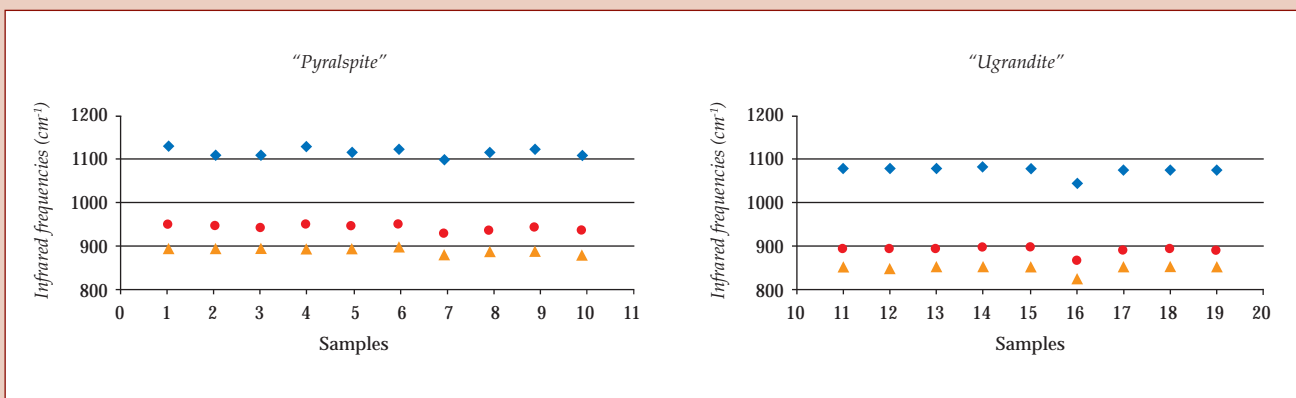
**Figure 5:** *Frequencies of the IR bands, measured in reflectance mode, over the 1150-800 cm$^{-1}$ range for the pyralspite and ugrandite series. Triangles, circles and diamonds correspond to the different IR vibrational frequencies (see also Table II).*
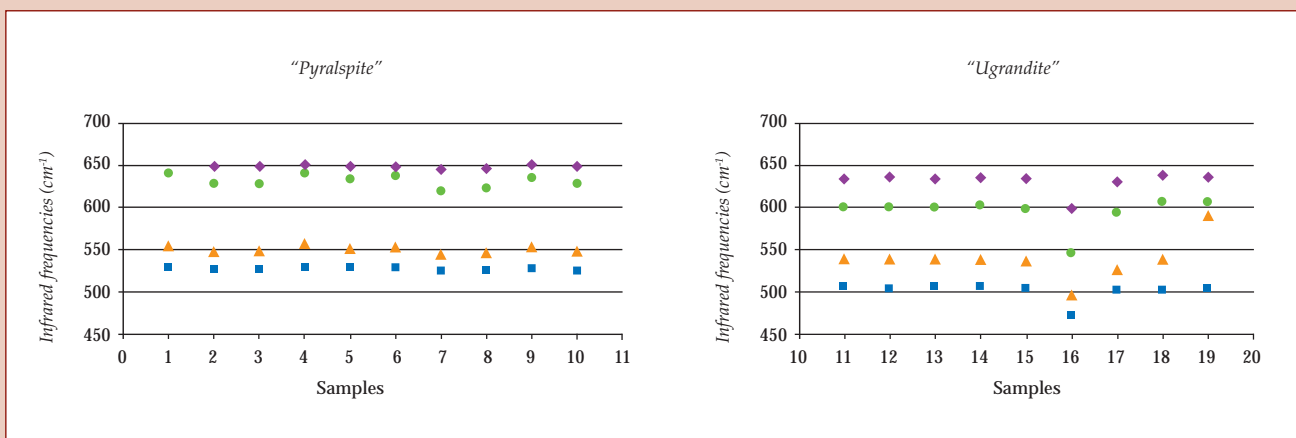


**Figure 6:** *Frequencies of the IR bands, measured in reflectance mode, over the 650-450 cm$^{-1}$ range for the pyralspite and ugrandite series. Again squares, triangles, circles and diamonds correspond to the different IR vibrational frequencies (see also Table II).*

col. 1) compared with the two shown by almandine at 624 and 648 cm$^{-1}$, which is consistent with the results of Moore and White (1971) and Tarte and Deliens (1973). By comparison with other *ugrandite* garnets, andradite has only a single peak at 423 or 436 cm$^{-1}$, in reflectance and transmittance mode, respectively, instead of two.

Lastly, both pink and green hydrogrossular garnets (samples 18 and 19) give IR transmission spectra exhibiting H$_2$O absorption bands, particularly prominent about 3620 and 3600 cm$^{-1}$, in keeping with the hydrogarnet substitution, i.e. [SiO$_4$] ↔

[H$_4$O$_4$]; a broad absorption band at about 3350-3400 cm$^{-1}$ is assigned to non-structural adsorbed H$_2$O (Rossman and Aines, 1991; Amthauer and Rossman, 1998).

## Conclusion

Although every garnet gemstone exhibits a unique set of gemmological characteristics defining its identity (colour, refractive index, specific gravity and visible spectral features, observed through a hand spectroscope), mid-infrared spectroscopy and electron micro-analytic methods yield

additional useful information. Electron microprobe analyses can enable specification of series, species and variety, providing a full compositional characterization. IR-spectroscopy in reflectance mode proves to be an effective auxiliary diagnostic tool. The positions of the IR absorption bands in the 1150-800 and 650-450 cm$^{-1}$ ranges allow an immediate discrimination between the *pyralspite* and *ugrandite* families. Moreover, pyrope, spessartine and andradite garnets possess such IR-patterns that are potentially useful in their identification.

## Acknowledgements

## References

Amthauer, G., and Rossman, G.R., 1998. The hydrous component in andradite garnet. *American Mineralogist*, 83(7-8), 835-40

Chaplin, T., Price, G.D., and Ross, N.L., 1998. Computer simulation of the infrared and Raman activity of pyrope garnet, and assignment of calculated modes to specific atomic motions. *American Mineralogist*, 83(7-8), 841-7

Deer, W.A., Howie, R.A., and Zussman, J., 1997. *Rock-forming Minerals. Vol. 1A: Orthosilicates (2$^{nd}$ edn)*. The Geological Society, London, 467-698

Droop, G.T.R., 1987. A general equation for estimating Fe$^{3+}$ concentrations in ferromagnesian silicates and oxides from microprobe analyses, using stoichiometric criteria. *Mineralogical Magazine*, 51, 431-5

Eeckhout, S.G., Castañeda, C., Ferreira, A.C.M., Sabioni, A.C.S., De Grave, E., and Vasconcelos, D.C.L., 2002. Spectroscopic studies of spessartine from Brazilian pegmatites. *American Mineralogist*, 87(10), 1297-306

Hofmeister, A.M., and Chopelas, A., 1991. Vibrational spectroscopy of end-member silicate garnets. *Physics and Chemistry of Minerals*, 17(6), 503-26

Hofmeister, A.M., Fagan, T.J., Campbell, K.M., and Schaal, R.B., 1996. Single-crystal IR spectroscopy of pyrope-almandine garnets with minor amounts of Mn and Ca. *American Mineralogist*, 81, 418-28

Johnson, M.L., Boehm, E., Krupp, H., Zang, J.W., and Kammerling, R.C., 1995. Gem-quality grossular-andradite: a new garnet from Mali. *Gems & Gemology*, 31(3), 152-66

Kane, R.E., Kampf, A.R., and Krupp, H., 1990. Well-formed tsavorite gem crystals from Tanzania. *Gems & Gemology*, 26(2), 142-8

Kanis, J., and Redmann, M., 1994. Four hessonite occurrences in Orissa, India. *Journal of Gemmology*, 24(2), 75-83

Krzemnicki, M.S., Hänni, H.A., and Reusser, E., 2001. Colour-change garnets from Madagascar: comparison of colorimetric with chemical data. *Journal of Gemmology*, 27(7), 395-408

Launer, P.J., 1952. Regularities in the infrared absorption spectra of silicate minerals. *American Mineralogist*, 37(1-2), 764-84

Manson, D.V., and Stockton, C.M., 1984. Pyrope-spessartine garnets with unusual color behavior. *Gems & Gemology*, 20(4), 200-7

Mercier, A., Moine, B., Delorme, J., and Rakotondrazafy, M.A.F., 1997. A note on a new occurrence of vanadian grossular garnet from Madagascar. *Journal of Gemmology*, 25(6), 391-3

Moore, R.K., and White, W.B., 1971. Vibrational spectra of the common silicates: I. The garnets. *American Mineralogist*, 56(1-2), 54-71

Phillips, Wm.R., and Talantsev, A.S., 1996. Russian demantoid, czar of the garnet family. *Gems & Gemology*, 32(2), 100-11

Rossman, G.R., and Aines, R.D., 1991. The hydrous component in garnets: grossular-hydrogrossular. *American Mineralogist*, 76(1-2), 1153-64

Schmetzer, K., and Bernhardt, H.-J., 1999. Garnets from Madagascar with a color change of blue-green to purple. *Gems & Gemology*, 35(4), 196-201

Schmetzer, K., Hainschwang, T., Kiefert, L., and Bernhardt, H.J., 2001. Pink to pinkish orange malaya garnets from Bekily, Madagascar. *Gems & Gemology*, 37(4), 296-308

Stockton, C.M., and Manson, D.V., 1985. A proposed new classification for gem-quality garnets. *Gems & Gemology*, 21(4), 205-18

Tarte, P., and Deliens, M., 1973. Correlations between the infrared spectrum and the composition of garnets in the pyrope-almandine-spessartine series. *Contributions to Mineralogy and Petrology*, 40(1), 25-37

Table Ia: Physical and chemical properties of pyralspite garnets

| Properties | Samples[a] 1 | 2 | 3 | 4 | 5 | 6 | 7 | 8 | 9 | 10 |
|---|---|---|---|---|---|---|---|---|---|---|
| | Pyrope var. chrome pyrope | Almandine | Almandine | Pyrope-almandine var. rhodolite | Pyrope-almandine var. rhodolite | Pyrope-almandine var. rhodolite | Spessartine | Almandine-spessartine | Pyrope-spessartine var. malaya | Pyrope-spessartine var. colour-change |
| Colour | red | purplish red | purplish red | red-purple | red-purple | red-purple | orange | orange-red | yellowish orange | green (daylight) purple (incandescent light) |
| Refractive index[b] | 1.741 | >1.79 | >1.79 | 1.750 | 1.778 | 1.778 | >1.79 | >1.79 | 1.754 | 1.775 |
| Specific gravity | 3.68 | 4.19 | 4.14 | 3.81 | 3.96 | 3.98 | 4.13 | 4.27 | 3.83 | 4.00 |
| Spectral absorption features (hand spectroscope) | a 445 nm cutoff; a weak band at 505 nm; a broad band at 564 nm; and a pair of thin bands at 684 and 670 nm | bands at 423, 438, 460, 505, 520, 573, 610 nm; a band at 690 nm | bands at 423, 438, 460, 505, 520, 573, 610 nm; a band at 690 nm | bands at 423, 438, 460, 504, 524, 574, 614 nm; a band at 691 nm | bands at 423, 438, 460, 505, 520, 573, 610 nm; a band at 690 nm | bands at 423, 438, 460, 505, 524, 575, 610 nm; a band at 690 nm | three bands at 410, 421 and 430 nm forming a cutoff at about 435 nm; bands at 460, 480, 520 nm; a weak band at 573 nm | a 435 nm cutoff; bands at 460, 480, 504 and 573 nm | three bands at 410, 421 and 430 nm forming a cutoff at about 435 nm; bands at 462, 480, 504, 520, 573 nm | three bands at 410, 421 and 430 nm forming a cutoff at about 435 nm; bands at 460, 480, 504, 520; a broad band at 573 nm |
| Oxide (wt.%)[c] | | | | | | | | | | |
| $SiO_2$ | 40.81 | 35.42 | 38.10 | 40.68 | 39.47 | 40.61 | 36.30 | 35.47 | 40.73 | 39.23 |
| $TiO_2$ | 0.21 | 0.02 | 0.01 | 0.02 | 0.04 | 0.01 | 0.13 | 0.03 | 0.03 | 0.08 |
| $Al_2O_3$ | 23.07 | 21.58 | 20.65 | 23.05 | 21.63 | 21.56 | 20.64 | 20.63 | 23.23 | 21.67 |
| $Cr_2O_3$ | 01.41 | 0.02 | 0.03 | 0.05 | 0.04 | 0.01 | bdl[d] | 0.01 | 0.01 | 0.36 |
| $Fe_2O_3$ | 03.00 | 03.52 | - | 1.86 | 0.18 | - | 0.19 | 02.14 | 0.06 | - |
| FeO | 07.03 | 34.32 | 33.20 | 11.23 | 24.36 | 27.36 | 05.23 | 24.08 | 03.53 | 0.51 |
| MnO | 0.34 | 0.47 | 3.47 | 3.09 | 1.04 | 0.33 | 37.28 | 16.75 | 15.99 | 24.18 |
| MgO | 20.49 | 03.68 | 4.47 | 18.11 | 10.83 | 10.53 | 0.01 | 0.44 | 14.23 | 8.71 |
| CaO | 03.81 | 0.76 | 0.57 | 1.52 | 1.86 | 0.47 | 0.33 | 0.26 | 02.34 | 3.56 |
| $Na_2O$ | 0.04 | 0.01 | 0.01 | 0.01 | 0.01 | 0.02 | 0.02 | 0.06 | 0.02 | 0.03 |
| $K_2O$ | 0.01 | bdl | bdl | 0.01 | 0.03 | 0.01 | bdl | bdl | 0.01 | 0.02 |
| $V_2O_3$ | bdl | bdl | bdl | bdl | bdl | bdl | bdl | bdl | 0.01 | 1.22 |
| Total | 100.22 | 99.80 | 100.51 | 99.63 | 99.49 | 100.91 | 100.13 | 99.87 | 100.20 | 99.57 |

| Numbers of ions on the basis of 12 oxygens | | | | | | | | | | |
|---|---|---|---|---|---|---|---|---|---|---|
| Si | 3.007 | 3.001 | 2.931 | 2.987 | 3.081 | 3.019 | 2.960 | 3.034 | 2.864 | 2.904 |
| Ti | 0.005 | 0.002 | 0.002 | 0.008 | 0.001 | 0.002 | 0.001 | 0.001 | 0.001 | 0.011 |
| Al | 1.958 | 2.016 | 2.009 | 2.002 | 1.928 | 1.950 | 1.976 | 1.938 | 2.056 | 1.935 |
| Cr | 0.022 | 0.001 | 0.001 | - | 0.001 | 0.002 | 0.003 | 0.002 | 0.001 | 0.079 |
| $Fe^{3+}$ | - | 0.003 | 0.133 | 0.012 | - | 0.011 | 0.102 | - | 0.214 | 0.161 |
| $Fe^{2+}$ | 0.033 | 0.218 | 1.664 | 0.360 | 1.736 | 1.558 | 0.683 | 2.211 | 2.320 | 0.418 |
| Mn | 1.570 | 0.998 | 1.173 | 2.598 | 0.021 | 0.067 | 0.190 | 0.234 | 0.032 | 0.021 |
| Mg | 0.995 | 1.563 | 0.054 | 0.001 | 1.191 | 1.235 | 1.964 | 0.531 | 0.444 | 2.174 |
| Ca | 0.293 | 0.184 | 0.023 | 0.029 | 0.038 | 0.152 | 0.119 | 0.049 | 0.066 | 0.291 |
| Na | 0.004 | 0.003 | 0.001 | 0.003 | 0.003 | 0.002 | 0.001 | 0.002 | 0.002 | 0.006 |
| K | 0.002 | 0.001 | - | - | 0.001 | 0.003 | 0.001 | - | - | 0.001 |
| V | 0.075 | 0.001 | - | - | - | - | - | - | - | - |
| **Mol.% end members** | | | | | | | | | | |
| Grossular | 5.42 | 6.10 | - | 0.38 | 1.25 | 4.41 | - | 1.50 | - | - |
| Almandine | 1.14 | 7.50 | 57.10 | 12.04 | 58.14 | 51.72 | 23.11 | 73.11 | 81.10 | 14.40 |
| Pyrope | 34.42 | 52.75 | 1.90 | 0.04 | 39.90 | 41.00 | 66.44 | 17.55 | 15.50 | 74.90 |
| Spessartine | 54.32 | 33.65 | 40.20 | 86.94 | 0.71 | 2.24 | 6.44 | 7.74 | 1.10 | 0.70 |
| Andradite | - | - | 0.80 | 0.60 | - | 0.53 | 4.01 | - | 2.30 | 8.30 |
| Uvarovite | 1.05 | - | - | - | - | 0.10 | - | 0.10 | - | 1.70 |
| Goldmanite | 3.65 | - | - | - | - | - | - | - | - | - |

[a] The localities of garnets are Arizona, India, Sri Lanka, Sri Lanka, Sri lanka, Sri Lanka, Namibia, Sri Lanka, Tanzania, Tanzania, Tanzania for 1, 3, 4, 5, 6, 7, 8, 9, 10 samples, respectively. The source of sample 2 is unknown.
[b] As observed through a Kruss refractometer.
[c] The number of averaged points are 10, 3, 5, 6, 4, 3, 3, 5, 4, 3 for 1, 2, 3, 4, 5, 6, 7, 8, 9, 10 samples, respectively.
[d] bdl=below detection limit (0.01 wt.%)

*Table Ib: Physical and chemical properties of ugrandite garnets*

| Properties | Samples[a] | | | | | | | | |
|---|---|---|---|---|---|---|---|---|---|
| | 11 | 12 | 13 | 14 | 15 | 16 | 17 | 18 | 19 |
| | Grossular | Grossular var. tsavorite | Grossular var. tsavorite | Grossular var. hessonite | Grossular var. hessonite | Andradite | Grossular-andradite | Hydrogrossular | Hydrogrossular |
| Colour | yellow | green | green | yellowish orange | yellowish orange | greenish yellow | greenish yellow | pink | green |
| Refractive index[b] | 1.738 | 1.741 | 1.743 | 1.742 | 1.754 | >1.79 | 1.766 | 1.72[c] | 1.73[c] |
| Specific gravity | 3.59 | 3.62 | 3.65 | 3.66 | 3.65 | 3.88 | 3.66 | 3.03 | 3.54 |
| Spectral absorption features (hand spectroscope) | none | none | none | bands at 407 and 430 nm | bands at 407 and 430 nm | none | band at 440 nm | none | none |
| **Oxide (wt%)[d]** | | | | | | | | | |
| $SiO_2$ | 39.49 | 39.43 | 39.13 | 38.48 | 39.13 | 34.87 | 38.59 | 36.87 | 38.64 |
| $TiO_2$ | 0.52 | 0.39 | 0.43 | 0.02 | 0.20 | 0.05 | 0.56 | 0.01 | 0.06 |
| $Al_2O_3$ | 21.31 | 19.61 | 20.39 | 20.64 | 18.34 | 0.10 | 17.38 | 20.89 | 20.05 |
| $Cr_2O_3$ | 0.02 | 0.34 | 0.18 | bdl[e] | 0.01 | 0.02 | 0.05 | 0.01 | 0.41 |
| $Fe_2O_3$ | 1.80 | 0.02 | - | 4.18 | 4.96 | 31.30 | 6.52 | 0.67 | 1.15 |
| FeO | - | - | 0.01 | - | - | 0.02 | - | - | - |
| MnO | 0.35 | 0.75 | 1.19 | 0.09 | 0.32 | 0.02 | 0.09 | 0.93 | 0.24 |
| MgO | 0.37 | 0.58 | 0.50 | 0.01 | 0.06 | 0.17 | 0.74 | 0.03 | 0.01 |
| CaO | 36.49 | 36.80 | 35.24 | 36.96 | 37.80 | 33.02 | 36.04 | 37.59 | 37.50 |
| $Na_2O$ | 0.03 | 0.02 | bdl | bdl | 0.01 | bdl | 0.02 | 0.01 | bdl |
| $K_2O$ | 0.02 | 0.01 | bdl | bdl | 0.01 | bdl | 0.01 | 0.01 | 0.01 |
| $V_2O_3$ | bdl | 1.14 | 1.48 | bdl | bdl | bdl | bdl | bdl | bdl |
| Total | 100.40 | 99.09 | 98.55 | 100.38 | 100.86 | 99.57 | 100.00 | 97.02 | 98.07 |

| Numbers of ions on the basis of 12 oxygens | | | | | | | | | |
|---|---|---|---|---|---|---|---|---|---|
| Si | 2.982 | 2.802 | 2.960 | 2.968 | 2.983 | 2.914 | 3.002 | 3.016 | 2.969 |
| Ti | 0.004 | 0.001 | 0.032 | 0.003 | 0.011 | 0.001 | 0.025 | 0.023 | 0.029 |
| Al | 1.823 | 1.871 | 1.571 | 0.010 | 1.647 | 1.842 | 1.843 | 1.768 | 1.889 |
| Cr | 0.025 | 0.001 | 0.003 | 0.001 | 0.001 | - | 0.011 | 0.021 | 0.001 |
| $Fe^{3+}$ | 0.067 | 0.038 | 0.377 | 2.004 | 0.284 | 0.238 | - | 0.000 | 0.102 |
| $Fe^{2+}$ | - | - | - | 0.002 | - | - | 0.000 | - | - |
| Mn | 0.016 | 0.060 | 0.006 | 0.001 | 0.021 | 0.006 | 0.077 | 0.049 | 0.022 |
| Mg | 0.002 | 0.003 | 0.085 | 0.021 | 0.006 | 0.001 | 0.057 | 0.067 | 0.042 |
| Ca | 3.101 | 3.060 | 2.962 | 3.010 | 3.087 | 2.998 | 2.897 | 3.016 | 2.940 |
| Na | - | 0.002 | 0.003 | - | 0.001 | - | - | 0.002 | 0.004 |
| K | 0.001 | 0.001 | 0.001 | - | 0.001 | - | - | 0.001 | 0.002 |
| V | - | - | - | - | - | - | 0.091 | 0.070 | - |
| **Mol.% end members** | | | | | | | | | |
| Grossular | 94.61[f] | 95.75[f] | 77.92 | - | 84.50 | 87.90 | 90.40 | 91.48 | 92.75 |
| Almandine | - | - | - | 0.06 | - | - | 0.01 | - | - |
| Pyrope | 0.05 | 0.10 | 2.80 | 0.70 | 0.20 | - | 1.90 | 2.12 | 1.40 |
| Spessartine | 0.51 | 1.91 | 0.20 | 0.04 | 0.66 | 0.20 | 2.54 | 1.55 | 0.70 |
| Andradite | 3.51 | 2.24 | 18.98 | 99.20 | 14.62 | 11.90 | - | 0.05 | 5.10 |
| Uvarovite | 1.32 | - | 0.10 | - | 0.02 | - | 0.54 | 1.09 | 0.05 |
| Goldmanite | - | - | - | - | - | - | 4.61 | 3.71 | - |

[a] The localities of garnets are Tanzania, Tanzania, Sri Lanka, Italy, Mali, South Africa, South Africa for 12, 13, 14, 15, 16, 17, 18, 19 samples, respectively. The source of sample 11 is unknown.

[b] As observed through a Kruss refractometer.

[c] By the distant vision method.

[d] The number of averaged points are 8, 3, 4, 7, 4, 5, 4, 3 for 11, 12, 13, 14, 15, 16, 17, 18, 19 samples, respectively.

[e] bdl=below detection limit (0.01 wt.%).

[f] Consisted of mol. % grossular and hydrogrossular, for samples 18 and 19.

*Table II: Infrared reflectance band frequencies (in cm⁻¹) for all garnets in study*

**Pyralspite**

| 1 | 2 | 3 | 4 | 5 | 6 | 7 | 8 | 9 | 10 |
|---|---|---|---|---|---|---|---|---|---|
| Pyrope var. chrome pyrope | Almandine | Almandine | Pyrope-almandine var. rhodolite | Pyrope-almandine var. rhodolite | Pyrope-almandine var. rhodolite | Spessartine | Almandine-spessartine | Pyrope-spessartine var. malaya | Pyrope-spessartine var. colour-change |
| 1125 | 1102 | 1103 | 1125 | 1112 | 1116 | 1094 | 1109 | 1118 | 1104 |
| 944 | 940 | 939 | 945 | 941 | 944 | 924 | 932 | 938 | 930 |
| 888 | 891 | 889 | 890 | 889 | 892 | 876 | 883 | 884 | 877 |
| - | 648 | 649 | 650 | 649 | 649 | 644 | 646 | 650 | 648 |
| 639 | 624 | 624 | 639 | 631 | 634 | 612 | 616 | 633 | 622 |
| 558 | 548 | 549 | 559 | 553 | 555 | 543 | 545 | 556 | 549 |
| 527 | 524 | 525 | 528 | 526 | 527 | 522 | 522 | 525 | 523 |
| 471 | 463 | 463 | 471 | 467 | 466 | 459 | 460 | 469 | 464 |
| 406 | 404 | 404 | 404 | 405 | 404 | 404 | 404 | 405 | 404 |

**Ugrandite**

| 11 | 12 | 13 | 14 | 15 | 16 | 17 | 18 | 19 |
|---|---|---|---|---|---|---|---|---|
| Grossular | Grossular var. tsavorite | Grossular var. tsavorite | Grossular var. hessonite | Grossular var. hessonite | Andradite | Grossular-andradite | Hydrogrossular | Hydrogrossular |
| 1081 | 1080 | 1081 | 1082 | 1079 | 1044 | 1075 | 1075 | 1077 |
| 893 | 893 | 893 | 897 | 897 | 867 | 891 | 893 | 891 |
| 853 | 850 | 852 | 853 | 853 | 825 | 853 | 851 | 851 |
| 634 | 635 | 633 | 636 | 633 | 595 | 630 | 639 | 635 |
| 599 | 600 | 599 | 601 | 597 | 549 | 593 | 606 | 605 |
| 534 | 535 | 534 | 535 | 532 | 492 | 528 | 534 | 533 |
| 505 | 505 | 506 | 506 | 503 | 467 | 500 | 500 | 502 |
| 469 | 469 | 469 | 472 | 468 | 423 | 465 | 470 | 470 |
| 408 | 410 | 410 | 413 | 411 | - | 408 | 410 | 407 |

*Table III: Infrared transmittance band frequencies (in cm⁻¹) for all garnets in study*

**Pyralspite**

| 1 | 2 | 3 | 4 | 5 | 6 | 7 | 8 | 9 | 10 |
|---|---|---|---|---|---|---|---|---|---|
| Pyrope var. chrome pyrope | Almandine | Almandine | Pyrope-almandine var. rhodolite | Pyrope-almandine var. rhodolite | Pyrope-almandine var. rhodolite | Spessartine | Almandine-spessartine | Pyrope-spessartine var. malaya | Pyrope-spessartine var. colour-change |
| 995 | 996 | 996 | 998 | 995 | 998 | 975 | 998 | 993 | 984 |
| 970 | 966 | 966 | 971 | 968 | 971 | 950 | 959 | 965 | 955 |
| 901 | 902 | 901 | 903 | 901 | 905 | 888 | 895 | 897 | 889 |
| 872 | 874 | 876 | 874 | 876 | 876 | 863 | 869 | 870 | 863 |
| - | - | - | - | - | - | - | - | - | - |
| - | - | - | - | - | - | - | - | - | - |
| - | 638 | 638 | 643 | 643 | 643 | 631 | 634 | 648 | 638 |
| 577 | 571 | 570 | 577 | 573 | 576 | 562 | 566 | 573 | 567 |
| 530 | 527 | 527 | 533 | 529 | 531 | 522 | 524 | 526 | 525 |
| 482 | 477 | 476 | 482 | 479 | 481 | 471 | 473 | 480 | 477 |
| 460 | 452 | 453 | 460 | 457 | 456 | 449 | 450 | 458 | 452 |

**Ugrandite**

| 11 | 12 | 13 | 14 | 15 | 16 | 17 | 18 | 19 |
|---|---|---|---|---|---|---|---|---|
| Grossular | Grossular var. tsavorite | Grossular var. tsavorite | Grossular var. hessonite | Grossular var. hessonite | Andradite | Grossular-andradite | Hydrogrossular | Hydrogrossular |
| 951 | 951 | 951 | 951 | 951 | 929 | 950 | 950 | 951 |
| 915 | 914 | 915 | 916 | 913 | 886 | 911 | 916 | 914 |
| 861 | 860 | 861 | 861 | 859 | 831 | 856 | 860 | 859 |
| 843 | 842 | 843 | 843 | 841 | 811 | 838 | 843 | 843 |
| - | - | 760 | - | - | - | 759 | - | - |
| - | - | 668 | - | - | - | - | 681 | 676 |
| 619 | 620 | 619 | 619 | 617 | 589 | 615 | 616 | 617 |
| 545 | 544 | 544 | 545 | 541 | 510 | 539 | 546 | 544 |
| 505 | 506 | 505 | 503 | 502 | 479 | 500 | 504 | 505 |
| 476 | 474 | 475 | 476 | 473 | 436 | 469 | 476 | 476 |
| 453 | 450 | 453 | 452 | 450 | - | 444 | 448 | 454 |

# Accordance in round brilliant diamond cutting

Michael Cowing, FGA

AGA Certified Gem Laboratory

**Abstract:** *Over more than 150 years, those involved in the diamond industry have worked to establish the ideal angles and proportions to cut the facets of the Standard Round Brilliant (SRB) diamond in order to produce the 'Ideal' gem. This paper reviews milestones in that work and demonstrates that the solutions by major contributors to this endeavour have surprising commonalities. These common aspects are in  accord with the research and investigation of the author as well as the knowledge of diamond cutters and the teaching of diamond cutting institutions.*

**Keywords:** *cut grading, diamond, round brilliant*

## Introduction

The 57-facet Standard Round Brilliant cut (SRB) has evolved over several hundred years. Its finest cut quality has historically been called 'Ideal'. Many consider the Ideal Round Brilliant style of cut superior because its cut quality (called its 'make') brings out the best in diamond beauty, brilliance, fire and sparkle. The quality of these attributes of diamond beauty is referred to as the diamond's 'optical performance' or its 'light performance' (Cowing, 2005).

Diamonds in a range of cut proportions that are seen by diamond cutters and many other experienced observers as having greatest beauty possess the best combination of brilliance, in both its aspects of brightness and contrast, fire, and scintillation (sparkle with movement) (Cowing, 2005). This is the essence of the 'Ideal Round Brilliant'.

Today, consumers in increasing numbers are looking for diamonds with the best possible beauty, i.e. the best light performance. They look to jewellery retailers for proof of perfection of cut. In turn, the jewellers often look to the diamond grading laboratories or gemmologist-appraisers for assistance in providing consumers with confirmation of the quality of their diamond's make.

The laboratories of the Gemological Institute of America (GIA) and the American Gem Society (AGS) appear to be divided as to the finest or ideal make in the round brilliant diamond. The AGS believes "Tolkowsky was right" (Bates, 2004) and that the angles and proportions within a narrow range of the Tolkowsky Ideal have the best optical performance. The GIA has found: "There is no one set of proportions that yields the most beautiful diamond" (Boyajian, 2004). Instead, there are many different proportion sets that are seen as top performers. "The long-held view that expanding deviations from a fixed arbitrary set of proportion

values produces diamonds with increasingly poorer appearances is simply not valid" (Boyajian, 2004).

GIA's grade or measure of make has five levels. The highest is 'Excellent'. The range of angles and proportions that attain the GIA 'Excellent' grade is larger than that of the AGS 'Ideal 0' grade. Although there are significant differences, the 'Excellent' grade is best compared to the top two grades of the 11 grade AGS system, each comprising the top approximately 20% of the grades in both systems.

Several diamond cutting houses and retailers, some grading laboratories, and some gemmologists and researchers including the author, set the bar for the best make higher in some respects than either GIA or AGS. In a sense you could say that they answer to a higher authority. For this investigator, that authority comes from a "direct assessment" of the diamond's optical performance in typical illumination circumstances (Cowing, 2005).

### Consider the commonalities

The question is how to reconcile the differing viewpoints. The answer is found by considering aspects that these different viewpoints have in common. I find that there are more aspects of agreement among the cut grading systems than disagreement. To discover the best round brilliant diamond make, let's look at the aspects in common between the grading systems of all these groups rather than their differences.

## The round brilliant cut sweet spot

If you play or watch golf or tennis, no doubt you will have heard about the 'sweet spot'. This is the area near the middle of a club or racket where the ball is struck with maximum control and speed. Striking the ball within the sweet spot causes it to respond with the best, most consistent performance.

There is also a 'sweet spot' in terms of cutting angles and proportions for peak

diamond performance. The range of this sweet spot encompasses pavilion and crown angles long associated with the 'Ideal' cut. In this sense, the range of angles and proportions said by GIA and AGS to give the best brilliance, fire and sparkle, are their respective sweet spots. When the cutter fashions the diamond with sufficient craftsmanship to obtain a diamond within the sweet spot range, the diamond responds with the best light performance and beauty.

In tennis the best athletes use a racket with the largest sweet spot and aim to hit its centre. In diamond design, the evolution of the 'Ideal' round brilliant has led cutters very close to the centres of the sweet spot of both grading systems. Today's cutters aim close to the centre of the round brilliant's sweet spot when they want to ensure the best light performance and beauty.

Seven parameters are used today to define the round brilliant cut. (Standard 'indexing' or placement of each facet is assumed). These seven parameters are the pavilion main angle, the crown main angle, the table size, the length of the pavilion halves (lower girdle facets), the length of the star facets, the girdle thickness and the culet size. What is most remarkable is the finding of close agreement in the locations of the centres of each group's sweet spot in all seven of these parameter dimensions. As an aid in discussing these parameters, here are descriptions and illustrations of the anatomy of a round brilliant.

## Anatomy of the 57-facet round brilliant cut

The round brilliant cut has two key parts, the top and the bottom known as the crown and pavilion. The diamond's crown and pavilion are joined together at the girdle, where the diamond is at its maximum width.

### The Crown

Most of the brilliance, fire and sparkle reflected to our eyes from within the finest round brilliant cut diamonds comes from light that entered the diamond through its
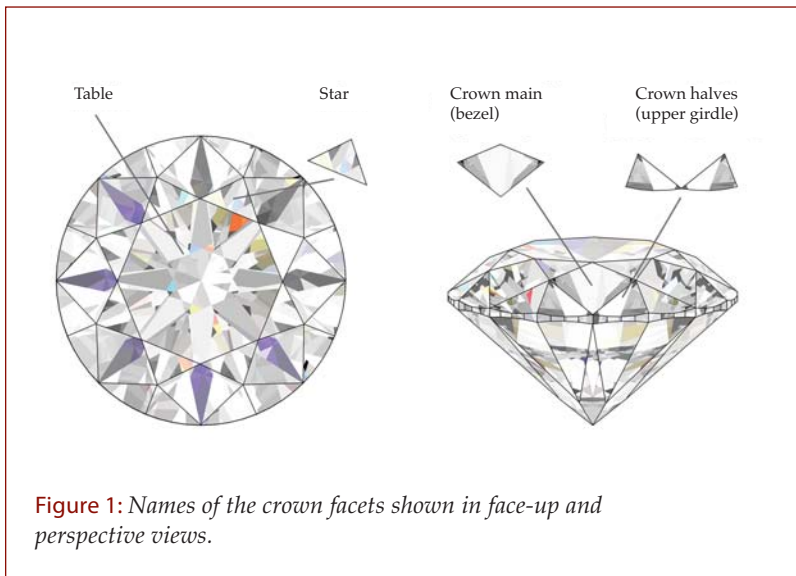
**Figure 1:** *Names of the crown facets shown in face-up and perspective views.*
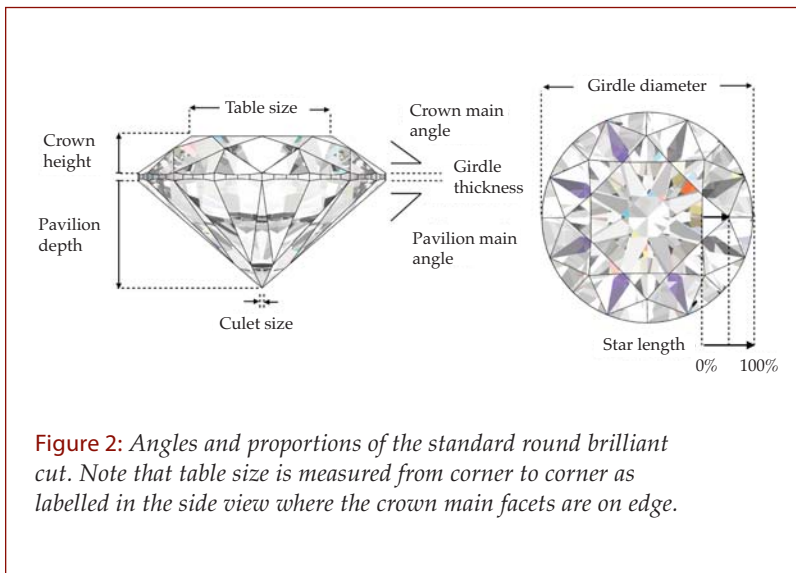


**Figure 2:** *Angles and proportions of the standard round brilliant cut. Note that table size is measured from corner to corner as labelled in the side view where the crown main facets are on edge.*
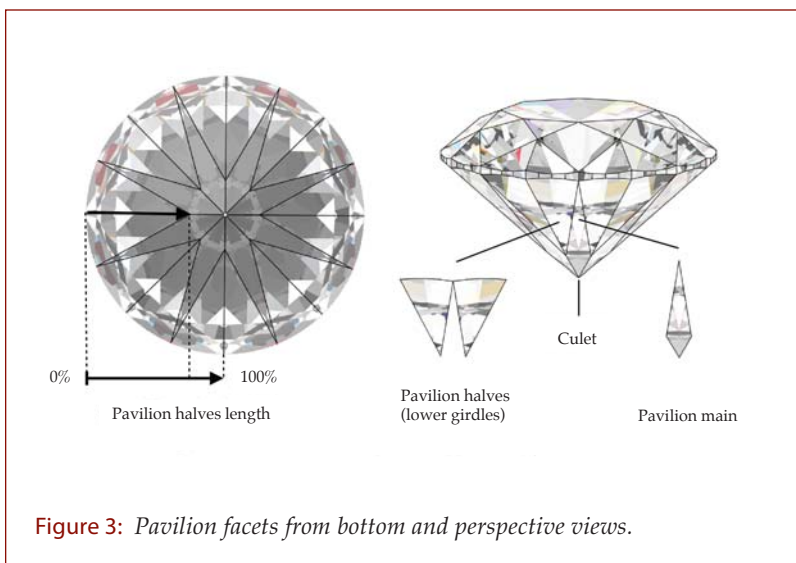


**Figure 3:** *Pavilion facets from bottom and perspective views.*

top section, the crown (see *Figure 1*).

The largest facet, which is centred on the crown, is the octagon-shaped table. Eight triangle-shaped facets called stars surround it. Next are the eight kite-shaped facets called crown mains or bezels. The sixteen crown halves follow the mains. These are also called upper girdle facets, because one of their three sides forms the upper outline of the girdle.

The parameters that uniquely define the crown of the standard round brilliant are shown in *Figure 2*. They are the crown main angle, the table size, the angle of the crown halves and the star angle. An alternative to listing the angle of the crown halves and the angle of the stars is to specify the star length percentage. The star length determines the angles of the stars and halves in the context of a specific crown main angle and table size.

### The pavilion

Below the girdle is the pavilion, which is the principal light-reflecting portion of the round brilliant (*Figure 3*).

The pavilion is comprised of 16 pie-shaped pavilion halves, also called lower girdle facets. Eight pavilion main facets intersect the pavilion halves. A small, octagon shaped, 58th facet may be present at the tip of the pavilion. This point, where the eight pavilion mains come together, is the culet, and this 58th facet is called the culet facet.

All the brilliance, fire and sparkle our eyes see emerging from within the round brilliant through its crown is reflected from either the pavilion mains or the lower halves. Changes in the sizes and angles of the pavilion mains and halves have the greatest effect on the diamond's beauty and optical performance.

### The girdle

The girdle is the thin section whose surface forms the diamond's perimeter. It joins the crown and pavilion. The upper and lower girdle facets, commonly called the halves, form the girdle's scalloped boundaries. The girdle itself may be polished or unpolished. Today it is generally faceted, as shown in *Figures 1, 2* and *3*.

### Facet alignment

In the round brilliant cut, the crown and pavilion halves are aligned across the girdle. The tail of the crown main, kite-shaped facet lines up directly across the girdle from the sharp point of the pavilion main facet.

## Tolkowsky's theory and Morse's Ideal angles

In the 1860s, Henry D. Morse, founder of the first successful American diamond cutting firm, discovered the centre of the diamond's sweet spot in two of the most important of the seven parameters. These are the pavilion main angle and the crown main angle. This was the greatest single stride in the evolution of what today is known as the 'Ideal'. A half-century later, the engineer and diamond cutter, Marcel Tolkowsky (1919) validated these angles theoretically using arguments based on both mathematics and physics.

Since that time, the term 'Ideal Cut' has come to be associated with the angles and proportions of Tolkowsky's theoretical determination. These are a pavilion main angle of 40.75, a crown main angle of 34.5 and a 53% table. However, this definition of the 'Ideal' is incomplete because it addresses only 17 of the 57 important facets defining the round brilliant cut diamond, and the range of the theoretical sweet spot for pavilion angle, crown angle, and table size is not addressed.

Because of the historical overemphasis on Tolkowsky's theoretical angles of 40.75 and 34.5 in association with 'Ideal', it is important to know that the five diamonds that Tolkowsky listed in his book as examples of maximally brilliant diamonds, had pavilion angles from 40 to 41, and crown angles from 33 to 35. These figures provide an implicit sweet spot range. Additionally, Tolkowsky notes in his book that American writers credit Henry D. Morse with first cutting for "maximum brilliancy". The angles that Morse first discovered that were said by writers like Frank B. Wade (1916) and Herbert Whitlock (1917) to yield an 'ideal brilliant' had a range that centred on a 41 pavilion and a 35 crown.

## The centre of the range of Ideal

Frank Wade was an American diamond expert who greatly influenced the thinking about the 'Ideal' cut. He said of Morse's angles: "Within the limits of one or two degrees there is little variation in brilliancy." This accords with today's consensus that there is a range of appropriate angles and proportions producing the best optical performance and beauty. This article calls that range the diamond cutting sweet spot. Differences of opinion are principally in the extent of variation in angles and proportions from those of Morse and Tolkowsky that retain the finest brilliance, fire and sparkle.

It is worth looking at those variations and the centre of the round brilliant cut diamond's sweet spot for not only the crown and pavilion main angles, but all seven of the parameters that define the important facets making up the round brilliant cut.

## Comparing the centres of the sweet spots

We compare the GIA's 'Excellent' range of crown and pavilion main angles in their 5 grade system and the top two grades in the AGS's 11 grade system, because both comprise approximately the top 20% of each laboratory's grading system. Because of the interaction and interrelationship between the diamond's parameters, they must be considered in relation to each other. This is why both GIA and AGS provide charts for each table size showing the range of crown and pavilion main angle combinations that comprise each grade.

## Centre of the sweet spot for the table

*Figure 4* shows, for each table size, the number of combinations of crown and pavilion main angles that may attain the top grade in GIA's and AGS's grading systems.
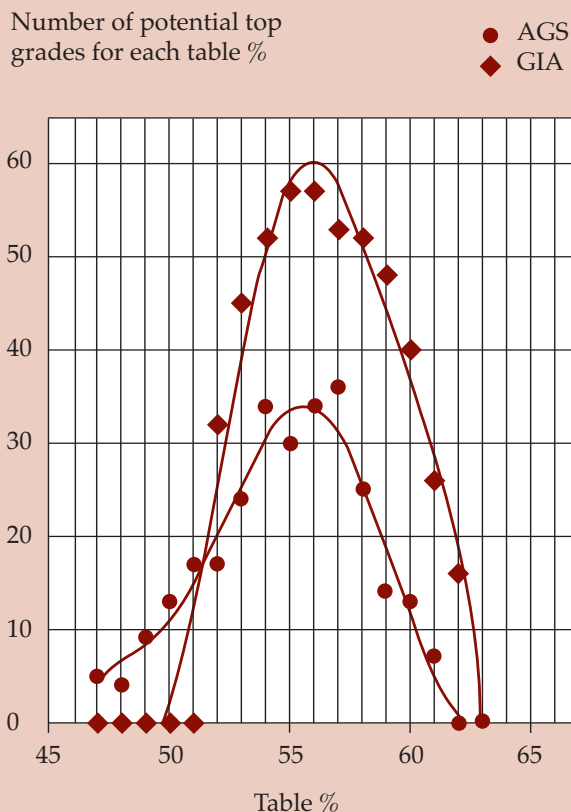


Number of potential top grades for each table %

● AGS
◆ GIA

Table %

**Figure 4**: *Number of combinations of crown and pavilion main angles for each table percentage that may attain the top cut grade.*

A visual assessment of the peak area of each of these curves indicates that the centre of the sweet spot of the table size is closest to 56% in both grading systems. These two curves indicate that table sizes within 2% to 3% of the sweet spot centre of 56% contain a majority of the best combinations of crown and pavilion main angles.

## Sweet-spot centre for the crown and pavilion angles

Let us analyze the combinations of crown and pavilion main angles that receive the top grades in each system for a 56% table. The centres of the GIA and AGS sweet spots are compared with the Morse and Tolkowsky 'Ideal' angle combinations in *Figures 5, 6* and *7*.

The sweet spot of potential 'Excellent' combinations of crown and pavilion angles is outlined in red in *Figure 5*. It has as its centre, indicated by the red spot, a pavilion main angle of 41.2 and a crown main angle of 34.0. Shown in cyan and green are the Tolkowsky angle combination of 40.75 and 34.5 and the Morse angle combination of 41 and 35.

### GIA 'axis of Excellent'

Also shown in *Figure 5* is the negative slope of approximately -4.5 to 1 (red line) that is the axis of the sweet-spot for crown and pavilion angle, the 'axis of Excellent' (The major axis of an ellipse fit to the 'Excellent' sweet spot would have this approximate slope.) Although the GIA 'axis of Excellent' is shown as a line, it is not necessary to be on that line in order to attain the 'Excellent' grade. The slope of this line indicates that a change in pavilion angle from either Morse's or Tolkowsky's angles is best compensated by a 4.5 times change in crown angle in the opposite direction. Notice that Morse's angles are closest to that line. Tolkowsky's angles are in the 'Excellent' range and only slightly shallower by 0.25 in pavilion angle and 0.5 in crown angle.

*Figure 6* is the corresponding AGS cut grade estimation chart for a 56% table. The sweet spot of potential AGS 0 and 1
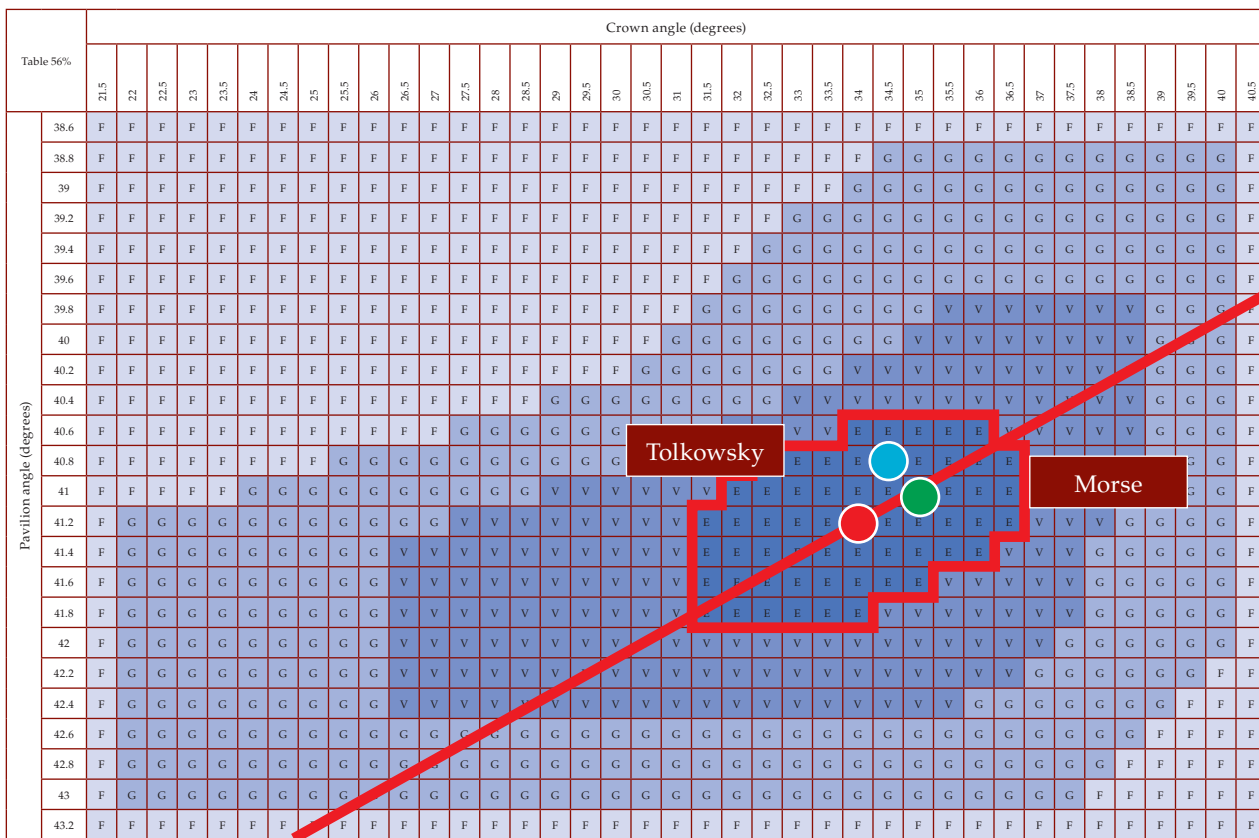
| Table 56% | | Crown angle (degrees) | | | | | | | | | | | | | | | | | | | | | | | | | | | | | | | | | | | | | | |
|---|---|---|---|---|---|---|---|---|---|---|---|---|---|---|---|---|---|---|---|---|---|---|---|---|---|---|---|---|---|---|---|---|---|---|---|---|---|---|---|---|---|
| | | 21.5 | 22 | 22.5 | 23 | 23.5 | 24 | 24.5 | 25 | 25.5 | 26 | 26.5 | 27 | 27.5 | 28 | 28.5 | 29 | 29.5 | 30 | 30.5 | 31 | 31.5 | 32 | 32.5 | 33 | 33.5 | 34 | 34.5 | 35 | 35.5 | 36 | 36.5 | 37 | 37.5 | 38 | 38.5 | 39 | 39.5 | 40 | 40.5 |

Figure 5: *GIA cut grade estimation for a 56% table. The 'sweet-spot' of potential 'Excellent' combinations of crown and pavilion angles is outlined in red. It has as its centre a pavilion main angle of 41.2° and a crown main angle of 34.0° (red spot) compared to the Tolkowsky angles of 40.75° and 34.5° (cyan spot) and the Morse angles of 41° and 35° (green spot).*

combinations of crown and pavilion angles is outlined in blue. It has as its centre, shown with the blue dot, a pavilion main angle of 41.1 and a crown main angle of 33.75

Remarkably, this centre of the sweet-spot for the top 20% of the AGS cut grades has the same pavilion angle within a tenth of a degree and a crown angle that is within a quarter degree of the corresponding centre of GIA's 'Excellent' grade.

## AGS 'axis of Ideal'

The axis of best angle combinations for the AGS 0 and 1, the 'axis of Ideal', also has about the same -4.5 to 1 negative slope as the GIA's 'axis of Excellent'. Tolkowsky's angles fall nearest this axis of best angle combinations. Morse's angles of 41 and 35 are just slightly steeper in crown angle and slightly deeper in pavilion angle. Notice that this range of AGS Ideal 0 and 1 grades, although having a similar slope as the GIA 'axis of Excellent',

is much narrower. It excludes Morse's Ideal angle combinations from the top two grades. Clarification on this point was obtained from AGS (P. Yantzer, pers. comm.) He indicated that the AGS charts are guidelines for the cutters, and the range of AGS 'Ideal 0' is somewhat wider than is shown by their charts. For example, Morse's 'Ideal' angles of 41 and 35 in proper combination with the other five parameters do attain the AGS 'Ideal 0' grade. This is in spite of the chart's indication that the combination of 41 and 35 is an AGS 2.

*Figure 7* is a combined comparison of the AGS 'Ideal 0 and 1' sweet spot with that of the GIA 'Excellent' showing their overlap and the close agreement of the sweet spot centres. So based upon the charts of both GIA and AGS, we observe that the target centre of the sweet-spot of the best round brilliant cut is Morse's 41 for pavilion angle and closer to Tolkowsky's crown angle of
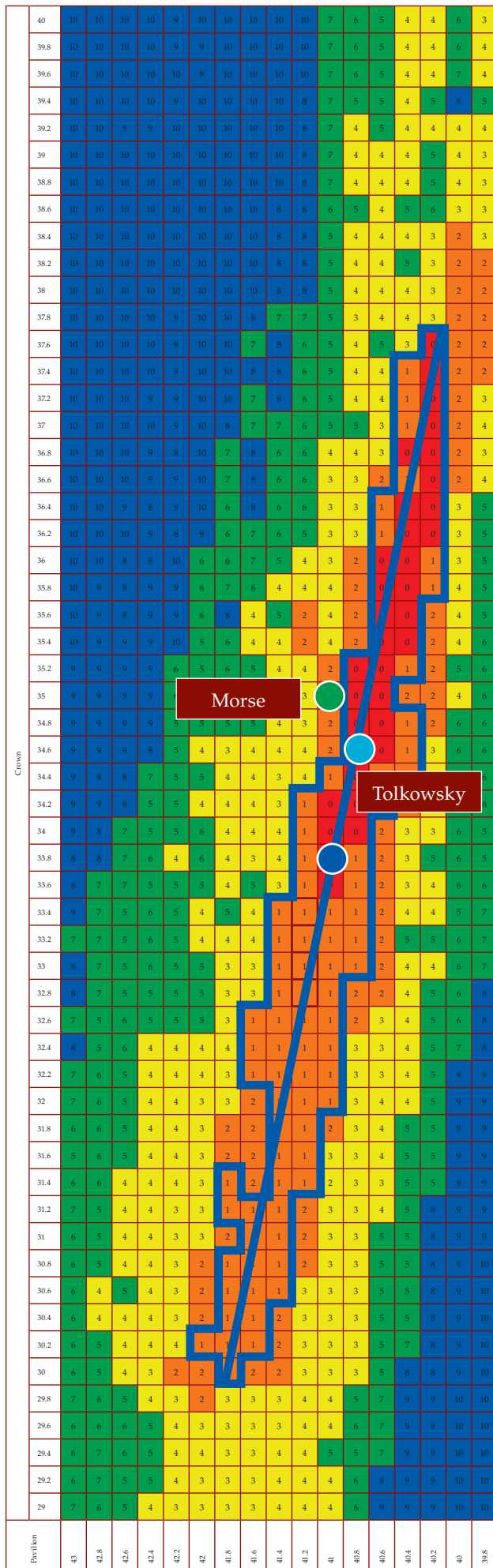
Figure 6: *AGS cut grade estimation for a 56% table. The 'sweet-spot' of potential AGS 0 and 1 combinations of crown and pavilion angles is outlined in blue. It has as its centre a pavilion main angle of 41.1° and a crown main angle of 33.75° compared to the Tolkowsky angles of 40.75° and 34.5° and the Morse angles of 41° and 35°.*

34.5 at 34 . Both 41 and 34 are very close to both the angles of Morse and Tolkowsky. In proper combination with the other five parameters, this sweet-spot centre of 41 and 34 along with the angle combinations of Morse and Tolkowsky all have ideal optical performance and beauty.

This sweet spot centre accords well with this investigator's findings based upon his direct assessment of the diamond's optical performance in typical illumination circumstances. The sweet spot centre of 41 and 34 is also in accordance with the teaching of diamond cutters and diamond cutting institutions. For example, from the 1970s the Institute for Technical Training in Antwerp, Belgium, taught angle combinations of 41 and 34 - 34.2 (pers. comm., D. Verbiest). In the same time frame, but a continent away in Johannesburg, South Africa, the Katz Diamond Cutting Factory was teaching its apprentices to cut the 'Ideal' round brilliant to a 41 pavilion main angle and 33 to 35 crown main angle (pers. comm., P. Van Emmenis).

What about the centre of the sweet spot for each of the other 4 of the 7 parameters defining the round brilliant?

# The importance of the length of the pavilion halves

There is general agreement that it is the interrelationship of all the individual proportions that determine the diamond's performance and beauty. However, the diamond's light performance is most sensitive to changes in the pavilion main angle, the crown main angle and the length of the pavilion halves (lower girdle facets.) We can explore the range of the pavilion
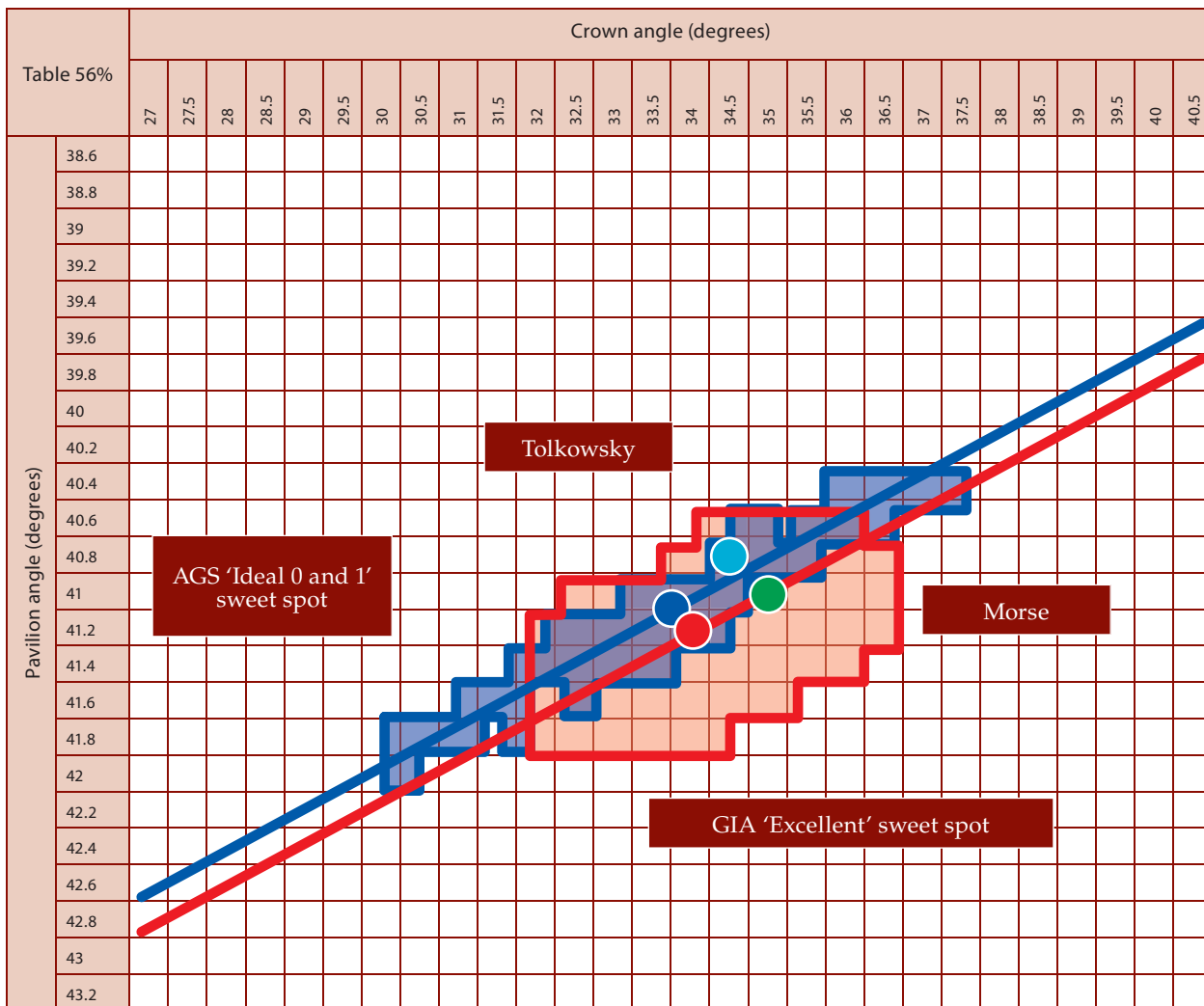
**Crown angle (degrees)**

Table 56%

Pavilion angle (degrees)

Crown angle columns: 27, 27.5, 28, 28.5, 29, 29.5, 30, 30.5, 31, 31.5, 32, 32.5, 33, 33.5, 34, 34.5, 35, 35.5, 36, 36.5, 37, 37.5, 38, 38.5, 39, 39.5, 40, 40.5

Pavilion angle rows: 38.6, 38.8, 39, 39.2, 39.4, 39.6, 39.8, 40, 40.2, 40.4, 40.6, 40.8, 41, 41.2, 41.4, 41.6, 41.8, 42, 42.2, 42.4, 42.6, 42.8, 43, 43.2

Chart labels: Tolkowsky · AGS 'Ideal 0 and 1' sweet spot · Morse · GIA 'Excellent' sweet spot

Figure 7: *A comparison of the AGS 'Ideal 0 and 1' (blue) sweet spot with that of the GIA 'Excellent' (red) showing their overlap and the close agreement of the sweet spot centres.*

halves and the other parameters in the context of the sweet spot centres of the table size, crown angle and pavilion angle.

In the early nineteenth century and before, most of the area of the pavilion was occupied by the main facets, which dominated the diamond's reflection pattern. As can be observed today in 58 facet, triple-cut diamonds from that era, the halves were small compared to those of the modern round brilliant. (Triple

Figure 8: *Modern 'Ideal' round brilliant cut (1.00 ct) and early triple-cut (2.38 ct) under the same 'fire friendly' illumination.*

cut is the term from the nineteenth century for the early 58 facet brilliant cut (Tillander, 1995) that today is popularly referred to as an Old European Cut (Gaal, 1977).) At that time the pavilion halves extended less than half the way to the culet. In contrast, Tolkowsky indicated in his book in 1919 that the high-class brilliant had lower halves two degrees steeper than the pavilion mains. This resulted in a length of the lower halves of about 60%, which was a significant increase in the length and size of the halves from those earlier times.

During the twentieth century, the pavilion halves were further increased in length with consequent increase in their area and influence on the diamond's beauty. The motivation for this increase in the length of the halves was the increased amount of sparkle or scintillation brought about by larger halves. However, a consequence of the increase in the halves in order to favour scintillation was a decrease in the size of the main facets. This brought an accompanying reduction in the desirable properties of large flash sparkle and fire that result from larger mains. This large flash fire and sparkle was a fundamental aspect of the appeal of the early round brilliant from the times of Morse and Tolkowsky.

*Figure 8* shows a 2.38 ct early triple-cut diamond with shorter pavilion halves compared to a 1 ct, 'Ideal' round brilliant with approximately 77% lower halves. Both were photographed in the same 'fire friendly', high contrast, spot illumination. This is lighting favourable to the display of fire. Both are impressive demonstrations of the diamond's fire resulting from white light dispersed into colours of the spectrum. However, larger flashes of fire, due principally to larger mains, are apparent in the early triple-cut compared to the more numerous but smaller flashes of fire in the 'Ideal' cut.

In illumination that is more favourable to brilliance and sparkle, such as that in a typical jewellery store, the comparison between diamonds with shorter and longer pavilion halves reveals a similar contrast in their light performance. That contrast is between the large flashes of brilliance, fire and sparkle due to the larger mains of the early 'Ideal'



Figure 10: *Computer image of a similar 'Ideal' cut diamond in typical viewing and illumination circumstances. The simulated diamond is inset at a smaller magnification to enable comparison at closer to actual size.*

cut and a greater amount of smaller sparkle and fire due to the larger halves and thinner mains of the modern 'Ideal' cut. To further demonstrate this contrast, a modern 'Ideal' cut was simulated (*Figure 10*) with proportions similar to those of the 'Ideal' cut photographed and shown in *Figure 9*. (Comparison of the actual photograph to the computer simulation of the diamond demonstrates the photo-realism and utility of today's computer imaging technology.) Changing just the length of the lower halves of the diamond in *Figure 10* to the 60% of Tolkowsky's time, causes the diamond's mosaic pattern of reflections to return to the large flash brilliance and fire in *Figure 11* that characterized the beauty and appeal of the older brilliant cuts. At the same time, we can appreciate in the modern 'Ideal'



Figure 9: *Photograph of an 'Ideal' cut diamond in typical viewing and illumination circumstances.*

Figure 11: *Computer image of the identical 'Ideal' cut diamond except for a 60% length of the lower halves. The simulated diamond is inset at a smaller magnification to enable comparison at closer to actual size.*



the retention of large flashes along with more numerous smaller flashes of sparkle and fire evident in *Figures 9* and *10*.

This comparison of optical performance and the previous one in *Figure 8* support the observation that an attractive balance between the areas occupied by the mains and halves is necessary for these two central reasons.

A number of individuals, diamond manufacturers, and this investigator agree that the best balance between the area of the main reflections and the area of the halves is obtained with a 75% to 80% length of the pavilion halves. This is the sweet spot range of lower half length that retains the large flash sparkle and fire and at the same time provides a greater amount of scintillation. The range of possible GIA 'Excellent' lower girdle facet lengths is 70% to 85%. Both ranges have the same 77.5% as the centre of the sweet spot of lower half length.

# Agreement on the parameters of girdle and culet size

Of the seven parameters, those of girdle thickness and culet size have the least influence on the brilliant cut's light performance. There is general agreement regarding these two parameters. The noticeably large culets of the past have been determined to detract from diamond beauty. Because it is parallel to the table, a large culet facet appears like a lifeless, dark 'window' in the diamond's centre. This can be seen in the early triple-cut in *Figure 8*. The culet facet has been minimized or eliminated in the modern round brilliant. The girdle thickness is kept thin to medium for two reasons. Any less thickness increases the vulnerability to chipping, and any greater thickness causes the diamond's apparent size (which the trade calls 'spread') to appear noticeably smaller than would be expected for its weight.
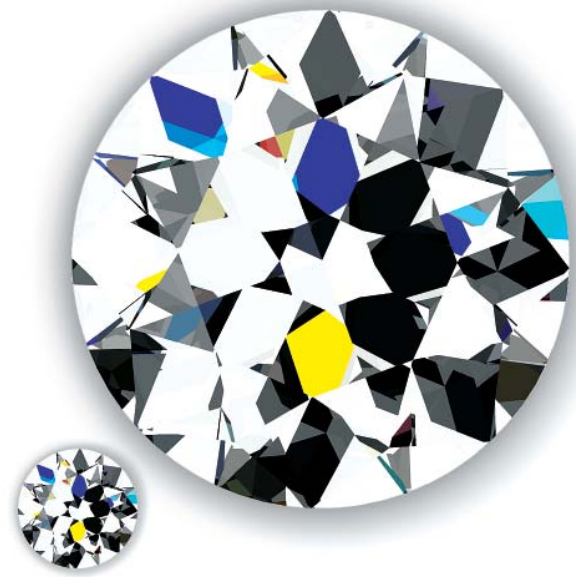
# Sweet spot centre of the star length

That leaves just the star length as the remaining parameter to consider. In the context of the table size and crown main angle, the star length determines the angles of the star facets and the crown halves or upper girdle facets. Although having less impact on diamond beauty than the pavilion mains and pavilion halves, the angles of the crown halves and stars do influence the diamond's light performance. Star lengths of 45% to 65% have the potential to receive a GIA 'Excellent' cut grade. This makes 55% the centre of the GIA sweet spot for star length. This accords with the findings of this investigator and the practice of many of today's cutters of the modern 'Ideal' cut. We find that the best optical performance is obtained with a star facet length between 50% and 60%, centred at the same 55%.

# Summary of the seven-parameter sweet spot centre

For a round brilliant cut diamond, the finest or ideal beauty is attained in the narrow range of parameters that in this paper is called the sweet spot. This is the range of angles and proportions historically called 'Ideal',

where the round brilliant cut exhibits the best distribution of brilliance (in both its aspects of brightness and contrast), fire and sparkle in typical real world illumination circumstances. Essential to this concept of 'Ideal' is the balance of the properties of reflections from the pavilion main facets and the pavilion halves (the lower girdle facets.)

Considering the GIA and AGS sweet-spot parameter centres and the knowledge gained from his own research, the author concludes that the seven-dimension, sweet-spot centre for the 'Ideal' round brilliant is as follows:

Listed in order of parameter importance:
1. Pavilion main angle = 41
2. Length of pavilion halves = 77%
3. Crown main angle = 34
4. Table size = 56%
5. Star Length = 55%
6. Girdle size = thin to medium
7. Culet size = small to none

These proportions accord with the author's knowledge of the parameters that yield the essence of ideal beauty in the standard round brilliant. That understanding is based upon direct assessment of the diamond's optical performance in typical real world illumination circumstances. There remain many important differences among the various grading systems, but we can all agree upon the centre of the 'Ideal' cut diamond's sweet-spot.

A conclusion reported by Cowing (2000) was that diamond cutters were correct in their adherence to close to a 41° pavilion angle. This angle is the most critical of the diamond's parameters. Further research by the author into all seven of the parameters that define the round brilliant has validated the accomplishments and progress of diamond cutters from the times of Morse and Tolkowsky until today. They would likely approve of today's 'Ideal' round brilliant, which evolved from their key contributions to the art and science of diamond fashioning.

## Acknowledgements

## References

Bates, Rob, 2004. AGS Changes Its Ideals. *The JCK*, November, p.30

Boyajian, W., 2004. Unlocking the secrets of the fourth c. *Gems & Gemology*, 40(3), 197-8

Cowing, M., 2000. Diamond brilliance: theories, measurement and judgement. *Journal of Gemmology*, 27(4), 209-227

Cowing, M., 2005. Describing diamond beauty – assessing the optical performance of a diamond. *Journal of Gemmology*, 29, 5/6, 274-280

Gaal, R., 1977. *The Diamond Dictionary*. Gemological Institute of America, California, 342pp.

*GIA Diamond Grading Lab Manual*, 2006. GIA, Carlsbad, CA

Tillander H., 1995. *Diamond Cuts in Historic Jewellery 1381-1910*. Art Books International, London, 248pp

Tolkowsky M., 1919. *Diamond Design*. Spon & Chamberlain, New York, 104 pp

Wade, Frank B., 1916. *Diamonds*. G. P. Putnam's Sons, New York and London, 150 pp

Whitlock, Herbert, 1917. Proportions of the Brilliant Cut. *The Jewelers' Circular-Weekly*, May, p. 45

# The causes of colour variation in Kashan synthetic rubies and pink sapphires

## Dr Karl Schmetzer[1] and Dr Dietmar Schwarz[2]

1. Taubenweg 16, D-85238 Petershausen, Germany
2. Gübelin Gem Lab, Lucerne, Switzerland

**Abstract:** *The trace element patterns of Kashan synthetic rubies and pink sapphires reveal two colour-causing transition metal elements, chromium and titanium, which are present in ranges of concentrations up to 0.23 wt.% $TiO_2$ and up to 0.62 wt.% $Cr_2O_3$. UV-visible absorption spectra consist of the absorption bands of $Cr^{3+}$ on which the absorption bands of $Ti^{3+}$ are superimposed. The titanium component of the spectra predominantly removes the purplish tint of the ordinary ruby colour and thus the saturated red or even orangey red coloration of the synthetic Kashan corundum material is developed. By heat treatment in air, titanium is oxidized from $Ti^{3+}$ to $Ti^{4+}$ and the influence of titanium on the ruby colour is removed.*

**Keywords:** *Heat treatment, Kashan, synthetic ruby, trace elements, visible-range spectra.*

## Introduction

Reference samples of natural and synthetic gem materials are frequently used in gemmological laboratories. In general, the properties of natural reference samples of known origin or the features of synthetic reference samples of a known producer are compared with properties of samples of unknown origin which are submitted for examination. In other cases, analytical instruments are calibrated using reference samples with known properties, e.g. of known chemical composition. During a re-examination of the properties of a large suite of Kashan synthetic rubies, the authors have observed some chemical and spectroscopic properties related to the causes of colour within these samples which have only

briefly been mentioned in the gemmological literature. In particular, the causes of colour and the correlation of trace element contents with spectroscopic properties in Kashan synthetic rubies have not been described and understood in detail.

Kashan synthetic rubies were produced by Ardon Associates in Austin, Texas, U.S.A., from the end of the 1960s to the mid-1980s with a short renaissance in the mid-1990s (Nassau, 1990; Laughter, 1994; Kammerling *et al.*, 1995; Hughes, 1997). The synthetic rubies are flux-grown from a cryolite-bearing melt (Gübelin, 1983; Henn and Schrader, 1985; Schmetzer 1986 a,b). Compared to various natural and synthetic rubies, some of the Kashan crystals contain unusually high

titanium in the range of 0.04 to 0.17 wt.% $TiO_2$ (Kuhlmann, 1983; Muhlmeister *et al.*, 1998) with high titanium contents reported especially for pink samples (Gübelin, 1983). These relatively high amounts of titanium are, most probably, related to an unusual pleochroism observed in part of the Kashan material with an extraordinarily strong yellowish red or orange parallel to the *c*-axis (Gübelin, 1983; Hughes, 1997). From the examination of absorption spectra it is known that some Kashan synthetic rubies reveal an absorption band due to $Ti^{3+}$ in addition to the ordinary $Cr^{3+}$ absorption spectrum (Schmetzer, 1986 b, p.102). This titanium-related absorption band reduces the violet to purplish tint of chromium on its own in many 'ordinary' rubies or pink sapphires (see Box).

## Materials and methods

For the present study, the authors examined 70 Kashan synthetic rubies in the range of 0.14 to 3.05 ct in weight, originating from the reference and teaching collection of one of the authors (DS) and from other reference collections. The samples (*Figure 1*) show clear ranges in colour from purplish



Figure 1: *Six Kashan synthetic rubies and pink sapphires showing a wide range of colour representative of our research material. Weight of samples from 0.96 to 1.60 ct, the sample at the lower left weighs 1.05 ct and measures 5 × 7 mm. Photo by H.A. Hänni.*

pink to pink and orangey pink, and from purplish red to red and orangey red. In general, those samples with a less intense violet or purplish tone tended to resemble 'Thai rubies', and those with a somewhat more intense violet to purplish hue tended to resemble 'Burmese rubies'. All 70 stones showed a small shift of colour between daylight and incandescent light.

Trace or minor element contents of all 70 samples were obtained using EDXRF spectroscopy. The analyses were performed with a Tracor Northern Spectrace 5000 system, using a programme specially developed for trace element geochemistry of corundum. The detection limit for these minor elements was in the range of 0.005 wt.%; consequently below detection limit (bdl) indicates a concentration below 0.005 wt.%.

Polarized UV-Vis absorption spectra of 15 samples with different trace element contents, especially with different titanium concentrations, were recorded with a Perkin-Elmer Lambda 19 spectrophotometer after orientation of the optic axis of each sample with the aid of an immersion microscope. Heat treatment of four samples with high titanium contents was performed in air at 1750 C over a period of 170 h, and then their polarized absorption spectra were recorded again.

## Results

### Chemical properties

On visual inspection, the synthetic rubies show a continuous range of colour (*Figure 1*) and cannot be subdivided into groups with specific colours. This visual impression is confirmed by their chemical compositions. EDXRF spectroscopy shows that two major colour-causing trace elements, namely chromium and titanium, are present with chromium contents between 0.09 and 0.62 wt.% $Cr_2O_3$ and titanium contents from bdl

According to a general practice in the gem trade, we are using the terms 'ruby' and 'pink sapphire' for chromium-bearing synthetic corundum. However, we would like to mention that there is no clear boundary between the two varieties due to a continuous range of chromium contents within the Kashan material.
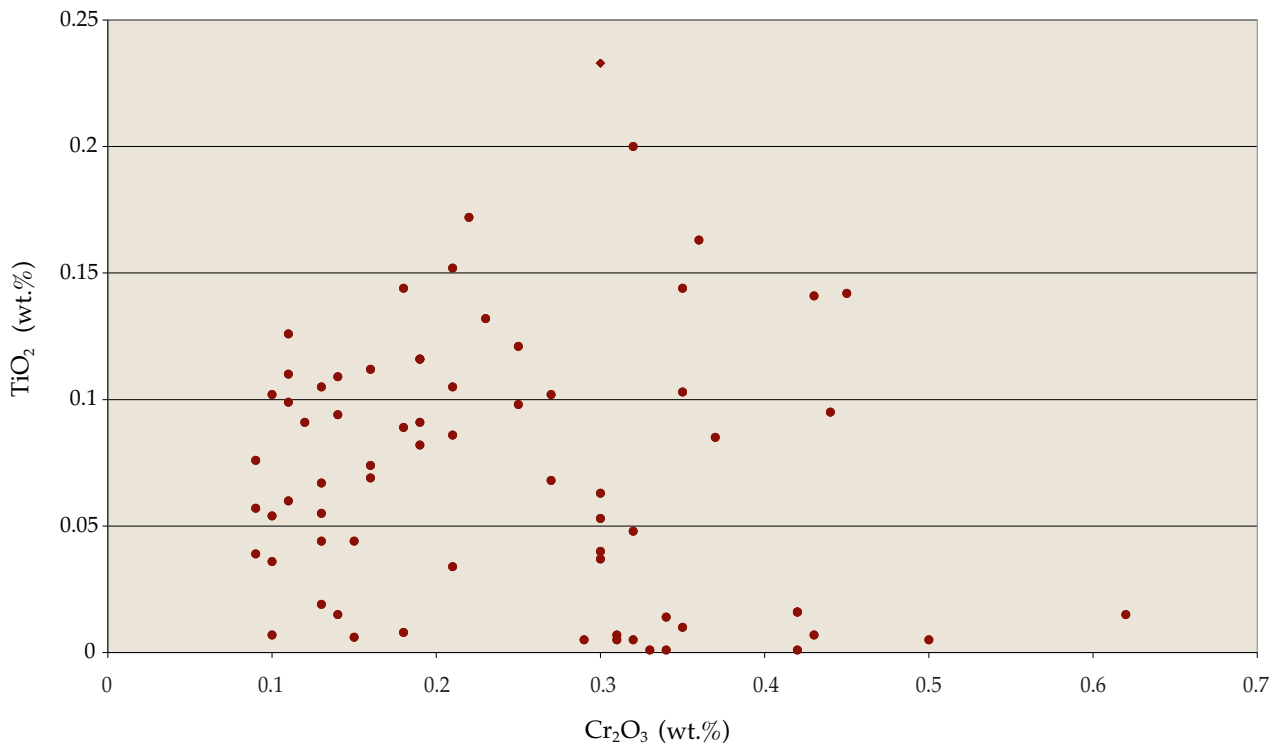
**Figure 2:** *Graphic representation of chromium and titanium contents as determined for 70 Kashan synthetic rubies and pink sapphires by energy-dispersive X-ray fluorescence spectroscopy (EDXRF); the chromium contents vary widely between 0.09 and 0.62 wt.% $Cr_2O_3$, and the titanium contents of the sapphires also show a wide variation from the detection limit of the instrument up to 0.23 wt.% $TiO_2$. No special clusters or concentration of samples around specific points in the diagram are evident.*

to 0.23 wt.% $TiO_2$. A correlation diagram of $Cr_2O_3$ versus $TiO_2$ contents (*Figure 2*) indicates a continuous range of trace element data for chromium and titanium with no clustering or concentration of data around specific points in the diagram. Consequently, these data do not indicate a limited number of specific colour types but a continuous range of coloration or variation in colour.

Other trace element values were relatively low: iron contents from bdl to 0.03 wt.% $Fe_2O_3$ and vanadium contents between 0.005 and 0.03 wt.% $V_2O_3$ were detected, no gallium contents above the detection limit of the instrument were found, as expected for Kashan synthetic corundums. These data indicate that only chromium and titanium have to be considered as colour-causing trace elements in Kashan synthetic rubies.

## Spectroscopic properties

All absorption spectra of different samples with various chromium and titanium contents (*Figure 3*) reveal the absorption bands of $Cr^{3+}$ on octahedral

**Table I:** *Spectroscopic properties of Kashan synthetic rubies and pink sapphires.*

| Colour cause | Absorption maximum (nm) and polarization relative to the **c**-axis | Intensity of absorption bands |
|---|---|---|
| $Ti^{3+}$ | 493 ∥c and⊥c | ∥c > ⊥c |
| | 542 (shoulder) ∥c and ⊥c | ∥c > ⊥c |
| $Cr^{3+}$ | 556 ⊥c; 542 ∥c | ⊥c > ∥c |
| | 410 ⊥c; 397 ∥c | ∥c > ⊥c |
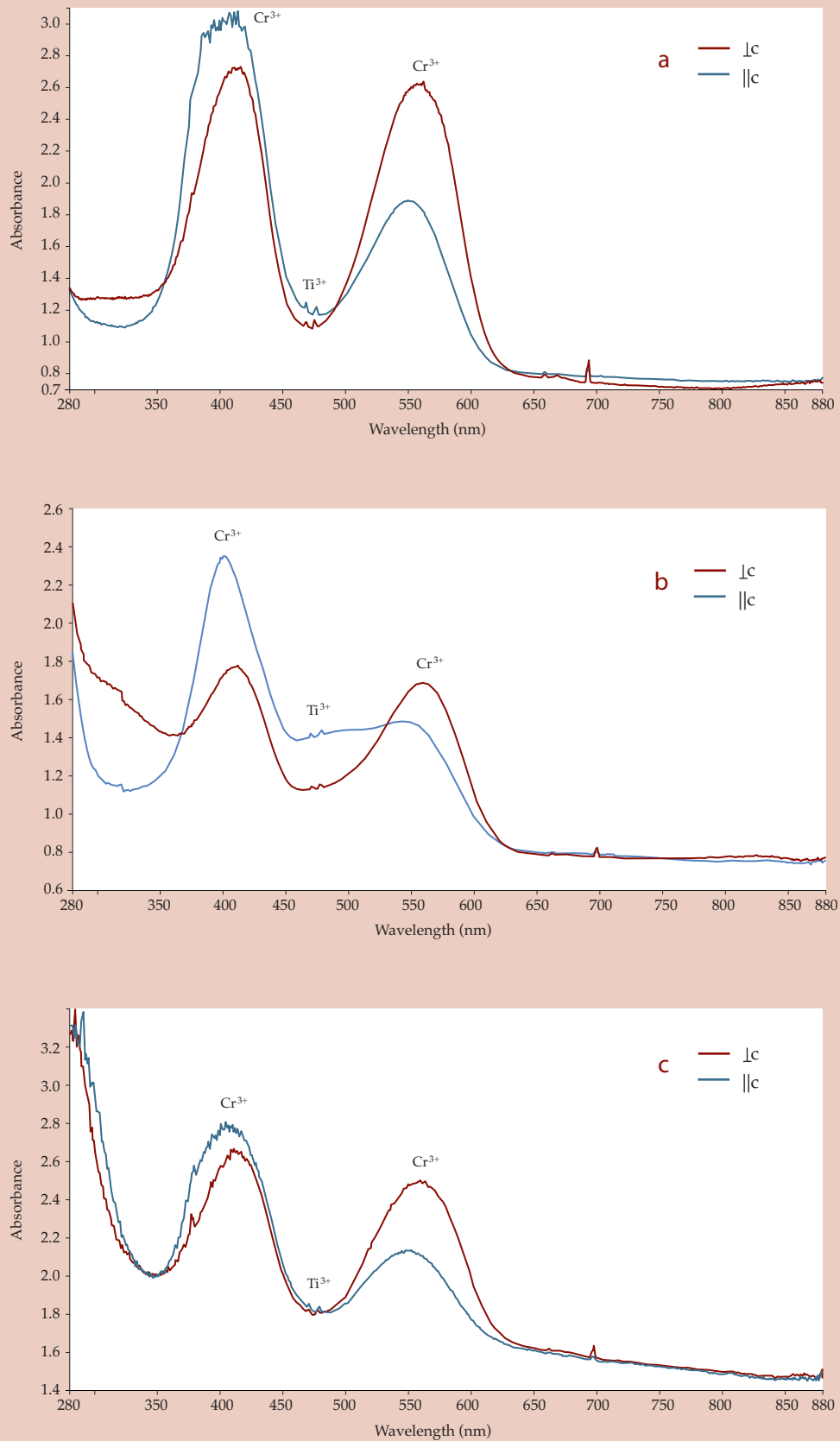
**Figure 3:** *Polarized UV-visible absorption spectra of two samples of Kashan synthetic rubies coloured by chromium and titanium; (a) sample I with trace element contents of 0.04 wt.% TiO$_2$ and 0.42 wt.% Cr$_2$O$_3$, (b) sample II with trace element contents of 0.15 wt.% TiO$_2$ and 0.21 wt.% Cr$_2$O$_3$, (c) spectrum of sample II after heat treatment in an oxidizing environment. The spectra represent samples with relatively low (spectrum a) and relatively high (spectrum b) titanium contents, in spectrum (c) the influence of titanium in spectrum (b) is removed after oxidation of Ti$^{3+}$ to Ti$^{4+}$.*

Figure 4: *Heat-treated Kashan synthetic ruby of 1.57 ct (left) with trace element contents of 0.15 wt.% $TiO_2$ and 0.21 wt.% $Cr_2O_3$ (spectrum see Figure 3c) compared to an untreated sample of 1.29 ct with similar trace element contents of 0.14 wt.% $TiO_2$ and 0.18 wt.% $Cr_2O_3$. The heat treated sample measures 6 × 8 mm. Photo by H.A. Hänni.*

aluminium sites of the corundum structure (*Table I*). This well known chromium spectrum of ruby or pink sapphire is accompanied by two absorption bands of $Ti^{3+}$, a strong band with a maximum at 493 nm and a somewhat less intense shoulder at 542 nm. Both the band and the shoulder due to $Ti^{3+}$ are more intense in spectra taken with polarization parallel to the *c*-axis than in spectra perpendicular to the *c*-axis (McClure, 1962; Moulton, 1986; Wong *et al.*, 1995; see again *Table I*).

In the UV-Vis absorption spectra of samples that were heat treated in an oxidizing environment, the absorption bands of $Ti^{3+}$ were completely removed (*Figure 3*). This is consistent with oxidation of $Ti^{3+}$ to $Ti^{4+}$, because $Ti^{4+}$ does not show any absorption bands in the visible range. A similar reaction has already been described for titanium-bearing synthetic corundum after annealing in an oxidizing environment by Moskvin *et al.* (1980). The remaining peaks in spectra of our annealed samples consisted only of $Cr^{3+}$ bands which were not affected by the heat treatment process. The colour of these Kashan synthetic rubies changed from orangey pink or orangey red before heat treatment to purplish pink or purplish red after heat treatment (*Figure 4*).

It is worth mentioning that a reverse process can occur by heat treatment of synthetic titanium-bearing sapphire in a reducing atmosphere, in which $Ti^{4+}$ is transformed to $Ti^{3+}$ and the colour of the samples is intensified (Moskvin *et al.*, 1980; Johnson *et al.*, 1995).

## Cause of colour and pleochroism

As indicated by chemical and spectroscopic properties of the samples, we have to consider a combination of two colour-causing trace elements to explain the colour of Kashan synthetic rubies. Synthetic sapphires doped with $Ti^{3+}$ alone show a pink coloration (see, e.g., Johnson *et al.*, 1995) and the purplish red colour of synthetic chromium-doped Verneuil rubies is known to all gemmologists. To understand the influence of titanium on the colour of chromium-bearing corundum, the position of the $Ti^{3+}$ absorption maximum becomes important; this is located just between the two strong chromium absorption bands



Figure 5: *Kashan synthetic rubies and pink sapphires arranged in groups with different trace element contents; the chromium contents are indicated below the samples (in wt.% $Cr_2O_3$) , the titanium contents are indicated left of the samples (in wt.% $TiO_2$). Lower line: samples with purplish pink to purplish-red coloration and titanium contents in the range of 0.01 to 0.02 wt.% $TiO_2$. Second line: samples with slightly purplish-pink to slightly purplish-red coloration and titanium contents in the range of 0.03 to 0.05 wt.% $TiO_2$. Third line: samples with pink to red coloration and titanium contents in the range of 0.06 to 0.09 wt.% $TiO_2$. Upper line: samples with orangey-pink to orangey-red coloration and titanium contents in the range of 0.10 to 0.14 wt.% $TiO_2$. The chromium contents of the samples within each of the four colour lines increases from left to right (compare also* Figure 2 *and* Table II*).*

*In general, the colour intensity from light pink to intense red is correlated with increasing chromium contents; with increasing titanium contents, the purplish to violet hue of the samples is reduced. Weight of samples from 0.96 to 3.05 ct, the sample at the lower left weighs 2.01 ct and measures 6 × 8 mm. Photo by H.A. Hänni.*

*Table II: Schematic overview of colour and pleochroism of Kashan synthetic rubies and pink sapphires.*

| Approximate titanium contents (range, wt.% TiO$_2$) | Overall body colour | Colour relative to the *c*-axis | |
| --- | --- | --- | --- |
| | | ‖c | ⊥c |
| 0.10 – 0.14 | *Very intense* <br><br> orangey pink to orangey red | *Very intense* <br><br> reddish yellow | *Intense* <br><br> pink to red |
| 0.06 – 0.09 | *Intense* <br><br> pink to red | *Intense* <br><br> pinkish yellow to orange | *Moderate* <br><br> pinkish red to purplish red |
| 0.03 – 0.05 | *Moderate* <br><br> Slightly purplish pink to slightly purplish red | *Moderate* <br><br> pinkish yellow to orange | *Not affected* <br><br> purplish pink to purplish red |
| 0.01 – 0.02 | *Not affected* <br><br> purplish pink to purplish red | *Not affected* <br><br> yellowish pink to yellowish red | *Not affected* <br><br> purplish pink to purplish red |

**NB:** The words in italics indicate the influence of each range of titanium content on the colour and pleochroism compared to titanium-poor or titanium-free rubies or pink sapphires.

in the visible range. We also have to consider that the intensity of the titanium absorption bands is much stronger in the spectrum parallel to the *c*-axis than in that perpendicular to the *c*-axis.

The visual impression of the overall body colour as well as the pleochroism of Kashan synthetic rubies and pink sapphires are summarized in *Table II* and correlated with approximate titanium contents of the samples; representative samples are pictured in *Figure 5*. However, it should be emphasized, that the coloration of each sample is a function of its trace element contents, in these stones, mainly of chromium and titanium. Due to the varying intensity of chromium and titanium absorption bands in the spectra parallel and perpendicular to the *c*-axis, the impression of the colour of a faceted stone is also influenced by the orientation of the table facet relative to this axis.

If only small amounts of titanium (in the range of 0.01 to 0.02 wt.% TiO$_2$) are present, the 'ordinary' colour of ruby or pink sapphire is little or not affected. With increasing titanium contents, the colour is affected in both directions of the pleochroism of uniaxial corundum, i.e. parallel and perpendicular to the *c*-axis. Due to the different intensity of the titanium absorption in both directions, relatively small amounts of titanium (in the range of 0.03 to 0.05 wt.% TiO$_2$) are sufficient to change the colour parallel to c, whereas higher titanium contents (in the range of 0.06 to 0.09 wt.% TiO$_2$) are needed to affect the visual impression of the colour perpendicular to c.

In general, the colour parallel to the *c*-axis becomes less red and more yellowish and the colour perpendicular to the *c*-axis becomes less violet and more pure red or pink (*Table II*). Thus, the colour parallel to the *c*-axis is shifted from yellowish red to reddish yellow and the colour perpendicular to the *c*-axis is changed from purplish pink or purplish red to a more pure pink or red

without any violet or purplish colour tone. The body colour of the samples is changed from purplish pink or purplish red to orangey pink or orangey red (*Figure 5*, *Table II*).

In heat-treated samples with complete oxidation of titanium from $Ti^{3+}$ to $Ti^{4+}$, the 'ordinary' chromium pleochroism of ruby or pink sapphire is observed and the stones are purplish red (see again *Figure 4*).

## Discussion

The synthetic rubies and pink sapphires examined were obtained during a period of several years by one author (DS). Thus, it may be concluded that they are a mixture of the Kashan production from several years, and cover at least a major range of the production of Ardon Associates in the 1970s and 1980s. It is obvious that the producer clearly recognized the influence of titanium and consequently used this trace element as dopant to produce rubies and pink sapphires with a saturated red coloration, i.e. by removing the purplish tint of purely chromium-doped synthetic corundum.

As comparable trace element contents or absorption spectra have not been described for rubies from any natural source or for synthetic stones from any other producer, these chemical and spectral features might be useful for recognising Kashan synthetic rubies or pink sapphires and distinguishing them from natural gems.

## Acknowledgement

## References

Gübelin E.J., 1983. The recognition of the new synthetic rubies. *Journal of Gemmology*, 18(6) 477–99

Henn, U., and Schrader, H.-W., 1985. Some aspects of identification of Kashan synthetic rubies. *Journal of Gemmology*, 19(6) 469–78

Hughes, R.W., 1997. *Ruby and sapphire.* RWH Publishing, Boulder, Colorado, USA. 512 pp

Johnson M.L., Mercer M.E., Fritsch E., Maddison, P., and Shigley, J.E., 1995. "Ti-sapphire": Czochralski-pulled synthetic pink sapphire from Union Carbide. *Gems & Gemology*, 31(3), 188–95

Kammerling, R.C., Koivula, J.I., Fritsch, E., Johnson, M.L., and DeGhionno, D.G., 1995. Faceted Kashan synthetic rubies and sapphires. *Gems & Gemology*, 31(1), 70

Kuhlmann, H., 1983. Emissionsspektralanalyse von natürlichen und synthetischen Rubinen, Sapphiren, Smaragden und Alexandriten. *Zeitschrift der Deutschen Gemmologischen Gesellschaft*, 32(4), 179–95

Laughter, T., 1994. Kashan makes a comeback. *JewelSiam*, 5(1), 79–83

McClure, D.S., 1962. Optical spectra of transition-metal ions in corundum. *Journal of Chemical Physics*, 36(10), 2757–79

Moskvin, N.A., Sandulenko, V.A., and Sidorova, E.A., 1980. Color centers and luminescence in corundum crystals containing titanium. *Journal of Applied Spectroscopy*, 32(6), 592–6

Moulton, P.F., 1986. Spectroscopic and laser characteristics of $Ti:Al_2O_3$. *Journal of the Optical Society of America B*, 3(1), 125–33

Muhlmeister, S., Fritsch, E., Shigley, J.E., Devouard, B., and Laurs, B.M., 1998. Separating natural and synthetic rubies on the basis of trace-element chemistry. *Gems & Gemology*, 34(2), 80–101

Nassau, K., 1990. Synthetic gem materials in the 1980s. *Gems & Gemology*, 26(1), 50–63

Schmetzer, K., 1986a. Production techniques of commercially available gem rubies. *Australian Gemmologist*, 16(3), 95–100

Schmetzer, K., 1986b. *Natürliche und synthetische Rubine – Eigenschaften und Bestimmung.* E. Schweizerbart'sche Verlagsbuchhandlung, Stuttgart, Germany. 131 pp

Wong W.C., McClure, D.S., Basun, S.A., and Kokta, M.R., 1995. Charge-exchange processes in titanium-doped sapphire crystals. I. Charge-exchange energies and titanium-bound excitons. *Physical Review B*, 51(9), 5682–92

# Abstracts

## Diamond

### Ein Schadenfall besonderer Art.

H.A. Hänni. *Gemmologie. Z. Dt. Gemmol. Ges.,* 55(3/4), 2006, 105-10. 3 photographs, 2 tables, bibli.

The origin of a crater-like pit in a cut diamond is explained as a consequence of a laser shot mistakenly directed into the stone during a repair of the setting. The laser transformed a little of the diamond into graphite, the increase of volume blasted a portion of the stone away and created the damage.                                  E.S.

### The Arkansas Diamond rush continues.

J. Houran. *The Mineralogical Record,* 37, 2005, 505-10.

Several major diamond crystals are reported from the Crater of Diamonds State Park, Arkansas, U.S.A. A Centennial book on the area and its diamonds is promised.          M.O'D.

### Diamond from the Los Coquitos area, Bolivar State, Venezuela.

F.V. Kaminsky (felixvkaminsky@cs.com), O.D. Zakharchenko, G.K. Khachatryan, W.L. Griffin and D.M. DeR. Channer. *The Canadian Mineralogist,* 44(2), 2006, 323-40.

A set of 77 diamond crystals (average weight 30 mg) from the Los Coquitos placer deposit on the Guaniamo River, Venezuela, have been examined comprehensively and compared with diamonds from the Quebrada Grande kimberlite sills and placer deposits, both ~ 50 km SE. The Los Coquitos diamonds are similar in general, but differ in having a higher proportion of octahedral crystals and a slightly higher total nitrogen content of 719 ppm. The $\delta^{13}C$ values of the Los Coquitos diamonds vary from +0.4 to -20.5 ‰. The garnet inclusions in the Los Coquitos diamonds are lower in Ca, the pyroxenes have a wider compositional range and olivine has a lower Fo content compared to inclusions in the Quebrada Grande suite, and the Los Coquitos diamonds show a greater depletion in LREE. It is considered that the Los Coquitos diamonds were derived, at least in part, from an undiscovered kimberlite source sampled from a different section of the subcontinental lithospheric mantle.          R.A.H.

### The impact of internal whitish and reflective graining on the clarity grading of D-to-Z color diamonds at the GIA Laboratory .

J.M. King, T.M. Moses and W. Wang. *Gems & Gemology,* 42(4), 2006, 206-20.

Unlike many other characteristics that affect the clarity grade of diamonds, determination of the impact of 'whitish' graining and 'reflective' graining as bands, lines or planes in extended areas through a range of motion requires analysis that goes beyond visibility at 10x magnification. The importance of this observation is underlined by such graining often being the only characteristic present in large, high-clarity, high-colour diamonds. The history of the reporting of such graining by the GIA Laboratory is reviewed, the causes of the different types of graining most commonly encountered are considered, and the methodology and critical assessment that GIA graders use to determine the impact of such graining on the clarity of the diamond are examined.          R.A.H

### Gem News.

B.M. Laurs (Ed.). *Gems & Gemology,* 42(4), 2006, 268-92.

Notes included an update is given on diamond trading in Sierra Leone.          R.A.H.

### Lab Notes.

T.M. Moses and S.F. McClure (Eds). *Gems and Gemology,* 42(4), 2006, 260-7.

A note is given of a fancy deep pink 0.84 ct diamond which became deep orange-pink after exposure to UV radiation, this colour persisting for about two weeks.          R.A.H.

### [Spectroscopic studies on irradiation-enhanced fancy colour diamonds.]

J.C.C. Yuan, M.-S. Peng and Y.-F. Meng. *Kuangwu Yanshi (Journal of Mineralogy and Petrology),* 25(3), 2005, 47-51. (Chinese with English abstract.)

Spectroscopic techniques ranging from FTIR, UV-visible-near infrared absorption, photoluminescence and Raman spectroscopy were used to study 10 natural diamonds with fancy colour induced by radiation. These diamonds are classified on their FTIR characteristics. Their visible absorption and low-temperature photoluminescence spectra indicate that there are a number of colour-centre peaks attributable to point defects. In addition to the N3 absorption peak, peaks at 595 and 637 nm are also observed. The colour-centre peaks at 575, 595 and 637 nm in the low-temperature photo-induced luminescence spectra, in combination with the $H_1b$

colour centre at 4929 cm$^{-1}$ and the H$_1$c colour centre at 5156 cm$^{-1}$ in the near infrared spectra, are not only reliable indicators for green diamonds having been irradiated, but are also an important characteristic of other colours in diamonds treated by irradiation. R.A.H.

# Gems and Minerals

## Andradit wom Pizzo Crampiolo, Grampelhorn.

C. ALBERTINI AND S. GRAESER. *Lapis,* 31(5), 2006, 28-31.

Non-gem andradite is described from Pizzo Crampiolo in the border area of Switzerland (Valais) with Italy. M.O'D.

## Fluorite; novo ed eccezionale ritrovamento al Chumar Bakhoor, in Pakistan.

R. APPIANI. *Rivista Mineralogica Italiana,* 30, 2006, 250-3.

Fluorite crystals of considerable size (around 12 cm) and predominantly pink to red are reported from a pegmatite at Chumar Bakhoor (5520 m) in the Hispar Valley, Pakistan. Some material appears to be of ornamental quality. M.O'D.

## Alchuri, Shigar Valley, Northern Areas Pakistan.

D. BLAUWET. *The Mineralogical Record,* 37, 2005, 513-40.

Minerals recently reported and with possible ornamental potential are described: fine green titanite, clinozoisite, Cr-diopside, zoisite and orthoclase. Exceptional crystals of red to orange väyrynenite are especially noteworthy; the source is probably the Braldu river valley. The Namlook mine in this valley has also produced fine translucent to transparent red crystals of triplite. M.O'D.

## The Jackson's Crossroads amethyst deposit, Wilkes County, Georgia.

R.L. BOWLING, R. MOORE AND T. LEDFORD. *The Mineralogical Record,* 36, 2005, 479-86.

Fine gem-quality amethyst crystals were discovered in 1988 in east-central Georgia, U.S.A. The host rock appears from investigations to be either a metadacite or a slightly metamorphosed granite. Amethyst crystals are found in a variety of pocket-types and are described as highly lustrous royal purple. A faceted specimen shown weighed 48.35 ct. M.O'D.

## Die Chromlagerstätte Sarany im Ural.

V. BURLAKOV AND V.V. AVDONIN. *Lapis,* 31(10), 2006, 53-60.

The geology and mineralization of the Sarany area in the Russian Urals are described. A list of minerals is given. Some chromian titanite is of ornamental quality M.O'D.

## Erongo Mountains, Namibia.

B. CAIRNCROSS. *The Mineralogical Record,* 37, 2005, 361-470.

Species of possible gem quality are described from the Erongo Mountains, Namibia. They include light blue jeremejevite, aquamarine, fluorite, orthoclase and topaz. M.O'D.

## Leopard opal: play-of-color opal in vesicular basalt from Zimapán, Hidalgo State, Mexico.

R.R. COENRAADS (coenraads01@optus. net.com.au) AND A.R. ZENIL. *Gems & Gemology,* 42(4), 2006, 236-46.

So-called 'leopard opal' consists of vesicular basalt impregnated with play-of-colour opal, and is known only from Zimapán, Hidalgo State, Mexico. Its occurrence is due to an abundance of silica derived from the chemical breakdown of overlaying layers of volcanic ash, the permeability of the underlying basalt and the presence in the basalt of pores of an aesthetically pleasing size. The even distribution and small size of the opal-filled vesicles makes for an attractive rock when cut or carved and polished. Veinlets and irregular masses of opal showing various body-colours (red, white and colourless to pale blue) have also been deposited along joints and fractures within the basalt. This opal deposit, which may

have been worked in pre-Columbian times, has been explored recently only by a number of test pits, leaving a potential for future development R.A.H.

## Die Mineraliensammlungen des Australian Museum, Sydney.

I. GRAHAM, R. POGSON AND G. WEBB. *Lapis,* 31(2), 2006, 33-7.

The mineral collections of the Australian Museum, Sydney are generally described with some features highlighted. M.O'D.

## Claro, Südschweiz: Aquamarin und seltene Titanmineralien aus Pegmatitdrusen.

R. GUERRA AND S. WEISS. *Lapis,* 31(12), 2006, 20-5.

Aquamarine of apparently near gem-quality is described from Claro, southern Switzerland. The beryl is accompanied in a pegmatite by uncommon titanium minerals. These and other minerals can be found in a descriptive list. M.O'D

## The cause of iridescence in rainbow andradite from Nara, Japan.

T. HAINSCHWANG (thainschwang@ yahoo.com) AND F. NOTARI. *Gems & Gemology,* 42(4), 2006, 248-58.

'Rainbow' andradite from the Yoshina area, Nara Prefecture, Japan, occurs as relatively small orange-brown crystals showing iridescence in almost the entire spectral range. It is an almost pure andradite. Two different types of lamellar structures appear to be responsible for the iridescence. These structures cause predominantly thin-film interference and probably diffraction of light. The terms of interference and diffraction are discussed and correlated to the iridescence observed in these garnets R.A.H.

## Pre-Columbian jadeite axes from Antigua, West Indies: description and possible sources.

G.E. HARLOW (gharlow@amnh.org), A.R. MURPHY, D.J. HOZJAN, C.N. DE MILLE AND A.A. LEVINSON.

*The Canadian Mineralogist,* 44(2), 2006, 305-21.

Excavation of workshop sites on Antigua uncovered jade axe forms and associated fragments, all of which are jadeite jade (jadeitite). This Antigua site dates as the Saladoid period (~ AD 250-500). Ten of these jade artefacts were examined mineralogically and petrographically. For six of them, the mineral assemblage includes jadeite, omphacite, albite, a white-tan mica, zoisite/clinozoisite and titanite; allanite was found in the cores of zoisite in two jades, and glaucophane and lawsonite were each seen in a single sample. EPMA results are reported. Quartz is found as a secondary matrix phase around corroded grains of jadeite and as inclusions in omphacite. Possible sources include Guatemala. R.A.H.

## Pencil garnet from the Haramosh Mountains, near Gilgit, Pakistan.

F.C. Hawthorne and W.W. Pinch. *The Mineralogical Record,* 36, 2005, 525-7.

Almandine with a very high spessartine content is described from the area of the Haramosh mountains in the northern areas of Pakistan near Gilgit. Crystals appear to show a first-order hexagonal prism terminated by a second-order hexagonal pyramid. None the less their identity is confirmed by electron probe microanalysis. Full details of the forms are given. M.O'D.

## Blauer, pinkfarbiger und hellgrüner Opal aus Peru.

U. Henn. *Gemmologie. Z. Dt. Gemmol. Ges.,* 55(3/4), 2006, 111-8. 11 photographs, 3 graphs, bibl.

Greenish-blue and blue opals from Peru have been on the market for thirty years, usually known as Andean opals. Today there are also pink opals available, the colour resembling angel-skin corals. E.S.

## Korallen im Edelstein – und Schmuckhandel.

U. Henn. *Gemmologie. Z. Dt. Gemmol. Ges.,* 55(3/4), 2006, 77-104. 41 photographs, 4 tables, bibl. (German with English abstract.)

After pearls, corals come second in the organic jewellery trade. This article deals with the description of different coral species, their characteristics,

treatments and imitations. The Mediterranean *corallium rubrum* is red to orange and was predominant until the nineteenth century, when Japan became the centre of the industry. The Japanese variety is dark red to salmon in colour, the Taiwanese dark red to white-pink. The white coral Shiro is found between Japan and the Philippines. The Hawaiian bamboo soft red coral is white to brownish and generally dyed red. The Indo-Pacific blue corals are commonly dyed and impregnated. Black corals can be bleached to a golden colour and are often impregnated to improve their lustre. True Hawaiian gold corals (narella) have a typical dimpled structure and can also be impregnated. Stone corals, such as tiger or apple coral, are less important in the trade. White porous stone corals can be dyed red to pink as well as blue. Today there are large amounts of red, pink and blue reconstructed corals on the market. They consist of powdered coral fragments bound with coloured resin. There are many types of imitations on the market: glass, porcelain, plastics, dyed chalcedony or agate, dyed mother-of-pearl and ceramics like the 'synthetic coral' by Gilson or Kyocera. E.S.

## "Regenbogen-Mondstein" aus Indien.

U. Henn. *Gemmologie, Z. Dt. Gemmol. Ges.,* 55(3/4), 2006, 133-5. 4 photographs.

Colourless to milky-white, transparent to semi-transparent feldspar is offered in the trade as rainbow-moonstone; the stones show adularescence and labradorescence. The physical properties are as for andesine feldspar. Typical inclusion patterns of labradorescent plagioclase feldspar, esp. polysynthetic twinning lamellae and cleavage cracks can be seen under the microscope. E.S.

## The Honourable George Knox, 1765-1827, Parliamentarian and Mineral Collector. His collections in Trinity College, Dublin, Ireland

P.N.W. Jackson. *The Mineralogical Record,* 37, 2005, 543-51.

An aquamarine of fine colour and measuring 5.1 cm is among

the geological collections of Trinity College, Dublin. A number of items were formerly in the collection of George Knox. M.O'D.

## Die schönen Feldspat-Kristalle aus Namibia.

S. Jahn. *Mineralien Welt,* 17(6), 2006, 66-72.

Amethyst, green fluorite, goethite and quartz in association with potassium feldspar are described from the Erongo area of Namibia. M.O'D.

## Neu: grüne Fluorit von Riemvasmaak, Northern Cape, Südafrika.

S. Jahn and J. Steinbinder. *Mineralien Welt,* 17(6), 2006, 62-5.

Fine green fluorite crystals are described from Riemvasmaak, Northern Cape, South Africa. Some crystals are found as octahedra. M.O'D.

## Achate aus Patagonien.

P.Jeckel. *Lapis,* 30(10), 2005, 29-33.

Agate specimens of good ornamental quality are described from the Esquel region of Patagonia, Argentina. M.O'D.

## Die Jagd nach den 'Puma-Achaten' in Argentinien.

P. Jeckel. *Mineralien Welt,* 16(4), 2005, 68-70.

'Puma-agate' is described from Mendoza Province of Argentina, close to the border with Chile. The occurrence is similar to some in Germany. M.O'D.

## [A study on the identification of turquoise by FT-IR.]

Y-C. Kim. *Journal of the Korean Crystal Growth and Crystal Technology,* 14(6), 2004, 272-6. (Korean with English abstract.)

Natural turquoise can be distinguished easily from its common substitutes using infrared spectroscopy in the range 2000~450 cm$^{-1}$, especially by features in the mid-infrared. Gilson turquoise exhibits a significantly smoother pattern when compared with natural turquoise, due to a different state of aggregation. Infrared spectra of natural, treated, synthetic and imitation turquoise (gibbsite, calcite) are shown and compared. I.S.

## Gem News.

B.M. Laurs (Ed.). *Gems & Gemology,* 42(4), 2006, 268-92.

Details are provided of a 2.9 cm prismatic crystal of bicoloured beryl from the Erongo Mts, Namibia, with a sharp division between bluish-green and brownish-orange parts. From Brazil, a vein of milky white quartz is described with yellow-orange areas which are marketed as 'sunset' quartz. R.A.H.

## Collecting cavansite in the Wagholi quarry complex, Pune, Maharashtra, India.

M.F. Makki. *The Mineralogical Record,* 36, 2005, 507-12.

Fine specimens of the vivid blue hydrated silicate of calcium and vanadium, cavansite, are described from a quarry complex at Pune, Maharashtra, India. Specimens occur in small vugs and irregular cavities beneath overlying compact basalt and many need careful handling and reinforcement. M.O'D.

## Gemmologie Aktuell.

C.C. Milisenda. *Gemmologie, Z. Dt. Gemmol. Ges.,* 55(3/4), 2006, 73-6. 2 photographs.

In the last few months large amounts of diffusion-treated sapphire cabochons have come on the market. The identification of cabochons is more difficult than of faceted stones as the coloured coating is not so obvious. However, these stones showed also a distinct blue coloration within hollow tubes and surface fissures. There are also a large number of fancy coloured – mostly orange and yellow – sapphires on the market which have been diffusion-treated with beryllium. The amount of beryllium intensifies the yellow. It is also possible to remove or brighten blue colour. There are often unusual, circular inclusions in these stones; however, tests showed that these inclusions can be called characteristic for high-temperature treatment, but not diagnostic for beryllium diffusion. Some pink beads were sold as pink opal, but proved to be dyed marble; when tested with hydrochloric acid, there was strong effervescence and infra-red spectroscopy confirmed the presence of carbonates. E.S.

## Alpine 'iron roses'.

T. Moore. *The Mineralogical Record,* 36, 2005, 491-503.

Fine brilliant hematite crystals are described from Alpine-type clefts in various localities, the name 'iron roses' having long been used for suitably shaped aggregate examples. Ilmenite occasionally occurs in similar shapes. M.O'D.

## What's new in minerals.

T. Moore. *The Mineralogical Record,* 36, 2005, 285-301.

Among apparent gem-quality specimens displayed at the 2005 Tucson Gem and Mineral Show were a crystal of väyrynenite from the Shengus area, Gilgit district, Northern Areas, Pakistan: this appeared a transparent to translucent reddish-orange in the photograph. Also described were two deep blue aquamarine crystals from Mount Amero, Chaffee county, Colorado, U.S.A. M.O'D.

## Lab Notes.

T.M. Moses and S.F. McClure (Eds). *Gems and Gemology,* 42(4), 2006, 260-7.

Notes are given of a 5.82 ct, transparent, green round-brilliant-cut demantoid, of exceptional colour and size, reportedly from Russia; a 3.96 ct cut poudretteite; and a 0.68 ct modified lozenge step cut pyroxmangite. R.A.H.

## Die Vervendung von Röntgenstrahlen in der Achatforschung.

T. Moxon. *Mineralien Welt*, 16(4), 2005, 71-2.

X-rays have been used in the investigation of agate structure in a study carried out at the University of Cambridge. M.O'D.

## [The colour enhancement of natural ruby produced from Mong Hsu.]

C-W. Park and P-C. Kim. *Journal of the Korean Crystal Growth and Crystal Technology,* 14(6), 2004, 290-7. (Korean with English abstract.)

A natural rough ruby from Mong Hsu containing colour patches ranging from blue to nearly black was heat treated to investigate colour enhancement. The optimum conditions to produce an overall clear red were found to be temperatures of 1400-1600 C, and duration of 12 hours in an oxygen atmosphere.

EPMA analyses indicated that part of the blue or black colour patches are due to charge transfer between $Fe^{2+}$ and $Ti^{4+}$. The contents of $Fe^{2+}$ or $Fe^{3+}$ and $Ti^{4+}$ were reduced by heat treatment. Due to recrystallization of $TiO_2$, silk was formed on the surface of the ruby when heat treated for 12 hours at 1700 C. I.S.

## The minerals of the Hunting Hill quarry, Rockville, Maryland.

F.J. Parker. *The Mineralogical Record,* 36, 2005, 435-46.

Specimens of red grossular garnet and green diopside are described from the Hunting Hill quarry, Rockville, Maryland, U.S.A. Some grossular has been faceted. A descriptive mineral list is provided. M.O'D.

## What's new in minerals?

J. Polityka. *The Mineralogical Record,* 37, 2005, 573-82.

Minerals of possible gem interest noted at recent shows include red tourmaline in divergent clusters from the Minh Tien pegmatite, Luc Yen, Yen Bei Province, Vietnam; proustite crystals from Chanarcillo, Chile, and fine blue euclase from near Ouro Preto, Minas Gerais, Brazil. M.O'D.

## Luc Yen: neue Edelstein-Turmaline aus einem Pegmatit in Nordvietnam.

P. Russo and F. Escaut. *Lapis,* 31(6), 2006, 49-51.

Gem-quality red liddicoatite tourmaline is described from the Luc Yen pegmatite in North Vietnam. M.O'D.

## Achate von der Teufelsrutsch.

H-P. Schröder. *Lapis*, 31(5), 2006, 38-42.

Ornamental agates are described from the Teufelsrutsch, between Nack and Wendelsheim, Rhineland, Germany. M.O'D.

## Das Laacher See-Gebiet. Feuer, Eis und edle Steine.

W. Schüller. *Lapis,* 31(10), 2006, 13-26.

Minerals, some of ornamental quality, are described from the area of the Laacher See, Germany. M.O'D.

## Blau-Quarz aus Minas Gerais, Brasilien.

R. Schultz-Güttler. *Gemmologie, Z. Dt. Gemmol. Ges.,* 55(3/4), 2006, 135-6. 1 photograph.

The amethyst mine of Montezuma in the northern part of the Brazilian state of Minas Gerais produces amethyst which can be modified to green by thermal treatment, the so-called prasiolite. Recent treatment with gamma rays produced a surprisingly blue colour. The pleochroism was strong; reddish along the *c*-axis and reddish-blue perpendicular to the *c*-axis.        E.S.

## Fifty-nine treasure hunts in Minas Gerais, 1969-2005. (Memoirs of a Collector, part 1.)

G. Steiger. *The Mineralogical Record,* 36, 2005, 531-49.

The author has visited, and describes specimens from, 59 different locations in Minas Gerais, Brazil. Tourmaline of gem quality features in this part.        M.O'D.

## Raman- und fluoreszenz-spektroskopische Eigenschaften von Zirkon-Einschlüssen in chrom-haltigen Korunden aus Ilakaka und deren Veränderung durch Hitzebehandlung.

B. Wanthanachaisaeng, T. Häger, W. Hofmeister and L. Nasdala. *Gemmologie, Z. Dt. Gemmol, Ges.,* 55(3/4), 2006, 119-32. 11 photographs, 7 graphs, bibl.

The samples came from the Ilakaka-Sakahara region in the south-west of Madagascar. Under the microscope zircon inclusions change their appearance above 1400 C. The authors used a heat treatment which allowed changes to be observed at 1000 C; this treatment varies not only the temperature, but also the duration of the treatment and heating and cooling rates. Remnant pressures acting on the zircon inclusions varied from 1 to 5 kbar — significantly lower than previously described pressures of up to 27 kbars.E.S

## Identification of 'chocolate pearls' treated by Ballerina Pearl Co.

W. Wang (wyul.wang@gia.edu),

K. Scarratt, A. Hyatt, A.H.T. Shen and M. Hall. *Gems & Gemology,* 42(4), 2006, 222-35.

Treated cultured pearls with a chocolate coloration have entered the market from several sources. Gemmological, spectroscopic and chemical analyses have been performed on both untreated and treated cultured pearls to provide a better understanding of the 'chocolate' treatment process used by one company and to determine how these products can be identified. It seems likely that the organic components in black cultured pearls were partially bleached to create the brown colour; no foreign colouring agent was detected. Cultured pearls so treated can be identified on the basis of their unusual coloration, characteristic fluorescence, UV-Vis-NIR reflectance and Raman spectra, and trace-element composition (Pb5-26 ppm).        R.A.H.

## The Mineralogical Record label archive.

W.E. Wilson. *The Mineralogical Record,* 36, 2005, 450-7.

Gemmologists who are also mineral collectors need to know that the *Mineralogical Record* has collected and preserved more than 6000 examples of specimen labels from many dealerships and other collections world-wide. It is believed to be the largest such collection outside major museums.        M.O'D.

## W.A. Thompson. A half century of collecting and dealing in minerals.

W.E. Wilson. T*he Mineralogical Record,* 37, 2005, 555-66.

Among the specimens in the Thompson collection are fine purple zoisite crystals, wulfenite and vanadinite, some of gem quality        M.O'D.

# Instruments and Techniques

## A study on the identification of ruby and garnet by optical method.

J-H. Hwang and J-K. Choi. *Journal of the Korean Crystal Growth and Crystal Technology,* 15(5), 2005, 182-7.

A new colour filter, called the

Hwang Ji Ho filter has been prepared, which enables one to distinguish ruby from other red gemstones. Through this filter, ruby appears blue, whereas red garnet is dark red. Other red stones such as spinel and tourmaline also appear dark red.        I.S.

## A Raman investigation of the amblygonite-montebrasite series.

B. Rondeau (rondeau@mnhm.fr), E. Fritsch, P. Lefevre, M. Guiraud, A.M. Fransolet and Y. Lulzac. *The Canadian Mineralogist,* 44(5), 2006, 1109-17.

Nine rough minerals and seven faceted gemstones of the amblygonite-montebrasite series were analysed by Raman spectroscopy, XRD, IR and gemmological properties (density and refractive indices); the Raman signal appears to be a good indicator of the F content. Three peaks evolve significantly as the F content increases: from 599 to 604, from 1056 to 1066 and from 3379 to 3348 cm$^{-1}$. Also, the FWMH (full width at half maximum) of the peak around 3370 cm$^{-1}$ increases from 11 to 57 cm$^{-1}$ as F content increases. All the faceted gemstones analysed were found to consist of montebrasite rather than amblygonite as claimed by the gem traders.  R.A.H.

# Synthetics and Simulants

## Experimental study on diamond dissolution in kimberlitic and lamproitic melts at 1300-1420°C and 1 GPa with controlled oxygen partial pressure.

Y. Kozai and M. Arima (arima@ed.ynu.ac.jp). *American Mineralogist,* 90(11-12), 2005, 1759-66.

Experiments were carried out in the graphite stability field to evaluate the dissolution processes of diamond crystals in kimberlitic and lamproitic magmas. Dissolution agents used include an aphanitic kimberlite from Wesselton mine, South Africa, and a lamproite from Mount North, West Kimberley, Australia. With increasing run duration, diamond morphology changed from a sharp octahedron

through a combination of octahedral and tetrahexahedroidal forms to spherical tetrahexahedroidal forms with rounded faces. Negatively oriented trigons formed on the octahedral {111} face. As the degree of diamond dissolution increased, the trigons changed from smaller shallow types to larger deep types. The dissolution rate in the kimberlite solvent at 1300 C was 0.12 mm/h under the HM buffer, 0.0034 mm/h under the MW buffer and 0.0017 mm/h under the WI buffer, whereas at 1420 C it was 0.014 mm/h under the WI buffer. In the lamproitic solvent, the dissolution rate was 0.0024 mm/h at 1420 C for the WI buffer. The data indicate that diamond dissolves in silicate melts as carbonate ions through an oxidizing reaction. The degree of dissolution depends greatly on temperature, oxidation state and the compositional dependence of $CO_2$ solubility in the melts. R.A.H.

## Luminescence study of defects in synthetic as-grown and HPHT diamonds compared to natural diamonds.

J. LINDBLOM (joachim.lindblom@utu.fi), J. HÖLSA, H. PAPUNEN AND J. HÄKKÄNEN. *American Mineralogist*, 90(2-3), 2005, 428-40.

Optically active defects in as-grown, high-pressure-high-temperature (HPHT), boron-doped, and synthetic diamonds (SD) grown with a nitrogen-getter, as well as in natural diamonds (ND), were characterized by absorption and luminescence spectroscopies using different excitation sources. The laser-excited photoluminescence (PL) spectra of SDs show numerous sharp lines characteristic for Ni-related centres, whereas NDs yield mainly broad PL bands. Under UV and electron beam excitation, the yellow synthetic diamonds display green luminescence patterns along octahedral directions. The UV-excited PL spectra of the yellow SDs show a green band associated with Ni-related optical species. NDs display broad bands centred at ~ 450 nm that are related to complex nitrogen-related aggregates formed in the mantle over a long period of geological time. The CL spectra of SDs reveal many Ni-related and simple nitrogen-vacancy defects. All synthetic diamonds were found to show luminescence from Ni-related defects centred at ~ 480 and 530 nm at room temperature and 77K, respectively, and a sharp luminescence band at 694 nm due to a $Cr^{3+}$ impurity in corundum inclusions. R.A.H.

## Diamond formation in metal-cabonate interactions.

J. SIEBERT (julieri.siebert@lmcp.jussieu.fr), F. GUYOT AND V. MALAVERGE. *Earth & Planetary Science Letters*, 229(3-4), 2005, 205-16.

Reduced silicon alloyed with Fe metal has been shown to react chemically with $FeCO_{3 \, siderite}$ at pressures of 10-25 GPa and temperatures of 700-1800 C according to: $2 \, FeCO_{3 \, siderite} + 3 \, Si_{in \, metal} = 2Fe_{in \, metal} + 3 \, SiO_{2 \, stishovite} + 2 \, C_{diamond}$. Since no carbon seeds were introduced, the only source of C for diamond formation was the carbonate phase. This observation provides a mechanism for diamond formation, possibly relevant to the early Earth. Thermodynamic modelling of these reactions shows that the stishovite/silicon oxygen fugacity buffer is far more reducing than the carbonate/diamond equilibrium; this is taken to imply that in Earth mantle conditions no silicon-bearing metal can exist with carbonates. The formation of diamond by reactions between carbonates and highly reducing metal phases containing significant amounts of silicon might have been expected to have occurred in the early Earth by the mixing of oxidized and reduced accretion components at pressures and temperatures greater than 10 GPa and 1700 C. R.A.H.

## The nature of Ti-rich inclusions responsible for asterism in Verneuil-grown corundum.

C. VITI (vitic@unisi.it) AND M. FERRARI. *European Journal of Mineralogy*, 18(6), 2006, 823-34.

Verneuil-grown star corundum with variable zoning and colouring (ruby and sapphire) host three sets of acicular inclusions at 120 . The inclusions are up to 20-30 μm long and 0.1-0.4 μm wide. Their cross-sections match the visible-light wavelength and explain the optical diffraction responsible for sharp six-arm stars in cabochon gemstones. The inclusions are elongated parallel to corundum {10$\bar{1}$1} faces and are polysynthetically twinned on {10$\bar{1}$1}. Electron diffraction and high resolution TEM show that the inclusions are almost isostructural with the corundum matrix, even if slightly distorted to a monoclinic lattice with *a* 5.00, *b* 4.63, *c* 13.08 Å, γ 118 . Nanochemical data point to a $TiO_2$ stoichiometry, thus indicating the occurrence of $Ti^{4+}$ cations, coupled with vacancies, within the distorted corundum-like structure (with only half of the octahedral sites occupied). Close to the apical terminations of the $TiO_2$ needles, local stoichiometry is consistent with the presence of $Ti^{2+}$ cations, formed by redox disproportionation during post-growth thermal annealing. R.A.H.

## Crystal morphology and feature of the diamond films by DC arc discharge.

X.-H. ZHANG, L. WANG (wangling@cdut.edu.cn), J.-P. LONG, S.-H. CHANG AND J.-G. ZHOU. *Kuangwu Yanshi (Journal of Mineralogy and Petrology)*, 25(3), 2005, 100-4. (Chinese with English abstract.)

Polycrystalline films of diamond with surface morphology with {100} and {111} faces were synthesized on an abraded tungsten carbide tool from a gas mixture of methane and hydrogen using DC arc discharge CVD. The morphology of the diamond film was examined by scanning electron microscopy. With increasing concentration of carbon gas, the morphology of the film of diamond changed from {111} to {100} and the diamond particle shape varied from octahedral to cubic. A lot of twin-like particles and ballast-like particles also exist in the diamond film. R.A.H.

# Abstractors

R.A. Howie    R.A.H.        M. O'Donoghue    M.O'D.        E. Stern    E.S.        I. Sunagawa    I.S.

# Book Reviews

## Minerals and Their Localities (2nd updated edn).

J.H. BERNARD AND J. HYRSL, 2006. Granit, Prague. 823 pp, illus. in colour. ISBN 80-7296-054-7.  98.

This very large book presents virtually all established mineral species in alphabetical order with a high proportion of examples illustrated in colour. This has given at least two photographs in each opening and often more. Data given for each species includes name, chemical composition and group membership, physical properties including crystal system and space group. Mode of occurrence and major localities complete each entry.

A number of appendices presents: the richest localities of the world; references; alphabetical list of mineral localities; brief biographies of the authors and a final appendix describing, with all the properties cited in the main text, recently published minerals.

This is a major achievement and the authors are to be congratulated; no doubt there are occasional slips/typos but a careful selection of entries failed to throw up any examples. The typeface is well chosen, bearing in mind that the print size has to be small. The binding appears to be secure. The standard of reproduction is also excellent, again bearing in mind that the photographs have to be small. Anyone with a serious interest in minerals should buy this most reasonably-priced book.        M.O'D.

## Symmetrielehre der Kristallographie. Modelle der 32 Kristalklassen zum Selbstbau.

R. BORCHARDT AND S. TUROWSKI, 1999. Oldenbourg, Munich.

ISBN 978-3-486-24648-3.  29.80.

Attractively produced and printed guide to making models of the 32 crystal classes. Many readers may prefer to keep the book whole or at least copy the drawings.        M.O'D.

## Russian Gemstones Encyclopedia.

V.V. BUKANOV, 2006. Granit, St. Petersburg. 472 pp. ISBN 80-7296-053-9.  79

The presentation and some of the photographs are similar to (and sometimes the same as) those in the excellent Bernard and Hyrsl 'Minerals and their localities' (2006), reviewed above. The page formats and the typeface are virtually identical (this is not a criticism as they are both excellent). The reader may ask whether or not the texts (where appropriate) are identical – they are not. The author has managed to incorporate a large number of gem species while acknowledging the scarcity of gem varieties of some of the species covered.

Entries are in general by alphabetical name of species: members of mineral groups are not always where the reader might expect to find them but this is a problem with any encyclopedic work. The author provides an alphabetical list of mineral names to make the problem less of a hindrance.

Appendixes deal with unique diamonds (giving date of discovery and covering world-wide deposits not just Russian ones), unique specimens of ruby and sapphire, beryl varieties, quartz and gold nuggets. There is a respectable list of references.

The book with its small but attractive colour photographs is pleasing to look at though this

reviewer would appreciate knowing where he is on any given page: though running heads are intrusive they would have been useful here. In addition it would have been good to have more detail about Russian deposits but this would have necessitated a much larger work.

I would strongly recommend an early purchase for this book and for Bernard and Hyrsl. Both books are printed in the Czech Republic but can be obtained most easily from Weise Verlag, Orleansstr 69, 81667 Munich, Germany.        M.O'D.

## A Journey with Colour. A History of South Australian Opal, 1840-2005.

L. CRAM, 2006. Len Cram, Lightning Ridge. 368pp, illus. in colour. Hard cover. ISBN 0-9585414. Approx. £77.

The third and final volume of Len Cram's superbly illustrated survey of Australian opal deals with the opal fields of South Australia. As in the previous two volumes the standard of colour photography and reproduction reaches ever-new heights and it is safe to say that these are among the very finest illustrated gemstone books ever printed. As before there is a great deal of history as well as accounts of mining and of the opals themselves. South Australian opal fields include both Andamooka and Coober Pedy, the latter being described for the years 1961-2005 and Andamooka from 1930-2005. The two fields occupy pages 15 to 298 of the book, which gives some idea of their importance. Other fields described include Mintabie and Stuart Creek.

The reader will feel that he has really met some of the larger-than-life characters whose doings, legal and

illegal, are described in Len Cram's easy-to-read prose.

The 'Special Collector's' edition, hardbound, is the version to go for and it may not be long before copies become unobtainable.          M.O'D.

## Feldspat.

[Contributions by various authors], 2006. Weise, Munich. 97 pp, illus. in colour. *(ExtraLapis* 30*)*. 17.80.

The complicated feldspar mineral group is most attractively illustrated in this excellent series – if precedent is followed an English-language version should appear in due course. As always the colour photographs are beautiful – the authors appear to favour microcline – and the text authoritative. The absence of red Oregon sunstone from the illustrations is my only, minor, criticism.     M.O'D.

## Jade.

C. Lam Shiu Ling, 2005. Lead On Publishing Co., Hong Kong. Illus. in colour. ISBN 962-86332-5-2. $380.

Attractively produced and informative guide to jadeite and nephrite jade. The text shares each page with colour photographs of jade varieties, some in mounts and with maps. The possible multiplicity of fanciful names is restricted and the reader can assume that nomenclature is up-to-date. Chinese characters are illustrated here and there (perhaps rather small for this reviewer's eyes). Details of fashioning and marketing are informative and useful as are the descriptions and illustrations of simulants and treatments.

The photographs, while certainly adequate, do not always show the best colour quality although most greens get away with it; there is a useful bibliography with one or two surprising omissions (Laufer, Ou Yang) but as a whole the book comes off very well and can be recommended to readers at any level.          M.O'D.

## [Catalogue of an] Exhibition held at Somerset House, London, 2 November 2002 – 26 January 2003.

J.A. Rosenthal, 2002. Art Books International, London. In slip case and with presentation bag. £200.00.

This is one of the most beautiful jewellery books that I have ever seen and also one of the largest and heaviest; the presentation bag is most welcome. The book illustrates and briefly describes 397 pieces, in almost all cases devoting a whole opening to each piece. Captions describe the stones used, with a few words on the design but the text has been kept economical to allow maximum space for the magnificent photographs – some of these have been enlarged to form front and back end-papers. The reader is encouraged (by the reviewer) to look at the pictures with the aid of a torch in a darkened room when the stones appear to be in relief.     M.O'D.

## Minerals of the Carpathians.

S. Szakall (Ed.), 2002. Granit, Prague. ISBN 80-7296-014-8. 59.

This publisher appears to be relatively new, at least in the mineral and gemstone field and the present book compares with others I have recently reviewed. The Carpathians spread into several countries; the Czech Republic, Hungary, Poland, Romania, Slovakia and Ukraine and the book describes deposits and individual species from all of them. As I have come to expect, the standard of presentation is high with an easily read typeface, small but excellent colour photographs and a wealth of appendices and maps in the text. There are species and locality indexes and a particularly valuable section describes the mineral museums in the area covered.

While the major gem minerals are generally absent from the area there are many species keenly sought by collectors. Fine green crystals of cuprite, groups of amethyst crystals (some with rhodochrosite), fire opal, chrysocolla and almandine catch the eye.

Organic substances are included and a section at the rear of the book presents idealized crystal diagrams, with notations, of some of the featured minerals. Photographs of the directors of the museums are welcome and there is an excellent bibliography, arranged by individual countries; this is useful as some entries are presented in the appropriate vernacular of the countries covered.          M.O'D.

## Surselva: Kristalle, Klüfte, Cavacristallas.

M.Wachtler (Ed.), 2006. Weise, Munich. 99 pp, illus. in colour. *(ExtraLapis* 31*)*. 17.80

Though this beautifully-illustrated survey of the geology, mineralization and species to be found in the general area of Disentis, Graubünden (Grisons), Switzerland, deals primarily with species too small for ornamental use, some are remarkable for their colour and form: a deep pink fluorite, variously-coloured rutile and rock crystal are notable. This series is essential for the serious collector.

M.O'D.

## Gemstones of Sri Lanka. Rarely Encountered Gemstones of Sri Lanka.

G. Zoysa, 2006. Speed Mark, Colombo, Sri Lanka. Illus. in colour. US$7.00 (US$10 laminated).

Two comprehensive charts, one displaying the major commercial gemstones and the other the rare gem varieties which have been recovered from the gem deposits of Sri Lanka.

R.R.H.

# The Journal of Gemmology Celebrates 60 years

The year 2007 marks the 60th anniversary of The Journal of Gemmology, the official journal of the Gemmological Association of Great Britain when it was incorporated under the Companies Act in 1947.

**1947...**

Printed in black-and-white with a grey cover, the 1947 Journal looked very different from the publication produced today.

Contributors to the first volume included names familiar to us all – B.W. Anderson, Prof. Edward Gübelin, R. Keith Mitchell and Robert Webster. In his editorial in the January 1947 issue, the then President of the Association, Dr G.F. Herbert Smith, concluded by saying: "The Association goes from strength to strength; it is a privilege which I greatly value to have been connected with the movement from the very start, and I hope that it may be my good fortune to aid its progress still further." He would have been justly proud to know the strength of the Association today, with a Journal that remains a leader in its field.
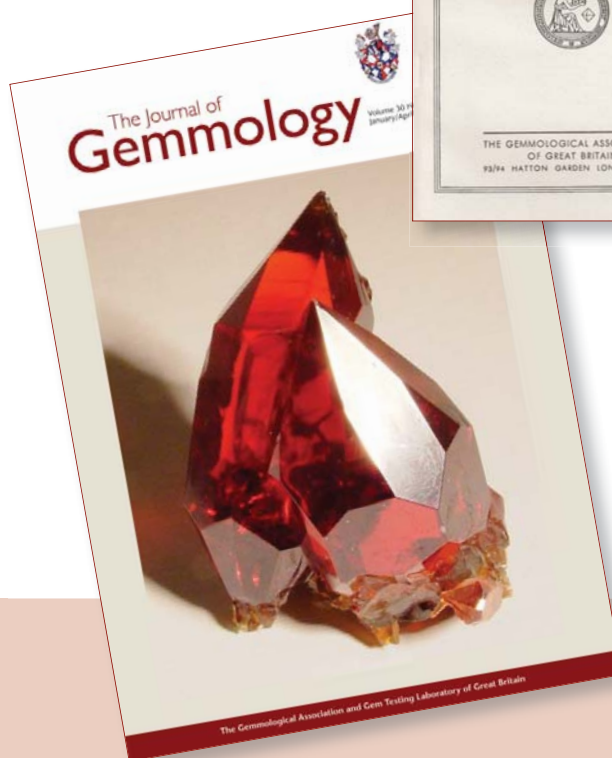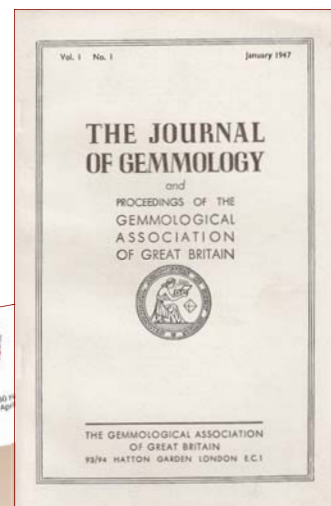
## Gem-A Conference theme

The first two articles of the January 1947 issue of the Journal were 'All pearls are not what they seem!' by Dr A.E. Alexander and 'Jade picture' by Elsie Ruff. To mark the anniversary of *The Journal of Gemmology*, the 2007 Gem-A Conference will focus on the subjects of these two articles with the theme 'Gems of the Orient'.

**...2007**

*So join us at the Gem-A Conference to celebrate the first sixty years of The Journal of Gemmology.*

## Gem-A Conference 2007    GEMS OF THE ORIENT

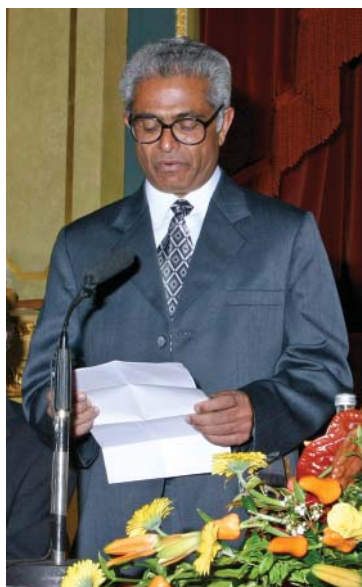Sunday 28 October - The Renaissance Heathrow Hotel

Presentations by an international panel of speakers will cover pearls from their history to the pearl market today, and the latest developments in jade.
Further details of the Conference will be published in the June issue of Gems & Jewellery.

# Proceedings of the Gemmological Association and Gem Testing Laboratory of Great Britain and Notices

## Conference and Presentation of Awards

The 2006 Gem-A Conference was held on Sunday 5 November at the Renaissance London Heathrow Hotel. Speakers at the event were Dr Ahmadjan Abduriyim, Victoria Finlay, Doug Garrod, Grenville Millington, Dr Jack Ogden, Dr Jayshree Panjikar and Benjamin Zucker. A programme of events was arranged to coincide with the Conference, including a private viewing and guided tour of the Crown Jewels with Crown Jeweller David Thomas, and a private viewing of the exhibition 'Bejewelled by Tiffany, 1837-1987' at the Gilbert Collection, Somerset House.



K.T. Ramchandran giving his address at the Presentation of Awards.

On Monday 6 November the Presentation of Awards gained in the 2006 Gem-A examinations was held at Goldsmiths' Hall in the City of London. Gem-A Chairman, Professor Alan Collins, presided, and K.T. Ramchandran, Executive Director of the Gemmological Institute of India, presented the awards. In his address, Mr Ramchandran emphasized the importance of education in the jewellery trade and the need for Gem-A graduates to act ethically and to continue to gain knowledge of the subject.

The presentation was followed by a reception for over 200 graduates and their guests.

Reports of both the Conference and Presentation of Awards were published in *Gems & Jewellery,* 2006, 15(5).

## R. Keith Mitchell Award

A new award, the R. Keith Mitchell Award for Excellence in the Field of Gemmological Spectroscopy, has been created in honour of Vice President R. Keith Mitchell who died in April 2006*. The first presentation of this award took place at the Presentation of Awards held at Goldsmiths' Hall on Monday 6 November 2006.

The award was presented to Colin Winter for his publication, lecturing and teaching that had done so much to spread the understanding of the importance of the hand-held spectroscope in gemmology.

*A tribute to Keith Mitchell was published in *The Journal of Gemmology,* 2006, 30(3/4), p.129.



From left: R. Keith Mitchell Award winner Colin Winter, with Keith Mitchell's sons Anthony and Graham at the Presentation of Awards ceremony at Goldsmiths' Hall.

# Gem-A Awards

Gem-A examinations were held in October 2006 and January 2007.
In the Examinations in Gemmology 177 candidates sat for the Diploma
Examination of whom 90 qualified, including seven with Distinction and 15 with
Merit. In the Foundation Gemmology Examination, 154 candidates sat of whom
92 qualified. In the Gem Diamond Examination 46 candidates sat of whom 29
qualified, including four with Distinction and three with Merit.
The names of the successful candidates are listed below.

## EXAMINATIONS IN GEMMOLOGY

### Gemmology Diploma
#### Qualified with Distinction

Dong Jin, Beijing, P.R. China
Frei, Thomas, Pratteln, Switzerland
Liu Tung-Wen, Taipei, Taiwan, R.O. China
Mahesh M. Babu, Kottayam, Kerala, India
Sinagra, Monika, Shanghai, P.R. China
Xu Baoqin, Wuhan, Hubei, P.R. China
Yan Xi, Wuhan, Hubei, P.R. China

#### Qualified with Merit

Barbour, Alexandra Frances, Dorchester,
    Dorset
Chang Qing, Beijing, P.R. China
Chen Yingying, Wuhan, Hubei, P.R. China
Gao Chujun, Wuhan, Hubei, P.R. China
Gourlet, Agnes, Chartres, France
Hug, Samuel, Gosport, Hampshire
Kaneyasu, Yoshimasa, Okayama-ken, Japan
Learmonth, Bryony, Stafford, Staffordshire
Mak Hoi Chuen, Jeff, Kowloon, Hong Kong
Newall, Myron, Colorado Springs,
    Colorado, U.S.A.
Peng Hui, Wuhan, Hubei, P.R. China
Peng Juan, Wuhan, Hubei, P.R. China
Puniani, Geeta, Surat, Gujarat, India
Wong Tung Wing, Shau Kei Wan,
    Hong Kong
Zhang Mengfei, Beijing, P.R. China

#### Qualified

Amicone, Maria, La Salle, Quebec, Canada
Andriasamy, Gisele, Paris, France
Bowers, Sally Faye, Fulham, London
Caplin, Marco, Lachine, Quebec, Canada
Chen Hsiu-Chuan, Taipei, Taiwan, R.O.
    China
Chen Cui, Guangxi, P.R. China

Chen Xi, Beijing, P.R. China
Cheng Chong Chuen, New Territories,
    Hong Kong
Cheung Ka Yan, Michiele, Ap Lei Chau,
    Hong Kong
Chung Yee Man, Stella, Kowloon,
    Hong Kong
Cote, Gaetan, St. Lambert, Quebec, Canada
Cui Lei, Beijing, P.R. China
Elles, Sarah Louise Jean, London,
Han Fen, Shanghai, P.R. China
Horn, Chandra Leah, Montreal, Quebec,
    Canada
Hossenlopp, Patricia, Chene-Bougeries,
    Switzerland
Hui Yuen Wah, Kowloon, Hong Kong
Kao Chen Li-Chen, Taipei, Taiwan, R.O.
    China
Katayama, Shinko, Colombo, Sri Lanka
Kemprud, Tanya D., Revelstoke,
    British Columbia, Canada
Khan, Ehtesham Ullah, Peshawar, Pakistan
Kim, Ji  A, Nam-Gu, Daegu, Korea
Ko Cheuk Wah, Robin, Quarry Bay,
    Hong Kong
Kong Yang, Guangxi, P.R. China
Kwok Sau Ying, New Territories,
    Hong Kong
Kwok Yuk Kuen, Kowloon, Hong Kong
Lau Kwan, May, Kowloon, Hong Kong
Lee, Ju Yeon, Daegu, Korea
Lee Wai Kwok, Simon, Kowloon,
    Hong Kong
Lefebvre, Alburt, Brampton, Ontario,
    Canada
Li Suet Lin, Happy Valley, Hong Kong
Li Hu, Wuhan, Hubei, P.R. China
Li Qiang, Wuhan, Hubei, P.R. China

# Gem-A Awards

Li Qianhe, Guangxi, P.R. China
Lin Chia Hui, Taipei, Taiwan, R.O. China
Liu Shuhan, Wuhan, Hubei, P.R. China
Luo Haiyan, Beijing, P.R. China
Lwin, Min, Yangon, Myanmar
Menekodathu Remanan, Amarnath, Surat, Gujarat, India
Micatkova, Lubica, London
Nam, Yong Ju, Seoul, Korea
Ng Sum Yi, Jordan, Kowloon, Hong Kong
Ngai Sheung Lau, Kowloon, Hong Kong
Oldbury, Christien, Poole, Dorset
Panidi, Lydia, Elefsina, Greece
Parhi, Chinmayee, Surat, India
Park, Ji Min, Daegu, Korea
Rajbanshi, Niren Man, South Ealing, London
Sherin, Saira, Peshawar, Pakistan
Sit Yat Sing, Shatin, Hong Kong
Thanattamkul, Pakamon, Nonthaburi, Thailand
Tian Cheng, Beijing, P.R. China
Tong Sen Yue, Sandy, Central, Hong Kong
Traill, Lillian, London
Tyler, Clare J., Den Bosch, The Netherlands
Wacyk, Carrein Tara, London
Wang Qi, Guangxi, P.R. China
Wat Wing Suet, Kowloon, Hong Kong
Watson, John Richard, Berkhamsted, Hertfordshire
Wong Yu Lap, Angel, Sha Tin Centre, Hong Kong
Wu Shih-Han, Taipei, Taiwan, R.O. China
Xie Yi, Shanghai, P.R. China
Zeng Fanrong, Wuhan, Hubei, P.R. China
Zhong Dan, Beijing, P.R. China
Zhou Chuanjie, Wuhan, Hubei, P.R. China
Zhou Yanfei, Wuhan, Hubei, P. R. China
Zong, Yue, Guangzhou, P.R.China
Zotta, Elisa, Parma, Italy

## Gemmology Foundation Certificate
### *Qualified*

Barker, Holly J., Johannesburg, South Africa
Chan Tat Hang, New Territories, Hong Kong
Chauhan, Rakesh, Chandigarh, India
Chen, Yu-Chen, Taipei, Taiwan, R.O. China
Cheng Yuan, Guangxi, P.R. China

Cheung Pui Shan, Alicia, New Territories, Hong Kong
Chiu Chun-Chieh, Taipei, Taiwan, R.O. China
Chokshi, Sheel Deepak, Vadodara, Gujarat, India
Chrismas, Jacqueline, Godalming, Surrey,
Cole, Natalie Rachel, Stone, Staffordshire
Daudin, Mathieu, Paris, France
De Alwis Dissanayake, Manoja Dilsiri, Colombo, Sri Lanka
De Barros, Valere, Maron, France
De Gaetano, Antonella, Genova, Italy
Ding, Hui, Surbiton, Surrey
Dong Haiyang, Guangxi, P.R. China
Drai, Stephanie, Clamart, France
Dufour, Gaspard, Chens Sur Laman, France
Efthymiadis, Avraam, Parga, Greece
Elles, Sarah Louise Jean, London
Faktor, Joanna, London
Feng, Jingling, Shanghai, P.R. China
Garcia-Agu, Cecile, Mouans-Sartoux, France
Gill, Julia Mary, Dudley, West Midlands
Goldman, Lucy, London
Griffiths, Neil Robert, Bromsgrove, Worcestershire
Guo Qian, Guangxi, P.R. China
Hailan Liu, Shanghai, P.R. China
Harris-MacNeil, Joanna, London
Ho Ching Yee, New Territories, Hong Kong
Ho Yue Yau, Tsuen Wan, Hong Kong
Hug, Samuel, Alverstoke, Gosport, Hampshire
Iozzino, Vittorio, Busalla, Genova, Italy
Jain, Aarti, Surat, Gujarat, India
Jayasuriya, Hasantha Udara Prem, Kandy, Sri Lanka
Jeong, Yu Joo, Korea
Jezova, Olesia, London
Kaneyasu, Yoshimasa, Okayama-ken, Japan
Learmonth, Bryony, Stafford, Staffordshire
Kathris, Ioannis, Holargos, Greece
Khan, Ehtesham Ullah, Peshawar, Pakistan
Khan, Nuzhat, London
Kiilu, Kyalo, Oldbury, West Midlands
Kim, Min Yeong, Ulsan-Si, Korea

# Gem-A Awards

Kim, Dong Hui, Daegu, Korea
Lai Tsz Wing, Aberdeen, Hong Kong
Lam Ying Kit, Hong Kong
Lau Man Yee, Chai Wan, Hong Kong
Lau Tsui Wah, Kowloon Tong, Hong Kong
Lee Ka Wai, Shatin, Hong Kong
Lee Seung Hee, Daegu, Korea
Lee Suk Wa, Ma Wan, Hong Kong
Lee Young Hee, Gyongsangbuk-Do, Korea
Lee Chi-Ju, Taipei, Taiwan, R.O. China
Li Po Shan, John, Central, Hong Kong
Liao, Tsai Chun, Taipei, Taiwan, R.O. China
Lin Li, Guangxi, P.R. China
Lin Wanchun, Guangxi, P.R. China
Lin Yu Chi, Taipei, Taiwan, R.O. China
Ling Xiaoqing, Shanghai, P.R. China
LiuTung-Wen, Taipei, Taiwan, R.O. China
Longini, Giovanni, Parma, Italy
Loo Shun Yee, Andrew, Kwai Chung,
    Hong Kong
Lui Ching Yi, Maggie, Hong Kong
Lung, Wan-Hui, Taipei, Taiwan, R.O. China
Maclellan, Kirstin, London
Mathieu, Clare Cecilia, London
Micatkova, Lubica, London
Mo Zurong, Guangxi, P.R. China
Monogyios, John, Athens, Greece
Nicolson, Anulak, Bangkok, Thailand
Park, Sun Young, Gyonggi-Do, Korea
Partridge, Jennifer Anne, Cambridge
Petit, Cyril, Ales, France
Raguin, Odiane, Aix-en-Provence, France
Rajbanshi, Niren Man, South Ealing,
    London
Rymer, Janine Felicia Mary, Twickenham
    Green, Middlesex
Sahabunyakul, Saran, Bangkok, Thailand
Santer, Kurt, St. Brelade, Jersey,
    Channel Islands
Sarraf, Kundan, Surat, Gujarat, India
Shen Jiani, Guangxi, P.R. China
Sherin, Saira, Peshawar, Pakistan
Shpartova, Irina, London
Sinagra, Monika, Shanghai, P.R. China
So Lai Yin, Kowloon, Hong Kong
Stefani, Helen, Ilioupoli, Athens, Greece

Tennant, Andrew, Leeds, West Yorkshire
Tsurkan, Anna, London
Vignal, Patrick, Ampus, France
Wan Moli, Guangzhou, P.R. China
Wang Qin, Guangxi, P.R. China
Wong Ka Yee, Hong Kong
Woo Ka Yin, Kwung Tong, Hong Kong
Wu Dan Dan, Guangzhou, P.R. China
Yan Ruogu, Guangzhou, P.R. China
Yang Jui Lin, Taipei, Taiwan, R.O. China
Yoo, Kkot Nim, Korea
Yoon, Hyun Ah, Seoul, Korea
Yu, Li, Guangzhou, P.R. China
Yu Kee Shun, Hong Kong

## Gem Diamond Diploma
### Qualified with Distinction

Chow Ho Man, Herman, Kowloon,
    Hong Kong
Flower, Caro, Melton Constable, Norfolk
Hall, Gregory Peter, Brighton, East Sussex
Leung, Vincent, Toronto, Ontario, Canada

### Qualified with Merit

Chen, Shioulin, Taipei, Taiwan, R.O. China
Chung Ka Yee, Anita, New Territories,
    Hong Kong
North, Sara, York

### Qualified

Bland, Claire, London
Blatherwick, Clare, Edinburgh
Chan Mei Fong, Frances, Kowloon,
    Hong Kong
Cheung Chi Shing, Peter, Kowloon,
    Hong Kong
Chu Yuen-Man, Alice, Braunstone, Leicester
Di Dongshuang, Wuhan, Hubei, P.R. China
Fisher, Fiona Jane, Dublin, Ireland
Freidericos, Nikitas, Athens, Greece
Kennedy, Martin, Belfast, N. Ireland
Lee, Sinnie, Kowloon, Hong Kong
Lee Wing Man, Vivian, Kowloon, Hong Kong
Li, Zhen, London
Lin, Lang-Dong, Taipei, Taiwan, R.O. China
Netsah, Maayane, Nairobi, Kenya

## Gem-A Awards

Ng Ka Wai, Annie, Kowloon, Hong Kong
Ngwe, Ohnmar, London
Poon Chor Wing, Hong Kong
Rose, Fiona Jane, Knutsford, Cheshire

Shen Hui, Wuhan, Hubei, P.R. China
Wang Zilei, Wuhan, Hubei, P.R. China
Wu, Shih-Han, Taipei, Taiwan, R.O. China
Zee Gar Bo, Michelle, Kowloon, Hong Kong

# Members' Meetings
## London

A private viewing of a sale which included the works of Andrew Grima was held on 5 December at Bonhams Auctioneers, New Bond Street, London W1.

## Gem Discovery Club
## Specialist Evenings

The Gem Club meets every Tuesday evening at the Gem-A London headquarters when Club members have the opportunity to examine a wide variety of stones, and once a month a guest gem or mineral specialist is invited to give a presentation.

The November guest was Jason Williams of gem dealers G.F. Williams & Co. of Hatton Garden, who demonstrated some of the skills needed to be a successful gem dealer. Members were given a series of activities to test their skills, including counting stones at speed, sorting by value, matching stones for colour, shape and weight, and folding stone papers. Cigdem Lule Whipp, the December specialist, gave a presentation on gem-quality diaspore. Club members were able to examine diaspore samples she had collected in Turkey. Freeform gem carving was Memory Stather's subject at the February specialist evening. In her presentation Memory described the process from the choosing of materials to the finished item, with the aid of a display of finished objects as well as raw materials, sketches and tools. In March Jack Ogden gave a presentation entitled 'Base Practices – The Decorative Etching of Gemstones in Antiquity' describing the use of the decorative etching of gem materials, especially carnelian, in Roman and earlier times. Jack brought along samples for members to examine.

## Midlands Branch

The Branch AGM was held on 26 January 2007 at the Earth Sciences Building, University of Birmingham, Edgbaston, at which Paul Phillips, Elizabeth Gosling and Stephen Alabaster were re-elected Chairman, Secretary and Treasurer respectively. The AGM was followed by a Bring and Buy Sale and a Team Quiz. Other events held at the Earth Sciences Building included a talk on 24 November 2006 by Peggy Hayden entitled 'Nineteenth century jet and other black jewellery', the Branch AGM, Bring and Buy and Team Quiz on 26 January 2007, a presentation entitled 'From paste to diamonds: shedding light on colourless gems' by Gwyn Green on 23 February, and 'The cravat pin, an almost forgotten item of jewellery', by James Gosling on 30 March. Events held at Barnt Green included an Instrument Training Day on 26 November and a Loupe and Lamp Training Day on 18 March, as well as the 54th Anniversary Branch Dinner on 9 December.

## North East Branch

On 1 November 2006 Brian Jackson gave a talk on 'Gem collecting in Russia' and on 14 March 2007 Alan Hodgkinson

## Gifts

The Association is most grateful to the following for their gifts
for research and teaching purposes:

Luella Woods Dykhuis FGA DGA, Tucson, Arizona, U.S.A., for rough specimens of Montana sapphire, tourmaline, Mexican topaz and quartz, and faceted amethyst, garnet and peridot. She also donated a large faceted quartz with lepidocrocite inclusions as featured on the cover of The Journal of Gemmology, 2006, 29(7/8).

Dennis Heyden, St. Louis, Missouri, U.S.A., for a purple jade carving of an owl.

John W. Nowak CEng FRAeS FGA, Bexley, Kent, for a large selection of faceted stones and crystals.

Pierre Salerno FCGmA, Luynes, France, for samples of ruby rough and a piece of rhodonite and garnet 'raisin bread', both from Greece.

Pierre Vuillet a Ciles FGA, Villards d'Heria, France, for three cream coloured quahog pearls.

Jason Williams FGA DGA, London, for a selection of faceted stones

---

gave a presentation entitled 'Stretching the refractometer'. Both meetings were held at the Ramada Jarvis Hotel, Wetherby.

### North West Branch

On 15 November 2006 at the YHA Liverpool International, Liverpool 1, the Branch AGM was held at which Deanna Brady was elected Chairman and Secretary of the Branch.

### Scottish Branch

Scottish Branch meetings included an opal workshop by Alan Hodgkinson on 27 November 2006 and Notes from the Gem Testing Laboratory by Stephen Kennedy on 27 February 2007, both held at the Napier University, Craiglockhart Campus, Colinton Road, Edinburgh. A Stone Setting Workshop by David Webster was held on 23 January at North Glasgow College. On 20 March, Brian Jackson spoke on the history of Scottish agates at Murchison House, West Mains Road, Edinburgh.

### South East Branch

The Branch AGM was held on 25 February at the Gem-A London Headquarters at which Peter Wates was elected Chairman,

Elizabeth Davidge Secretary and Lawrence Hudson re-elected Treasurer. The AGM was followed by a talk by David Lancaster entitled 'Cataloguing and Preparing a Sale of Antique Jewellery'.

## Membership

Between November 2006 and March 2007, the Council approved the election to membership of the following:

### Fellowship and Diamond membership (FGA DGA)

Andrews, Kitiya, Birmingham, West Midlands. 1996/2005

Slovak, Kate, Leicester, Leicestershire. 2005/2006

Ward, Louisa, London. 1996/1998

### Fellowship (FGA)

Bellec, Marion, Ergue-Gaberic, France. 2006

Bergeron, Elise, Montreal, Quebec, Canada. 2006

Cardew, Charles Julian, Penzance, Cornwall. 1982

Chan Wing Sze, Herleva, Kowloon, Hong Kong. 2006

Forsberg, Erika, Stockholm, Sweden. 2006
Goncalves Coelho, Ana Christina,
    Johannesburg, South Africa. 2006
Hartley, Pauline, Dewsbury,
    West Yorkshire. 2006
Holmes, Lissa, London. 2003
Kronis, Lynne, Toronto, Ontario, Canada. 2006
Offord, Nigel, Romsey, Hampshire. 1987
Tantisiriohaiboom, Yenrudee, Ho Chi Minh
    City, Vietnam. 2002
Turner, John, Burlington, Ontario,
    Canada. 2004
Win, Mai Mu Mu, Yangon, Myanmar. 1995
Xue Xiaoxin, Wuhan, Hubei, P.R.China. 2006

## Diamond membership (DGA)
Lo Wing See, Hong Kong. 2006
Mchugh, Trudi, Eastleigh, Hampshire. 2006
Wong Kwun Tong, Lever, Hong Kong 2006

## Associate membership
Abey, Sara, London,
Aderhold, Bryan, Ridgewood, New Jersey,
    U.S.A.
Allen Amanda, Northampton,
    Northamptonshire
Allsop, Jenny, Hythe, Kent
Amorena, Juan, Pamplona, Spain
Arlabosse, Jean-Marie, Cagnes s/Mer, France
Bamba, Tatsuya, Tokyo, Japan
Bartsch, Vanessa, London
Berney, Natalie, London
Biagi, Simon, London
Blacklock, Graeme John, Sydney,
    New South Wales, Australia
Boddunagula, Mahendra Babu, Hyderabad,
    India
Brook, Charlie, London
Brownwynne, James, St Albans, Hertfordshire
Bubnova, Michaela, Hinckley, Leicestershire
Charles, Anita Louise, London
Coene, Helena, Brussels, Belgium
Dereszewska, Basia, London
Dighton, Anna Louise, Saffron Walden, Essex
Efthymiadis, Avraam, Parga, Greece
Faktor, Joanna Deborah, London
Franklin, Dale, London
Franks, Jill, London
Fukaya, Keiko, Tokyo, Japan
Gordon, Pippa, London
Greenwood, Debbie, London

Griffiths, Sara, London
Halliday, Jilly, London
Han, Jie, London
Hara, Kiyo, Nishimuro-gun, Wakayama Pref.,
    Japan
Hawkins, Silas, London
Hawthorne, Eamonn, Carlisle, Cumbria
Hirayama, Chieri, Osaka City, Japan
Hu, Xiao Yu, London
Huang Chiao-Ying, London
Huybrechts, Thomas, Salisbury, Wiltshire
Ismain, Errico, London
Ikeda, Tomoka, Imari City, Saga Pref., Japan
Ito, Takako, Tokyo, Japan
Iwamoto, Akiko, London
Jara, Gonzalo, Bogota, Colombia
Jeong, Eun Ah, Kofu City, Yamanashi Pref.,
    Japan
Joshi, Rekhabensunil, Ahmedabad, India
Joshi, Sunil, Ahmedabad, India
Kamharn, Pranom, London
Kanatsu, Takeshi, Matsue City, Shimane Pref.,
    Japan
Keenan, Alison, London
Kishi, Tomoo, Himeji City, Hyogo Pref., Japan
Klein-Bernhardt, Ute, Wausau,
    Wisconsin, U.S.A.
Kobayashi, Nobue, Kofu City,
    Yamanashi Pref., Japan
Lacosta, Patricia, London
Little, Anne, Holmfirth, West Yorkshire
Mahoud Al-Musallam, Zainab, Kuwait
Manabe, Go, Tokyo, Japan
Marmont, Joan, London
Martin, Helen, Liverpool, Lancashire
Mashiko, Fumiko, Yachiyo City,
    Chiba Pref., Japan
Mori, Hirokazu, Osaka City, Japan
Nishimura, Fumiko, Kofu City,
    Yamanashi Pref., Japan
Novak, Daniel, Amarillo, Texas, U.S.A.
Ohara, Youhei, Nagaokakyo City, Kyoto, Japan
Oike, Akane, Tokyo, Japan
Oliver, Wendy, Aberystwyth, Ceredigion
Quintin-Baxendale, Brian, Ruislip Manor,
    Middlesex
Roberts, Julia, London
Ross, Antonia, Fleet, Hampshire
Sekine, Shunji, Tokyo, Japan
Smith, Gary, Montoursville,
    Pennsylvania, U.S.A.

## Donations

The Council of the Association is most grateful to the following for their donations.
Donation levels are Diamond (£1000 to £4999), Ruby (£500 to £999),
Emerald (£250 to £499), Sapphire £100 to £249) and Pearl (£24 to £99)

*Sapphire Donations*

Torbjorn Lindwall FGA DGA, Lannavaara,
   Sweden
Robert L. Rosenblatt FGA, Salt Lake City,
   Utah, U.S.A.

*Pearl Donations*

Raed Mustafa Al-Hadad FGA, Abu Dhabi,
   United Arab Emirates
Alexander Armati DGA, Reading, Berkshire
Burton A. Burnstein, Los Angeles,
   California, U.S.A.
Anthony J. Boyce FGA., Doncaster,
   South Yorkshire
Dennis Durham, Kingston upon Hull,
   East Yorkshire

Robin Fletcher, Reading, Berkshire
Gwyn Green FGA DGA, Barnt Green,
   Hereford and Worcester
Masao Kaneko FGA., Tokyo, Japan
Sandra Lear, FGA, Morpeth,
   Northumberland
Ernest R. Mindry FGA, Chesham,
   Buckinghamshire
Sara Naudi FGA., London
David J. Sayer FGA DGA, Wells, Somerset
Moe Moe Shwe FGA, Singapore
U Myint Tun FGA, Lulea, Sweden
Penny A Vernon FGA DGA, London
Nancy Warshow FGA DGA, Nairobi, Kenya
Ka Yee Yeung DGA, Hong Kong

Sonoda, Yasuko, Kofu City, Yamanashi Pref.,
   Japan
Sugiyama, Chika, Osaka City, Japan
Sutton, Claire, London
Tayler, Kathy, London
Tejima, Yuko, Ichikawa City, Chiba Pref., Japan
Tsai, Yi-Han Emma, London
Tsukamoto, Hiroyo, Kyoto City, Japan
Tsuruta, Miho, Onga-gun, Fukuoka Pref.,
   Japan
Ueda, Kenji, Osaka City, Japan
Ueno, Ingrid, Hyogo-Ken, Japan
Vasdekis, Lukas, Athens, Greece
Veerasingam, Jacob, Windhoek, Namibia
Wakabayashi, Takuji, Tokyo, Japan
Wakita, Youko, Osaka City, Japan
Wang, Songfang, Kofu City, Yamanashi Pref.,
   Japan
Watanabe, Yoshiko, Minamitsuru-gun,
   Yamanashi Pref., Japan
Williams, Anne-Marie, Amersham,
   Buckinghamshire
Yamada, Mayumi, Kobe City, Hyogo Pref.,

Japan
Yamaguchi, Yuko, Gerrards Cross,
   Buckinghamshire
Yoshida, Ayana, Tokyo, Japan
Zebrowski-Jensen, Catherine, Pena Bianca,
   New Mexico, U.S.A.

### Laboratory Membership

P. Fisher Ltd, London
Graus Antiques, London

## Obituary

It is with deep regret that we announce
the death on 17 April of David Kent FGA
(D. 1948), a Vice President of the Association
since 1992. A full obituary will be published
in the next issue of *The Journal*.

Hsieh Juan Ku-Wei FGA (D.1997), Taipei,
   Taiwan, died in November 2006.
Joan M. Hull FGA, Leighton Buzzard,
   Bedfordshire, died on 3 January 2007.

George M.A. McChlery MA CA FGA (D.1962), Glasgow, died on 26 December 2006.

John W. Nowak CEng FRAeS FGA (D.1974), Bexley, Kent, died on 16 April 2007.

Pekka J. Parikka FGA (D. 1989), Helsinki, Finland, died in August 2006.

Philip Riley FGA (D.1960 with Distinction), Kimpton, Hitchin, Hertfordshire, died in August 2006. Philip had served on the Council of the Gemmological Association of Great Britain for many years and was Vice Chairman of the Association from 1965-1970.

Peter A. Waters FGA DGA, Aldcliffe, Lancaster, died on 11 December 2006. Peter was awarded the Tully Medal in 1962 and had been a Gem-A correspondence course tutor for many years.

# Forthcoming Events

## Gem-A Annual General Meeting

The Gem-A AGM is to be held on Monday 18 June at 6:00 p.m.
at the National Liberal Club, Whitehall Place, London SW1A 2HE.

| | |
|---|---|
| Tuesday 1 May | Gem Discovery Club Specialist Evening. Gemstones in 18th century Portuguese jewellery. RUI GALOPIM DE CARVALHO |
| Friday 4 to Monday 7 May | Scottish Branch Annual Conference: Keynote speaker: PROFESSOR EMMANUEL FRITSCH |
| Saturday 12 May | South East Branch. Viewing of a private collection of African gems and minerals. |
| Thursday 17 May | North West Branch. Lord Derby – 15th Earl of Derby's agate collection. WENDY SIMKISS |
| Thursday 24 May | North East Branch. Coloured stone market. TRACEY JUKES |
| Tuesday 5 June | Gem Discovery Club Specialist Evening. The development of the Lennix synthetic emerald. ROY HUDDLESTONE |
| Saturday 16 June | Midlands Branch. Summer Supper Party |
| Thursday 21 June | North West Branch. Opals. ALAN HODGKINSON |
| Sunday 23 September | Hong Kong Dinner and Graduation Ceremony. To be held at The Salisbury, Kowloon, Hong Kong |
| Sunday 28 October | Gem-A Annual Conference. Gems of the Orient |
| Monday 29 October | Presentation of Awards and Graduation Ceremony. |

## Contact details

*When using e-mail, please give Gem-A as the subject:*

| | |
|---|---|
| London: | Karolina Grobelski on 020 7404 3334; e-mail karolina.grobelski@gem-a.info |
| Midlands Branch: | Paul Phillips on 02476 758940; email pp.bscfgadga@ntlworld.com |
| North East Branch: | Mark Houghton on 01904 639761; email sara_e_north@hotmail.com |
| North West Branch: | Deanna Brady on 0151 648 4266 |
| Scottish Branch: | Catriona McInnes on 0131 667 2199; e-mail scotgem@blueyonder.co.uk |
| South East Branch: | Peter Wates; email peter_at_GASEB@yahoo.co.uk |
| South West Branch: | Richard Slater on 01635 553572; e-mail rslater@dnfa.com |

## Gem-A Website

For up-to-the-minute information on Gem-A events visit our website on www.gem-a.info

# Guide to the preparation of typescripts for publication in The Journal of Gemmology

The Editor is glad to consider original articles shedding new light on subjects of gemmological interest for publication in The Journal. Articles are not normally accepted which have already been published elsewhere in English, and an article is accepted only on the understanding that (1) full information as to any previous publication (whether in English or another language) has been given, (2) it is not under consideration for publication elsewhere and (3) it will not be published elsewhere without the consent of the Editor.

**Typescripts** Two copies of all papers should be submitted on A4 paper (or USA equivalent) to the Editor. Typescripts should be doubled spaced with margins of at least 25mm. They should be set out in the manner of recent issues of The Journal and in conformity with the information set out below. Papers may be of any length, but long papers of more than 10 000 words (unless capable of division into parts or of exceptional importance) are unlikely to be acceptable, whereas a short paper of 400-500 words may achieve early publication.

The abstract, references, notes, captions and tables should be typed double spaced on separate sheets.

**Title page** The title should be as brief as is consistent with clear indication of the content of the paper. It should be followed by the names (with initials) of the authors and by their addresses.

**Abstract** A short abstract of 50-100 words is required.

**Key Words** Up to six key words indicating the subject matter of the article should be supplied.

**Headings** In all headings only the first letter and proper names are capitalized.

## A This is a first level heading

### B This is a second level heading

First and second level headings are ranged left on a separate line.

Third level headings are in italics and are indented within the first line of the text.

**Illustrations** High resolution digital files, for both colour and black-and-white images, at 300 dpi TIFF or JPEG, and at an optimum size, can be submitted on CD or via email. Vector files (EPS) should, if possible, include fonts. Match proofs are essential when submitting digital files as they represent the colour balance approved by the author(s).

Transparencies, photographs and high quality printouts can also be submitted. It is recommended that authors retain copies of all illustrations because of the risk of loss or damage either during the printing process or in transit.

Diagrams must be of a professional quality and prepared in dense black ink on a good quality surface. Original illustrations will not be returned unless specifically requested.

All illustrations (maps, diagrams and pictures) are numbered consecutively with Arabic numerals and labelled Figure 1, Figure 2, etc. All illustrations are referred to as 'Figures'.

**Tables** Must be typed double spaced, using few horizontal rules and no vertical rules. They are numbered consecutively with Roman numerals (Table IV, etc.). Titles should be concise, but as independently informative as possible. The approximate position of the Table in the text should be marked in the margin of the typescript.

**Notes and References** Authors may choose one of two systems:

(1) The Harvard system in which the authors' names (no initials) and dates (and specific pages, only in the case of quotations) are given in the main body of the text, (e.g. Collins, 2001,341). References are listed alphabetically at the end of the paper under the heading References.

(2) The system in which superscript numbers are inserted in the text (e.g. ... to which Collins refers.[3]) and referred to in numerical order at the end of the paper under the heading Notes. Informational notes must be restricted to the minimum; usually the material can be incorporated in the text. If absolutely necessary both systems may be used.

References in both systems should be set out as follows, with double spacing for all lines.

**Papers** Collins, A.T., 2001. The colour of diamond and how it may be changed. J.Gemm., 27(6), 341-59

**Books** Balfour, I., 2000. Famous diamonds. 4th edn. Christie's, London. p.200

Abbreviations for titles of periodicals are those sanctioned by the World List of scientific periodicals 4th edn. The place of publication should always be given when books are referred to.

# Contents

Cover Picture: Two red synthetic zincite crystals. Photograph by M. Krystek.
(See Formation of large synthetic zincite (ZnO) crystals during production of zinc white, p.257)